SYNTHESIS AND CHARACTERIZATION OF WATER-SOLUBLE POLYANILINE FOR HYDRAZINE DETECTION

HAZIRA BINTI HUSSIN

FACULTY OF SCIENCE
UNIVERSITI MALAYA
KUALA LUMPUR

2020

SYNTHESIS AND CHARACTERIZATION OF WATER-SOLUBLE POLYANILINE FOR HYDRAZINE DETECTION

HAZIRA BINTI HUSSIN

DISSERTATION SUBMITTED IN FULFILMENT OF THE REQUIREMENTS FOR THE DEGREE OF MASTER OF SCIENCE

DEPARTMENT OF CHEMISTRY
FACULTY OF SCIENCE
UNIVERSITI MALAYA
KUALA LUMPUR

2020

UNIVERSITI MALAYA

ORIGINAL LITERARY WORK DECLARATION

Name of Candidate: **HAZIRA BINTI HUSSIN**

Matric No: **SGR150015**

Name of Degree: **MASTER OF SCIENCE**

Title of Dissertation ("this Work"):

SYNTHESIS AND CHARACTERIZATION OF WATER-SOLUBLE POLYANILINE FOR HYDRAZINE DETECTION

Field of Study:

POLYMER CHEMISTRY

I do solemnly and sincerely declare that:

(1) I am the sole author/writer of this Work;
(2) This Work is original;
(3) Any use of any work in which copyright exists was done by way of fair dealing and for permitted purposes and any excerpt or extract from, or reference to or reproduction of any copyright work has been disclosed expressly and sufficiently and the title of the Work and its authorship have been acknowledged in this Work;
(4) I do not have any actual knowledge nor do I ought reasonably to know that the making of this work constitutes an infringement of any copyright work;
(5) I hereby assign all and every rights in the copyright to this Work to the University of Malaya ("UM"), who henceforth shall be owner of the copyright in this Work and that any reproduction or use in any form or by any means whatsoever is prohibited without the written consent of UM having been first had and obtained;
(6) I am fully aware that if in the course of making this Work I have infringed any copyright whether intentionally or otherwise, I may be subject to legal action or any other action as may be determined by UM.

Candidate's Signature Date:

Subscribed and solemnly declared before,

Witness's Signature Date:

Name:

Designation:

SYNTHESIS AND CHARACTERIZATION OF WATER-SOLUBLE POLYANILINE FOR HYDRAZINE DETECTION

ABSTRACT

In this study, polyaniline (PAni) was synthesized through the chemical oxidation method using aniline (Ani) as a monomer, hydrochloric acid (HCl) as a dopant, and ammonium persulphate (APS) as an initiator. PAni was rendered water soluble through treating with cellulose derivatives. Cellulose derivatives such as methylcellulose (MC), hydroxypropyl cellulose (HPC), and hydroxypropyl methylcellulose (HPMC) were used as a stabilizer to improve the solubility of PAni in an aqueous medium. The water-soluble PAni-cellulose derivative was applied as a chemical sensor for hydrazine detection. The chemical structures and electrical conducting behaviours of PAni-cellulose derivatives were investigated using Fourier transform infrared (FTIR) and Ultraviolet- visible (UV-Vis) spectroscopic analyses. The conductivities of water-soluble PAni-cellulose derivatives were measured using conductivity meter. In calibrating the hydrazine detection, water-soluble PAni-cellulose derivatives were mixed with various concentrations of hydrazine and the sensor responses were measured using the conductivity meter. At the early stage of the application, the range from 10 ppm to 100 ppm of hydrazine concentration was used. There were several parameters that have been studied, these include: (i) different volume ratio of PAni to hydrazine, (ii) different types of cellulose derivatives, (iii) different mass ratio of Ani to MC, and (iv) the detection at different concentration of hydrazine (1 ppm to 10 ppm). From the results obtained, all water-soluble PAni-cellulose derivatives showed a decrease in the electrical conductivities with the increasing of hydrazine concentration. This happens due to the reduction of PAni from conducting emeraldine salt (ES) to non-conducting leucoemeraldine (LE) by hydrazine. The PAni-MC (ratio 2:5) showed the best result with a good linearity of 0.9832, hence was selected to study the sensor

performance. The calibration plot was constructed from 0.05 ppm to 5.00 ppm of hydrazine. From the calibration curve, it showed a good linear correlation determination of 0.9953, a good sensitivity of 0.0132 ppm^{-1}, the limit of detection (LOD) of 0.55 ppm, and the limit of quantitation (LOQ) of 1.82 ppm. This study showed that the LOD achieved was lower than the OSHA standard of 1 ppm. Besides, the sensor performance was supported by UV-Vis and FTIR analyses. UV-Vis spectra show a significant decrease in absorbance at the bipolaron band (~821 nm) from 3.27 to 0.63 and at polaron band (~450 nm) from 2.89 to 0.55. A notable change in the chemical structures analyzed by FTIR for the quinoid to benzenoid (I_Q / I_B) intensity ratio of 1.03 before the addition of hydrazine decreased to 0.97 after the addition of hydrazine. Both UV-Vis and FTIR analyses significantly proved that the ES of water-soluble PAni-MC has turned to LE because LE consists of the more benzenoid units compared to ES. The water-soluble PAni-MC eventually indicated a good recovery range of 96 - 136 % and a good relative standard deviation (RSD) of 2.69 - 5.84 % in the real sample analysis study. As a conclusion, the water-soluble PAni-MC showed good potential as a chemical sensor for hydrazine detection.

Keywords: Water-soluble polyaniline, cellulose derivatives, hydrazine, electrical conductivity, sensor performance

SINTESIS DAN PENCIRIAN POLIANILINA LARUT AIR UNTUK PENGESANAN HIDRAZINA

ABSTRAK

Dalam kajian ini, polianilina (PAni) telah disintesis melalui kaedah pengoksidaan kimia dengan menggunakan anilina (Ani) sebagai monomer, asid hidroklorik (HCl) sebagai dopan, dan amonium persulfat (APS) sebagai pemula. PAni menjadi larut air melalui proses dengan terbitan selulosa. Terbitan selulosa seperti metilselulosa (MC), hidroksipropil selulosa (HPC), dan hidroksipropil metilselulosa (HPMC) telah digunakan sebagai penstabil untuk meningkatkan keterlarutan PAni dalam medium akueus. PAni-terbitan selulosa larut air telah digunakan sebagai sensor kimia untuk pengesanan hidrazina. Struktur kimia dan sifat kekonduksian elektrik PAni-terbitan selulosa dikaji dengan menggunakan analisis spektroskopi *Fourier* transformasi inframerah (FTIR) dan Ultra lembayung-nampak (UV-Vis). Kekonduksian PAni-terbitan selulosa larut air diukur dengan menggunakan meter kekonduksian. Dalam menentukur pengesanan hidrazina, PAni-terbitan selulosa larut air telah dicampur dengan pelbagai kepekatan hidrazina dan gerak balas sensor telah diukur dengan menggunakan meter kekonduksian. Pada peringkat awal aplikasi, kepekatan hidrazina dari 10 ppm hingga 100 ppm telah digunakan. Terdapat beberapa parameter yang telah dikaji, seperti; (i) perbezaan nisbah isipadu PAni kepada hidrazina, (ii) jenis terbitan selulosa yang berbeza, (iii) perbezaan nisbah jisim Ani kepada MC, dan (iv) pengesanan pada kepekatan hidrazina yang berbeza (1 ppm hingga 10 ppm). Daripada hasil yang diperoleh, semua PAni-terbitan selulosa larut air telah menunjukkan penurunan kekonduksian elektrik dengan peningkatan kepekatan hidrazina. Ini berlaku kerana penurunan PAni daripada konduksi garam emeraldin (ES) kepada penebat leukoemeraldin (LE) oleh hidrazina. PAni-MC (nisbah 2:5) menunjukkan hasil terbaik dengan garis lurus yang baik iaitu 0.9832. Oleh itu, campuran ini dipilih untuk mengkaji

prestasi sensor. Pengesahan kaedah dibina dalam julat 0.05 ppm hingga 5.00 ppm hidrazina. Daripada lengkung penentukuran, ia menunjukkan penentuan korelasi linear yang baik iaitu 0.9953, kepekaan yang baik iaitu 0.0132 ppm^{-1}, had pengesanan (LOD) sebanyak 0.55 ppm, dan had kuantiti (LOQ) sebanyak 1.82 ppm. Kajian ini menunjukkan bahawa LOD dicapai adalah lebih rendah daripada piawaian OSHA iaitu 1 ppm. Disamping itu, gerak balas sensor disokong oleh analisis UV-Vis dan FTIR. Spektrum UV-Vis menunjukkan penurunan ketara pada puncak bipolaron (~ 821 nm) dari 3.27 hingga 0.63 dan pada puncak polaron (~ 431 nm) dari 2.89 hingga 0.55. Perubahan yang ketara dalam struktur kimia juga dianalisis oleh FTIR untuk nisbah keamatan kuinoid kepada benzenoid (I_Q / I_B) dari 1.03 sebelum penambahan hidrazina menurun kepada 0.97 selepas penambahan hidrazina. Kedua-dua analisis UV-Vis dan FTIR telah membuktikan bahawa PAni-MC larut air telah berubah daripada keadaan ES kepada LE kerana LE mempunyai lebih banyak unit benzenoid berbanding ES. PAni-MC larut air akhirnya menunjukkan pemulihan yang baik antara 96 - 136 % dan sisihan piawai relatif yang baik (RSD) sebanyak 2.69 - 5.84 % dalam kajian analisis sampel sebenar. Sebagai kesimpulan, PAni-terbitan MC larut air menunjukkan potensi yang baik sebagai sensor kimia untuk pengesanan hidrazina.

Kata kunci: Polianilina larut air, terbitan selulosa, hidrazina, kekonduksian elektrik, prestasi sensor

ACKNOWLEDGEMENTS

All praises to Allah by whose Grace and Mercy all good deeds have been accomplished and may the peace and blessings of Allah be upon his Messenger. Alhamdulillah ‘Ala Kulli Haal.

First and foremost, I would like to express my sincere gratitude to all of my great supervisors; Prof. Dr. Gan Seng Neon, Assoc. Prof. Dr. Phang Sook Wai, and Assoc. Prof. Dr. Sharifah Mohamad for their continuous guidance, assistance, knowledge, and encouragement to help me out since I started this master’s journey until the end. I appreciate and grateful for their kindness.

A massive thanks to the members of the lab team; Mariam, Aziera, Yka, F iqah, Kavirajaa, Kak Shafiza, Kak Rohani, Mr. Abbas, Mr. Pejvak, and Mr. Pedram, I cannot thank you enough for how grateful I am for your help during my difficult time. I also would like to thank Prof. Dr. Wan Jefrey for permitting me to use the conductivity meter in his laboratory and all the staff of the Chemistry Department that always give me a hand with the instruments and other matters.

I would like to acknowledge the University of Malaya through the following grants; UMRG (RG271-13AFR) and PPP (PG198-2016A), and the Ministry of Higher Education Malaysia (MOHE) for their financial support and scholarship (MyMaster) to complete this research study.

Last but not least, my biggest appreciation to my awesome parents, Hussin bin Ab.Talib and Bidah binti Yunus@ Junoh for always sticking by me through thick and thin, loving, and supporting me. For always being on my side, for your protection and support, for sharing my dreams I do thank you, my big family.

TABLE OF CONTENTS

LIST OF FIGURES

LIST OF TABLES

LIST OF SYMBOLS AND ABBREVIATIONS

G	:	Conductance
σ	:	Conductivity
R^2	:	Coefficient of determination
mm^3	:	Cubic millimetre
°C	:	Degree celcius
e^-	:	Electron
σ_f	:	Final conductivity
g	:	Gram
σ_i	:	Initial conductivity
kDa	:	Kilodaltons
µA	:	Microampere
µg	:	Microgram
µm	:	Micrometre
µM	:	Micromolar
µS	:	Microsiemens
mg	:	Milligram
mL	:	Millilitre
mm	:	Millimetre
mmol	:	Millimol
mM	:	Millimolar
mS	:	Millisiemens
mV	:	Millivolt
M	:	Molarity
nm	:	Nanometer

nM	:	Nanomolar
Ω	:	Ohm
ppb	:	Parts per billion
ppm	:	Parts per million
% T	:	Percentage of transmission
π	:	Pi
pM	:	Picomolar
R	:	Resistance
s	:	Seconds
Q	:	Selectivity coefficient
S	:	Siemens
w/w %	:	Weight percentage
HAF	:	2-hydroxyethylammoniumformate
APBA	:	3-aminophenylboronic acid
AC	:	Alternating current
Al_2O_3	:	Alumina
NH_3	:	Ammonia
Ani	:	Aniline
APS	:	Ammonium persulphate
ATR	:	Attenuated total reflection
AOT	:	Bis-2-ethylhexyl sulfosuccinate sodium salt
CO	:	Carbon monoxide
CMC	:	Carboxymethyl cellulose
$HAuCl_4$	:	Chloroauric acid
CPs	:	Conducting polymers
DSA	:	Dextran sulfate

DF	:	Dilution factor
DMF	:	Dimethyl formamide
DMSO	:	Dimethylsulfoxide
DBSA	:	Dodecyl benzenesulphonic acid
EIS	:	Electrochemical Impedance Spectroscopy
ECL	:	Electroluminescence
ES	:	Emeraldine salt
FTIR	:	Fourier transform infrared
GOD	:	Glucose oxidase
AuNPs	:	Gold nanoparticles
GO	:	Graphene oxide
HFIP	:	Hexafluoroisopropanol
HOMO	:	Highest occupied molecular level
N_2H_4	:	Hydrazine
$N_2H_4.H_2O$	:	Hydrazine hydrate
HCl	:	Hydrochloric acid
HPC	:	Hydroxypropyl cellulose
HPMC	:	Hydroxypropyl methylcellulose
IDLH	:	Immediately Dangerous to Life or Health Concentration
ITO	:	Indium tin oxide
IARC	:	International Agency for Research on Cancer
I_B	:	Intensity of benzenoid
I_Q	:	Intensity of quinoid
LB	:	Langmuir-Blodgett
LE	:	Leucoemeraldine
LED	:	Light emitting diode

LOD	:	Limit of detection
LOQ	:	Limit of quantitation
LR	:	Linear range
LUMO	:	Lowest unoccupied molecular level
MC	:	Methylcellulose
MWCO	:	Molecular weight cut-off
NIOSH	:	National Institute for Occupational Safety and Health
NTP	:	National Toxicology Program
NIR	:	Near Infrared
NO_2	:	Nitrogen dioxide
OCSP	:	Organic crystal surface-induced polymerization
OSHA	:	Occupational Safety and Health Administration
PEL	:	Permissible exposure limit
PAMPS	:	Poly(2-acrylamido-2-methyl-propanesulphonic acid)
PEDOT	:	Poly(3,4-ethylenedioxythiophene)
PA	:	Polyacetylene
PAni	:	Polyaniline
PEO	:	Polyethylene oxide
Ppy	:	Polypyrrole
PPV	:	Poly(p-phenylene vinylene)
PSS	:	Poly(styrenesulfonate)
PTh	:	Polythiophene
PVA	:	Poly(vinyl acetate)
PVP	:	Poly(vinylpyrrolidone)
REL	:	Recommended exposure limit
rGO	:	Reduced graphene oxide

RSD	:	Relative standard deviation
SDS	:	Sodium dodecylsulfate
SD	:	Standard deviation
THF	:	Tetrahydrofuran
TLV	:	Threshold limit value
UV-Vis	:	Ultraviolet – visible

LIST OF APPENDICES

CHAPTER 1: INTRODUCTION

1.1 Conducting Polymers (CPs)

Conventionally, polymer serves as an insulator that cannot conduct electricity. Therefore, a polymer is used as the electric wire coating to prevent a short circuit. However, this perception had been changed after the discovery of conducting polymers (CPs) in 1977. CPs exhibit good electrical properties similar to metals and possess advantages over metals in certain applications. Historically, CP was discovered by Shirakawa and co-workers accidentally during the preparation of black powder polyacetylene (PA). The silvery PA thin film was obtained due to the excessive catalyst added. This silver PA possessed high electrical conductivity when it exposed to halogen vapour. This finding has attracted the interest of researchers all over the world to study in-depth about the chemical and physical properties of CPs (The Royal Swedish Academy of Sciences [RSAS], 2000).

CPs are organic polymers that can conduct electricity. They consist of conjugated double bonds, where the "pi" (π) bonds of the polymer backbone are separated by a single "sigma" (σ) bond (RSAS, 2000). Over recent decades, CPs have attracted scientific attention due to their special properties such as low cost, simple preparation method, possess redox behaviour, high electrical conductivity, and good mechanical resistance (Li et al., 2012; Sambasevam et al., 2015). **Figure 1.1** shows the well-known examples of CPs include polyaniline (PAni), polythiophenes (PTh), poly(p-phenylene vinylene) (PPV), poly(ethylenedioxythiophene) (PEDOT), and polypyrrole (PPy), (RSAS, 2000).

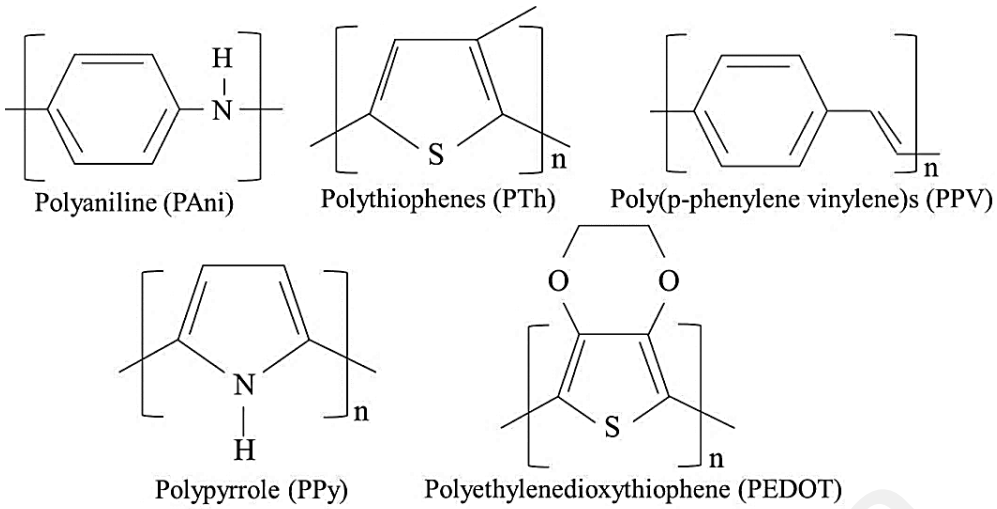

Figure 1.1: Main classes of CPs (RSAS, 2000).

All CPs can be synthesized through chemical or electrochemical methods with different types of monomer, synthesis temperature, and types of dopants (Li et al., 2012; Sambasevam et al., 2015). CPs have been utilized in various applications such as corrosion inhibitors, antistatic coating, electromagnetic interference shielding, smart windows, transistors, light-emitting diodes, solar cells, sensors, and secondary batteries (Hino et al., 2006; RSAS, 2000).

1.2 Polyaniline (PAni)

Polyaniline (PAni) is one of the oldest CPs and has been extensively studied by researchers since the 1980s due to its unique properties (Shao et al., 2011; Yin & Ruckenstein, 2000). Historically, PAni was discovered by F. Ferdinand Runge in 1834, started with initial oxidation of aniline (Ani). The experimentation on Ani was continued by many researchers until it was concluded by Henry Letheby in 1862, introducing a new approach to oxidize Ani using the electrochemical oxidation method. The reaction of Ani was carried out in the presence of dopant and oxidant in acidic

medium to the Ani monomer (Rasmussen, 2017; RSAS, 2000). In general, PAni can exist in four distinct oxidation states with a different colour; (a) blue emeraldine base (half oxidized), (b) green emeraldine salt (half oxidized, protonated), (c) violet perningraniline (fully oxidized), and (d) yellow leucoemeraldine (fully reduced) as shown in **Figure 1.2**. All states depend on the degree of protonation and oxidation (Hino et al., 2006; RSAS, 2000; Smith et al., 2005).

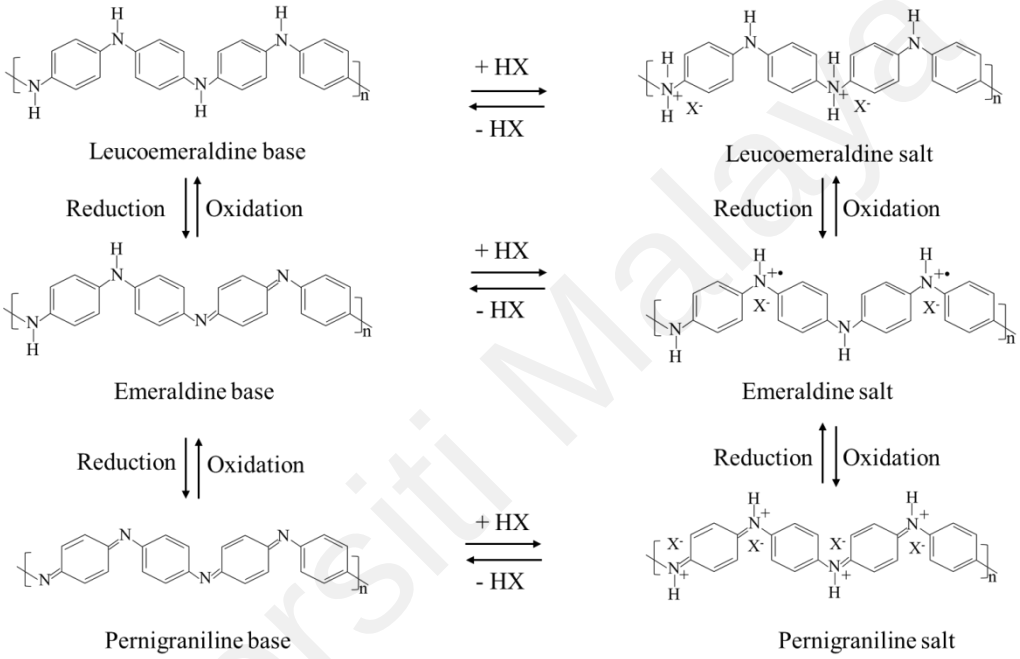

Figure 1.2: Different oxidation states of PAni (Smith et al., 2005).

Besides, the doping level of PAni can be switched by the doping/dedoping process (Shao et al., 2011). PAni exhibits many advantages such as ease of synthesis, high electrical conductivity, facile redox behaviour, high chemical stability, low cost, good environmental stability, and undergoes doping and dedoping by simple acids and bases (Barik et al., 2010; Chattopadhyay & Bain, 2008; Chattopadhyay & Mandal, 1996; Rahy et al., 2011; Su & Kuramoto, 2000; Virji et al., 2005; Yuan & Kuramoto, 2002). PAni can be synthesized by chemical and electrochemical methods (Li et al., 2012). The chemical route is preferred because it produces a large amount of PAni that is needed

for application compared to the electrochemical route which produces low yield polymer thus limits its application (Li et al., 2012; Rana et al., 2014). Owing to its desirable features, PAni has been applied in various fields in industry such as rechargeable batteries, electromagnetic shielding, light-emitting diodes (LED), corrosion protection, solar cells, electrochromic devices, smart windows, and chemical sensors (Barik et al., 2010; Chattopadhyay & Bain, 2008; RSAS, 2000; Sambasevam et al., 2015).

However, PAni as well as other CPs exhibit drawbacks such as insoluble in aqueous medium, soluble in limited organic solvents, poor mechanical strength, non-biodegradable, difficult to process due to its intrinsic intractability and infusibility thus limiting their potential application in the manufacturing industry (Casado et al., 2012; Jia et al., 2007; Luong et al., 2013; Sambesevam et al., 2015). Attempts have been made to improve the solubility of PAni such as dope with suitable surfactants and use steric stabilizers (Chattopadhyay & Bain, 2008; Sambesevam et al., 2015; Shao et al., 2011; Yin & Ruckenstein, 2000). In this research study, cellulose derivatives are utilized to synthesis PAni to produce PAni that is soluble in aqueous solution.

1.3 Hydrazine

The history of hydrazine began in 1875 when a German chemist, Emil Fischer discovered it. The work to isolate pure hydrazine was started by Theodor Curtius in 1887, however, the attempts were unsuccessful. In 1893, the preparation of pure hydrazine was accomplished by a Dutch chemist, Lobry De Bruyn. The first chemical production process of hydrazine was patented by Raschig in 1907 (Schirmann & Bourdauducq, 2012).

Hydrazine is one of the pollutants that have attracted enormous interest among researchers in developing chemical sensors. Hydrazine is a colourless, oily liquid, strong reducing agent, highly reactive base in the presence of oxidizing materials and metals, highly toxic, and explosive chemical (George et al., 2008; Sinha et al., 2015; Tsubakizaki et al., 2009; Zargar & Hatamie, 2013). There are two forms of hydrazine; anhydrous hydrazine (N_2H_4) and hydrazine hydrate ($N_2H_4.H_2O$) (Tsubakizaki et al., 2009). Although hydrazine is a toxic material, it has been used extensively in industrial fields (**Figure 1.3**) such as in the production of azo compounds, as a precursor to pesticides, as a fuel propellant for rockets, an oxygen scavenger for corrosion control in the boiler water treatment power plant, as a chemical in the production of airbag for cars, and an intermediate in the production of drugs in pharmaceutical industries (Arulraj et al., 2015; Schirmann & Bourdauducq, 2012; Sinha et al., 2015; Tsubakizaki et al., 2009).

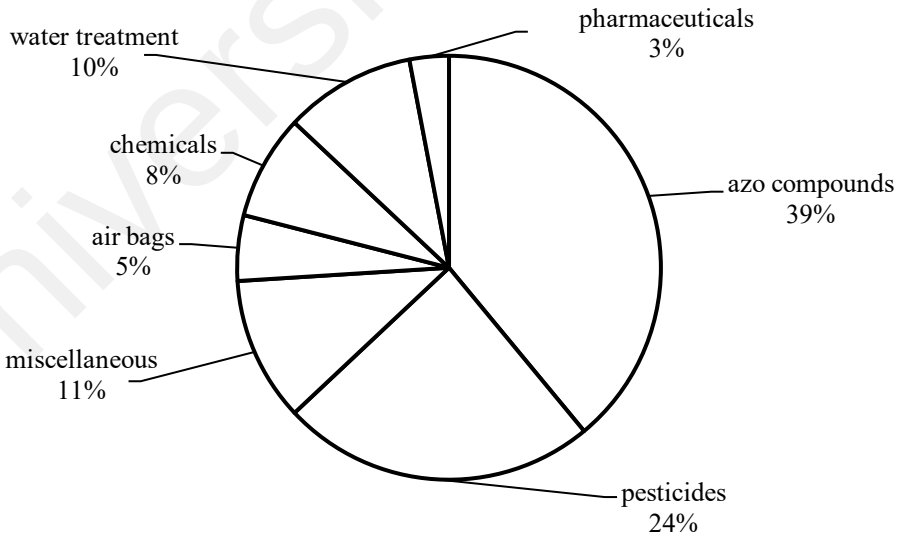

Figure 1.3: Hydrazine consumption in the industry (Schirmann & Bourdauducq, 2012).

However, it is a genotoxic carcinogen that is harmful to human and animal life. The prolonged exposure or inhalation to hydrazine can cause adverse health effects such as irritation to nose, eye, throat, dizziness, nausea, temporary blindness, pulmonary edema and coma, which can lead to the damage of lungs, liver, kidneys, central nervous and respiratory systems, and seriously affect the reproductive system in animals (Arulraj et al., 2015; Madhu et al., 2014; Sambasevam et al., 2015; Schirmann & Bourdauducq, 2012; Tsubakizaki et al., 2009; United States Department of Labor [DOL], 2018).

Therefore, the drainage of wastewater to the environment that contains hydrazine is not allowed and must be treated according to the environmental act. The concentration of hydrazine in the air does not exceed 0.1 ppm in Europe and 0.01 ppm in the United States. The threshold limit value (TLV) has been fixed at 0.1 ppm (0.13 mg/mm^3). The olfactory detection limit is between 3 to 5 ppm.

1.4 Problem Statement

Recently, environmental awareness of toxicity issues has arisen in society since it can cause poisonous effects on human health and the environment. Consequently, a number in sensor study has been increased in order to develop a good sensor to trace hazardous analytes. One of the chemicals that contribute to the toxicity problem is hydrazine.

Hydrazine and its derivatives are classified as group 2B toxic chemicals, which are carcinogenic to humans by the National Toxicology Program (NTP) and the International Agency for Research on Cancer (IARC) (Arulraj et al., 2015; DOL, 2018). Exposure to the high level of hydrazine can cause damage to the liver, kidneys, central

nervous system, and respiratory system of humans (Arulraj et al., 2015; DOL, 2018; Sambasevam et al., 2015). According to the National Institute for Occupational Safety and Health (NIOSH), the recommended exposure limit (REL) is 0.03 ppm, NIOSH Immediately Dangerous to Life or Health Concentration (IDLH) is 50 ppm, and the Occupational Safety and Health Administration (OSHA) standard is 1 ppm. Therefore, a reliable and sensitive analytical technique to trace the hydrazine level in the environment needs to be developed.

In developing a chemical sensor for hydrazine, CPs have gained prominent attention by scientists because CPs exhibit large electrical property changes when undergoing a redox reaction upon analyte. Among all CPs, PAni is one of the promising materials to be used as a sensor due to its doping and dedoping behaviour of acids and bases (Virji et al., 2005). As discussed earlier, PAni exhibits drawbacks of insolubility in an aqueous medium, soluble in limited organic solvents, non-biodegradable, and difficult to process due to its inherent intractability and infusibility (Casado et al., 2012; Jia et al., 2007; Luong et. al., 2013). In most cases, organic solvents were commonly used in the polymerization of Ani that can raise the toxicity issue to the environment. By addressing this issue, the researchers have put a lot of effort to develop green materials such as water-soluble material which is more environmentally friendly.

The study aims to establish a simple and high sensitivity sensor to detect hydrazine using water-soluble PAni. Water-soluble PAni was synthesized through a chemical oxidation method with different types of cellulose derivatives; methylcellulose (MC), hydroxypropyl cellulose (HPC), and hydroxypropyl methylcellulose (HPMC) as a steric stabilizer to enhance both the solubility and processability. Ammonium persulfate (APS) was used as an initiator and hydrochloric acid (HCl) was used as a dopant during

polymerization. These kinds of materials are relatively low cost, more environmentally friendly, high stability, non-toxic, and biodegradability compared to the traditional hydrazine sensor.

1.5 Research Objectives

The research objectives of this study are listed below:

1. To synthesize water-soluble PAni using different types of cellulose derivatives (MC, HPC, and HPMC) through chemical oxidation method and to characterize using Fourier transform infrared (FTIR) spectrometer, Ultraviolet-visible (UV-Vis) spectrophotometer, and electrical conductivity meter.
2. To study the effect of different concentration of hydrazine on the water-soluble PAni as a chemical sensor.
3. To study the effect of functional groups in the cellulose derivatives on PAni-based sensor in hydrazine detection.
4. To study the sensor performance of water-soluble PAni hydrazine sensors such as sensitivity, the limit of detection (LOD), the limit of quantitation (LOQ), coefficient of determination (R^2), interference study, and real sample analysis.

CHAPTER 2: LITERATURE REVIEW

2.1 Chemical Sensor

For decades, human activities such as manufacturing, agriculture, households, water treatment systems, laboratories, hospitals, and other production activities have yielded a lot of potentially hazardous or toxic by-products year by year. The generated waste can be in the form of liquid, solids, sediments, chemicals, heavy metals, and other harmful substances. All the hazardous wastes generally may end up in the soil, in the waters, or the atmosphere and eventually may risk, environmental health, including humans, animals, and plants (Wolters, 2019). The consequences of this issue, the scientists around the globe are endeavouring to fabricate a chemical sensor that can trace the hazardous analytes (e.g., ammonia, chloroform, hydrazine, and cyanide) that present in the environment to preserve human health and sustainability of the ecosystem.

A chemical sensor can be defined as a device or analyzer that reacts to a specific analyte and transfers the chemical information originated from chemical reactions into the analytical signal (Hulanicki et al., 1991; Wen, 2016). Generally, the sensors are designed to perform in good conditions upon specified analytes in particular sample types. The chemical sensors can be classified into many classes such as optical devices, magnetic devices, thermometric devices, mass sensitive devices, electrochemical devices, electrical devices, and other physical properties (**Figure 2.1**). The classification of chemical sensors is based on the method used for the effect, the application to detect specified analytes, and the techniques of application (Hulanicki et al., 1991).

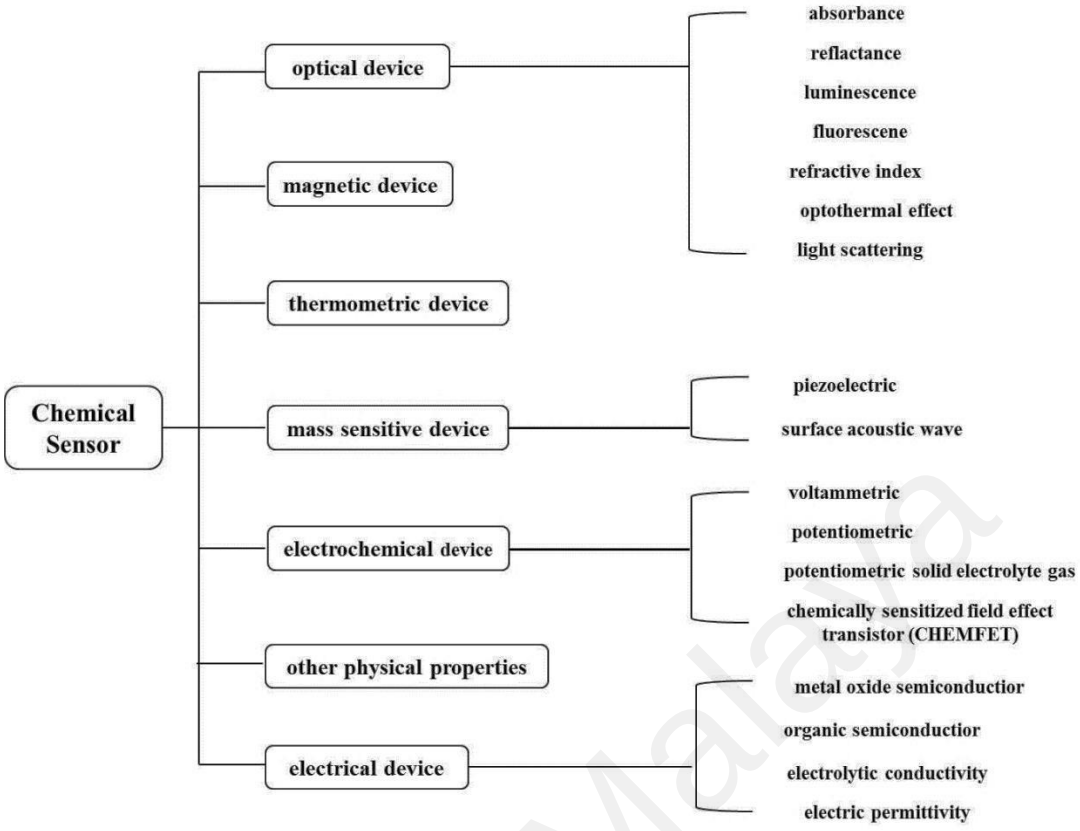

Figure 2.1: The classification of chemical sensors (Hulanicki et al., 1991).

2.1.1 Optical Device

An optical sensor is one of the devices that attracted many researchers to identify an analyte by changing the optical properties. Fluorescence is a well-suited method in the optical sensing which works by the changes in fluorescence intensity through the quenching process. The effectiveness of the quenching process depends on the type of fluorophores (Urbano et al., 1984).

The first optical sensor for halides and pseudohalides was established using acridinium and quinolium as fluorophors. The fluorescence signal had been excited from 360 nm to 405 nm of the absorption during the sensing upon the halides (Urbano et al., 1984). In the recognition of amino acids, anthroyloxy-stearate and perylene

arachidate were used as fluorophors. The amino acids had been permeated into the Langmuir-Blodgett (LB) films for both fluorophors and quenched the fluorescene intensity from 366 nm to 430 nm of anthroyloxy-stearate LB film and from 412 nm to 470 nm of perylene arachidate LB film (Aizawa et al., 1987).

Although this optical sensor offers good benefits of reversible and sensitive at low concentration, however, it needs the improvement of suitable reagents, limited dynamic range, and slow response time. All these disadvantages are caused by the mass transport barriers at the polymeric support, low sensitivity, low stability, and weak adhesion on fiber optics (Jones & Porter, 1988; Seitz, 1984).

2.1.2 Electrochemical Device

Besides, the electrochemical device also had been extensively studied by the researchers mostly in the clinical study of the biosensor. It works by converting the effect of the electrochemical interaction between analyte and electrode into an analytical signal in terms of current and potential (Hulanicki et al., 1991). The selection of catalase is crucial to catalyze analyte in giving an output signal.

In the detection of hydrogen peroxide, Aizawa and co-workers used the catalase-collagen membrane to maintain enzyme activity. During the catalysis process, hydrogen peroxide was decomposed into oxygen and water. The electrochemical current output was given by the amount of oxygen released. In the concentration range of peroxide from 0.00-0.15 $mmol^{-1}$, the current was increased from 100 μA to ~220 μA within 1-2 minutes (Aizawa et al., 1974). For the same analyte detection through the electrochemical method, Jonsson and Gorton used the horse-radish peroxidase catalase adsorbed on modified graphite as a hydrogen peroxide sensor in a flow injection system.

The increment of current response was observed from +600 mV to -200 mV in the range of concentration from 0.1 to 500 μM (Jonsson & Gorton, 1989).

This electrochemical sensor possessed some advantages such as fast response, direct evaluation, suitable for coloured and opaque solution, and high reusability of catalase and sample solution. Despite these advantages, it also exhibited some drawbacks such as complicated setup, lacking process control, poor stability of electrode, required skilled operations, and costly lab equipment (Jonsson & Gorton, 1989; Kulys & Costa, 1991).

2.1.3 Electrical Device

Besides chemical sensor types, the electrical device also gained enormous attention from scientists. This device performs by changing the electrical properties regarding conductance, resistance or capacitance resulted from the interaction between the sensor and the analyte (Hulanicki et al., 1991). The preference of semiconductors based on two types; (1) the electrical conductivity must change with the concentration of analyte at the ambient temperature and reversible, (2) stable at high temperature during the reaction (Bott & Jones, 1984).

The organic semiconductor-based sensor was developed using lead phthalocyanine films in the identification of nitrogen dioxide (NO_2) gases that were analyzed through the electrical device. The adsorption of NO_2 (as an electron acceptor) on the film surface (as a hole conductor) had affected the electrical conductivity of the organic semiconductor. During the sensing, the electrical conductivity changed from $\sim 10^{-9}\ \Omega^{-1}$ to $\sim 10^{-8}\ \Omega^{-1}$ upon the 2 ppb of NO_2 (Bott & Jones, 1984). Furthermore, the metal oxide semiconductor such as alumina (Al_2O_3) was used as a humidity sensor. The sensor

response was determined by the electrical device. The physical absorption of water molecules onto the porous alumina films through hydrogen bonding had induced electrical conductivity changes of alumina. As the relative humidity increased, the electrical conductivity showed an increment from ~10^{-8} S cm^{-1} of 30 % relative humidity up to ~10^{-6} S cm^{-1} of 65 % relative humidity (Nahar et al., 1984).

This type of electrical sensor, conventionally and yet became an option among researchers because it is possible to detect the analyte at very low concentration, facile method, and economical instrument (Bott & Jones, 1984).

Table 2.1 summarized the types of chemical sensors in the detection of chemical analytes. All these devices still have been used until now in the fabrication of chemical and biosensor. Conventional material such as metal ions usually was used as a sensing material. However, metals are toxic and may harm the environment (Harun et al., 2007). For the several past years, the polymer-based sensor has drawn scientist's attention to broadening its usefulness such as uncomplicated operation, pleasant selectivity at normal temperature, and low-cost, in the detection of hazardous analyte (Seitz, 1984; Wen, 2016).

Generally, polymer works as an insulator that cannot conduct electricity. However, the invention of electrically conducting polymers (CPs) had turned this perception and their applications were developed widely, including CPs-based sensor due to their great advantages such as exhibit redox behaviour, high electrical conductivity, and good mechanical strength (Li et al., 2012; Sambasevam et al., 2015).

Table 2.1: Different types of chemical sensors in the detection of chemical analytes.

Chemical sensor	Materials	Analyte	Technique	References
Optical device	Acridinium and quinolium	Halides and pseudohalides	Fluorescence	Urbano et al., 1984
	Anthroyloxy-stearate and perylene arachidate	Amino acid	Fluorescence	Aizawa et al., 1987
Electrochemical device	Catalase-cellulose membrane with teflon	Hydrogen peroxide	Amperometric	Aizawa et al., 1974
	Horse-radish peroxidase with modified graphite	Hydrogen peroxide	Flow injection system	Jonsson & Gorton, 1989
Electrical device	Lead phthalocyanine film	NO_2 gas	Organic semiconductor	Bott & Jones, 1984
	Alumina (Al_2O_3) film	Humidity	Metal oxide semiconductor	Nahar et al., 1984

2.2 Conducting Polymers (CPs)

In 1977, a group of scientists consists of Shirakawa, Heeger, and MacDiarmid had made a noble discovery of electrically conductive polymer; polyacetylene (PA). Upon the oxidation of *trans*-PA silvery film with halogen vapours through the doping process, the electrical conductivity was remarked by many orders of magnitude which is 4.40 X 10^{-5} Ω^{-1} cm^{-1} higher than its original *cis*-PA which is 1.70 X 10^{-8} Ω^{-1} cm^{-1} at room temperature. This finding has captivated other scientists to treasure a new class of semiconductor material and applied in various applications (Shirakawa et al., 1977).

Conducting polymers (CPs) or known as synthetic metals are organic polymers that possessed the electrical properties while maintaining mechanical properties. CPs consist of conjugated polymers with alternated single and double bonds in the polymer backbone generally are classified as semiconductors. The electrical properties of CPs are depended on the dopant. By adjusting the doping levels, the CPs may appear as an insulator (non-doped), semiconductor, or metal (fully doped). The prevalent CPs are polythiophenes (PTh), poly (p-phenylene vinylene) (PPV), polypyrrole (PPy), poly(ethylenedioxythiophene) (PEDOT), and polyaniline (PAni) (MacDiarmid, 2001).

In the past decades, a reliable and sensitive CPs-based sensor has attracted much attention in modern analytical science for chemical detection because of their electrical properties transition and redox behaviour. Upon the exposure of CPs to oxidant and reductant, CPs show rapid conductivity changes by enhancing the conductivity and decreasing conductivity, respectively. Both of the processes generally are reversible at room temperature. In comparison with most of the commercially-available sensors that usually based on metal oxides and operated at high temperatures, the CPs-based sensors have many better characteristics such as significant electrical conductivity changes upon

protonated and deprotonated, high mechanical strength, good redox behaviour, and can be operated at low temperature (Lange et al., 2008; Li et al., 2012; Sambasevam et al., 2015; Weiller et al., 2005).

PPy is one of the popular CPs that has been adapted in a chemical sensor application. In recognition of hazardous gases such as hydrochloric acid (HCl) and ammonia (NH_3), the ultra-thin PPy nanosheets (UPNSs) were synthesized in an aqueous suspension through the organic crystal surface-induced polymerization (OCSP). The hydrated crystals of sodium decylsulfonate ($C_{10}SO_3Na$) were used as a template and $FeCl_3$ as an oxidant. The as-synthesized electrical conductivity of UPNSs reported was much higher than PPy nanoparticles, which are 30.6 S/cm (UPNSs) compared to 2.4 S/cm (PPy). When the UPNSs exposed to 100 ppm of HCl and NH_3, the relative resistances were increased by almost ~10^1 S/cm and decreased to more than 10^{-1} S/cm, respectively. This eventually proved that PPy exhibited fine doping and dedoping process upon the detecting analyte by tuning the electrical properties (Jeon et al., 2011).

In the identification of hydrogen gas, PEDOT also has gained the attentiveness of researchers to use PEDOT as the sensing material. PEDOT: poly(styrenesulfonate) was named as (PEDOT: PSS) nanocomposites were chemically modified with graphene oxide (GO) and reduced graphene oxide (rGO) to enhance the sensor sensitivity during the detection of hydrogen gas. Both nanocomposites were doped using dimethylsulfoxide (DMSO). The electrical conductivities attained for PEDOT: PSS, GO/PEDOT: PSS, and rGO/PEDOT: PSS were ~110 S/cm, ~90 S/cm, and ~330 S/cm, respectively. Upon sensing the various concentrations of hydrogen, the electrical properties of both modified-PEDOT had been altered through redox reactions and charge transfer. As a result, the resistance was decreased from 159.0 Ω to 149.0 Ω for

GO/PEDOT: PSS and from 49.6 Ω to 49.0 Ω for rGO/PEDOT: PSS. This showed that the modified-PEDOT has a promising sensing behaviour towards hydrogen gas with the limit of detection (LOD) achieved was near to 30 ppm (Zheng et al., 2015).

Besides PEDOT, PTh also has been applied as a sensor by the analyst. The highly conductive PTh films were successfully doped with chloroauric acid (HAuCl4) using the solution-processing method. The electrical conductivity was increased from 47.2 μS/cm to 71.7 S/cm concomitant with the color changes of PTh films from red-brown to light blue upon doping. These happened due to the doping effect of HAuCl4 by generating a large number of free charge carriers in PTh films. After exposure to 500 ppm of volatile organic amines and thiols, the light blue color of PTh-doped HAuCl4 has reversed to red-brown when evaluated through electrochemical measurements. Besides, the electrical conductivity significantly decreased from 71.7 S/cm to 7.74 mS/cm as exposure upon 1000 ppm of amine vapor. These properties of PTh had made it applicable as a potential sensor in the detection of volatile amines and thiols as it can be reversible through the doping and dedoping process. Besides, these films can achieve the LOD lower than 1 ppm as the threshold limit for volatile amines and thiols is 10 ppm (Zhao et al., 2017).

Besides, in the sensing of carbon monoxide (CO) gas, PAni doped with a binary dopant of hydrochloric acid/β-cyclodextrin (PAni/HC) was used as a sensing material. PAni/HC was synthesized successfully through oxidative polymerization of aniline using ammonium persulfate as an oxidant. The binary dopant was used to enhance stability and prolong the shelf life of PAni as a sensor, as well as to enhance the electrical conductivity of PAni. The effect of binary dopant contributes to the higher electrical conductivity of PAni/HC of 0.282 S/cm than 0.034 S/cm of pristine PAni

through facilitating the electric path for the movement of charge carriers. Consequent to the exposure of CO gas, the conductivity of PAni/HC notably increased to ~0.86 S/cm due to the increment of the number of charge carriers along PAni/HC chain by CO. The LOD achieved by PAni/HC was 75 ppm in agreement with the reported PEL of below 100 ppm (Sen et al., 2017).

Table 2.2 shows a list of CPs-based sensors discussed previously. All CPs exhibited the changes in the electrical conductivities when reacting with an oxidizing agent and reducing agents by increasing or decreasing conductivity, respectively. Besides, the LODs achieved by all CPs were below the threshold limit by OSHA. Among all the CPs, PAni is the most prominent CPs used in the chemical sensor study. It is because PAni offers great advantages such as highly reversible upon doping/dedoping process, tunable electrical conductivity by acids and bases, adjustable pH, and good environmental stability (Sen et al., 2017).

Table 2.2: A list of CPs-based sensors.

CPs sensor	Technique	Analyte	Electrical conductivity	LOD	References
UPNSs	Flow injection	HCl gas and NH_3 gas	30.6 S/cm	-	Jeon et al., 2011
Modified graphene PEDOT: PSS films	Flow injection	Hydrogen gas	~90 S/cm and ~330 S/cm	30 ppm	Zheng et al., 2015
PTh-doped $HAuCl_4$	Electrochemical	Volatile organic amines and thiols	71.7 S/cm	< 1 ppm	Zhao et al., 2017
PAni-doped HC	Current flow measurement	CO gas	0.282 S/cm	75 ppm	Sen et al., 2017

2.3 Polyaniline (PAni)

PAni is the most favoured among the other CPs that has been explored by the researchers since the 1980s as a promising efficient sensor. PAni exhibits fascinating features such as highly sensitive to the analytes, reversible oxidation state due to the doping/dedoping and reduction/oxidation process, high electrical conductivity, and excellent environmental stability. Among all these unique properties, the doping and

dedoping process plays the main role in fabricating the PAni-based sensor (Li et al., 2012; Sambasevam et al., 2015; Wang et al, 2017).

One of the earliest PAni-based sensors was recorded in 1988 by Shinohara and co-workers. PAni film immobilized with glucose oxidase (GOD) (PAni-GOD) was synthesized through the electrochemical polymerization method of aniline (Ani). GOD was used as an enzyme for microsensor to enhance selectivity towards glucose detection. The detection was successfully determined by amperometrically in the linear range (LR) of glucose from 10^{-4} to 5.0 X 10^{-3} M. The addition of 5 mM - 10 mM of glucose to the solution caused a fast decrease in current within 10 s. This happened because oxygen was consumed by GOD, thus reduced the oxygen concentration. This process occurred at the surface of the PAni-GOD film, in which glucose was oxidized to gluconolatone. Meanwhile, oxygen was reduced to hydrogen peroxide (Shinohara et al., 1988).

The developments of PAni-based sensors are growing in the current decade. Various modifications on PAni were done in upgrading the electrical and mechanical properties of PAni as a sensor. The grafting of cellulose onto PAni (PAni-cellulose) through copolymerization method is one of the ways to enhance electrical conductivity and hydrophilicity of copolymer for humidity sensing. Cellulose was chosen because of the hydrophilic character and provided adsorption sites for water molecules, thus making it potentially applied as a humidity sensor. This resulted in PAni-cellulose with high electrical conductivity of 1.25 X 10^{-2} S/cm. The sensing process was observed by the changes in the electrical resistance of copolymer. As the relative humidity increased from 5 - 90 %, the resistance declined linearly from ~32 MΩ to 10 MΩ within 40 s owing to the adsorption of water molecules on PAni-cellulose (Shukla, 2012).

Besides copolymerization of PAni, doping with conducting filler also may improve the electrical and optical properties of PAni. The conducting filler provides a percolation pathway for the mobility of free charge carriers as well as decreases the optical bandgap by increasing localized state in the forbidden gap, respectively. Thus, when the PAni-based sensor exposes to the analyte, the changes in resistivity would be easier to monitor, as well as increasing sensitivity and selectivity of the sensor. The filler like Sn(IV)iodophosphate was incorporated into PAni to form PAni-SnIP nanocomposite via the sol-gel chemical polymerization method. It was observed that the increase of SnIP filler content, the conductivity also increased from 1.6 X 10^{-4} of pure PAni to 0.5- 1.5 X 10^{-3} S/cm of PAni-SnIP. The ethanol vapour detection by PAni-SnIP was monitored by resistivity measurement. As the ethanol concentration elevated, the resistivity responded linearly, raised from 0.4 Ω cm to 1.8 Ω cm. The sensitivity of 0.003 and the LOD of 5 ppm were obtained for PAni-SnIP (Khan et al., 2015).

PAni-based sensor not only applied in the chemical analyte sensing but also as a sensor for clinical diagnosis of biomolecules. In 2017, a promising sensor was fabricated by Zuo et al. by synthesizing PAni with 3-aminophenylboronic acid (APBA/PAni). APBA/PAni had been utilized as a quencher for the emission of graphite-like carbon nitride (g-C_3N_4) in the electrochemiluminescence (ECL) sensor for dopamine. Throughout dopamine sensing, the redox current was elevated from -100 μA to +150 μA concomitant with the decrease of ECL intensity. This might be happened due to the high electrical conductivity of PAni and the transfer of resonance energy from g-C_3N_4 to PAni. Besides, PAni/APBA also showed a great quenching effect and exhibited good sensitivity to dopamine with the LOD of 0.033 pM in the concentration range of dopamine from 0.10 pM to 5.00 nM (Zuo et al., 2017).

In addition, for the recognition of nucleic acid in blood cancer, Soni and co-workers had synthesized PAni nanostructures (PAni-NC) in 3D coral form using an oxidative template method. This 3D coral form of PAni-NC significantly enhances the electrochemical performance and electrical conductivity by providing a continuous conductive path to transfer ions rapidly. The conductivity attained by PAni-NC was 9.41 X 10^{-2} S/cm. PAni-NC had been deposited onto indium tin oxide (ITO) glass substrate to fabricate the biosensor electrode. During nucleic acid detection through electrochemical impedance spectroscopy (EIS), the resistance of PAni-NC/ITO obviously increased from 909.48 Ω to 2887.76 Ω with the nucleic acid concentration range from 10^{-6} M to 10^{-17} M. The LOD obtained was as low as 7 X 10^{-18} M. This showed that this biosensor was highly sensitive and selective for nucleic acid (Soni et al., 2019).

Table 2.3 displays a summary of PAni-based sensors that have been described above. Although PAni possessed many advantages to be applied in various sensor applications, it also has some drawbacks of limited solubility in organic solvents, insoluble in water, non-biodegradable, and difficult to process due to its inherent intractability and infusibility (Casado et al., 2012; Jia et al., 2007; Luong et. al., 2013). Therefore, the water-soluble PAni is a good solution to troubleshoot these problems.

Table 2.3: A list of PAni-based sensors.

PAni sensor	Technique	Analyte	LOD	References
PAni-GOD film	Amperometry	Glucose	-	Shinohara et al., 1988
PAni-grafted cellulose	Resistivity	Humidity	-	Shukla, 2012
PAni-SnIP nanocomposite	Resistivity	Ethanol	5 ppm	Khan et al., 2015
APBA-PAni	Electrochemiluminescence	Dopamine	0.033 pM	Zuo et al., 2017
PAni-doped HC	Current flow measurement	CO gas	75 ppm	Sen et al., 2017
PAni-NC/ITO	Impedance spectroscopy	Nucleic acid	7 X 10^{-18} M	Soni et al., 2019

2.4 Water-soluble PAni

Many research efforts have been devoted to improve the solubility and processability of PAni. The researchers have modified the properties of PAni using protonic acid and anionic surfactant (Chattopadhyay & Bain, 2008; Hino et al., 2006; Shao et al., 2011; Yin & Ruckenstein, 2000) as a dopant such as sodium dodecyl sulfate (SDS) (Hino et al., 2006), dodecyl benzenesulphonic acid (DBSA) (Hino et al., 2006; Su & Kuramoto, 2000; Yadav et al., 2019; Yin & Ruckenstein, 2000) dextran sulfate (DSA) (Yuan & Kuramoto, 2002) and poly(2-acrylamido-2-methyl propanesulphonic acid) (PAMPS) (Barik et al., 2010; Shao et al., 2011), bis-2-ethylhexyl sulfosuccinate sodium salt (AOT) (Sambasevam et al., 2015).

Niyazi Bicak and co-workers reported that the introduction of new ionic liquid, 2-hydroxyethylammoniumformate (HAF) as a solvent in the polymerization of anilium chloride with ammonium persulfate can improve solubility of PAni in organic solvents such as acetone, tetrahydrofuran (THF), dioxane, dimethylformamide (DMF), and N-methyl, 2-pyrrolidinone (Bicak et al., 2005). A.T. Ramaprasad and partner have worked on blended PAni with chitin to get better processability of PAni in common organic solvents (Ramaprasad & Rao, 2008). Moreover, an Ani aromatic ring substitution with substituent groups such as $–OCH_3$, $–SO_3$, and long alkyl chain also can alter the solubility of PAni in organic solvents and aqueous media (Chattopadhyay & Bain, 2008; Su & Kuramoto, 2000; Yin & Ruckenstein, 2000).

Besides, the steric stabilizer is also a popular dopant to produce water-soluble PAni through oxidative polymerization (Chattopadhyay & Mandal, 1996; Jia et al. 2007). Water-soluble steric stabilizer divided into two groups; (i) natural stabilizer such as cellulose ethers derivatives and (ii) synthetic stabilizer such as poly (ethylene oxide) (PEO), poly (vinyl methyl ether (PVME), poly-(vinylpyrrolidone) (PVP), and poly (vinyl alcohol)-coacetate) (PVA) (Chattopadhyay & Bain, 2008; Chattopadhyay & Mandal, 1996; Glass, 2000; Luong et al., 2013; Su & Kuramoto, 2000).

In addition, polysaccharide derivatives have been used to promote the solubility of PAni in aqueous media and organic solvents. Abdelaziz Rahy and partners described that the addition of sucrose enabled PAni to dissolve and stabilize easier in water and polar solvent by forming a hydrogen bond between PAni and the media (Rahy et al., 2011). Cellulose is a natural polymeric material which possesses good properties like chemical stability, mechanical strength, biocompatibility and biodegradation (Luong et al., 2013; Mo et al., 2009). Abdul Barik and co-workers used carboxymethyl cellulose

(CMC) as a steric stabilizer to yield stable dispersion of PAni (Barik et al., 2010). Nguyen Dang Luong et al. employed cellulose nanofibrils in aqueous suspension as a stabilizer in PAni through in-situ polymerization (Luong et al., 2013). In addition, cellulose nanofibrils possess many advantages such as low cost, non-toxicity, renewable nature, biodegradability, and able to form stable aqueous suspension (Casado et al., 2012).

MC is a non-ionic and water-soluble polymer that has been incorporated into PAni through oxidative polymerization in an acidic solution to produce water-soluble PAni. MC acts as a steric stabilizer and a molecular template to improve the dispersion of PAni (Chattopadhyay & Mandal, 1996; Jia et al., 2007; Sohouli et al., 2019). Principally, the acid dopant is commonly used during the dispersion polymerization of PAni. This is because acid dopant can activate the cellulose by breaking the hydrogen bonds and induce the accessibility and reactivity of the O-H groups into PAni to be easier (Mo et al., 2009).

A few research works based on the water-soluble PAni as a sensor was reported. Li and co-workers had suggested using poly (styrenesulfonic acid) (PSSA) as a template and PVA as an additive to produce the water-soluble PAni films through chemical oxidation polymerization in the aqueous solution using ammonium persulfate (APS) as an oxidant. The characteristics of PAni-PSSA and PAni-PSSA/PVA for humidity sensing were investigated at room temperature. In the range of 15 – 97 % relative humidity, both of the water-soluble PAni composites exhibit high sensitivity and good sensing linearity concomitantly with the change of impedance values over three orders of magnitude from 9.5 X 10^6 Ω to 6.3 X 10^3 Ω. Moreover, the response times as fast as

6 s to 10 s were recorded. It concluded that PAni-PSSA and PAni-PSSA/PVA has a potential sensor for humidity sensing (Li et al., 2010).

The modification of insoluble PAni into water-soluble PAni exhibited high performance and good sensitivity in gas sensing mechanism. Hao and Liu had prepared water-soluble PAni with $SmBaCuMO_{5+\delta}$ (M=Fe, Co, Ni) (SBCM) powders through a sol-gel technique in the fabrication of the ammonia gas sensor. When ammonia was introduced to the chamber, the resistance of PAni/SBCM increased from 0.5 X 10^4 Ω to 5.0 X 10^4 Ω in the concentration range from 10 ppm to 300 ppm. This happened due to the exchange of holes in the valence band of SBCM with the adsorbed ammonia gas by releasing electrons and recombines with holes to decrease the electrical conductivity. Among all the metals used, PAni/$SmBaCuFeO_{5+\delta}$ (SBCF) exhibited greater resistance sensitivity, higher selectivity and quick response-recovery time of less than 10 s (Hao & Liu, 2014).

In the detection of ascorbic acid, Gautam and partners developed a novel composite material using PAni, multiwalled carbon nanotubes (MWCNTs), and carboxymethyl cellulose (CMC) through the in-situ chemical polymerization in the aqueous suspension. In this composite, MWCNTs acted as conductive nanofillers to enhance the electrical and electrocatalytic properties, meanwhile, CMC improved the dispersion of MWCNTs in the aqueous medium and supplied negatively charged of carboxylate groups to form ionic bonding with protonated amine/imine of PAni. The water-soluble PAni/MWCNTs/CMC composite was applied as an electrode material, exhibited high surface area, good dispersion ability in the aqueous phase, good electrocatalytic properties, and high selectivity. The ascorbic acid sensor was monitored electrochemically by cyclic voltammetry (CV) technique. In the linear range of 0.05

mM – 5 mM with the scan rate of 5 mV s^{-1}, ascorbic acid was oxidized on the modified electrode with a lower potential of ~350 mV, thus, enhancing the sensitivity of 100.63 μAmM^{-1} cm^{-2} and the LOD of 0.01 mM during the sensing responses. It concluded that PANI/MWCNTs/CMC is suitable nanocomposite material for the electrode in the electrochemical sensor application (Gautam et al., 2018).

In the chemical sensor field, the water-soluble PAni has not been widely explored and applied as a sensor yet especially in the detection of hydrazine. In this study, the water-soluble PAni modified with cellulose derivatives was firstly fabricated as a sensor to identify hydrazine analytes.

2.5 Cellulose and Cellulose Derivatives

Cellulose ($(C_6H_{10}O_5)_n$) is one of the carbohydrate polymers that are naturally available in large quantities in the world. In cellulose, the glucopyranose chains are linked through beta-1,4-linkages with strong intramolecular and intermolecular hydrogen bonding, which has given the excellent properties to cellulose (Glass, 2000; Iglesias et al., 2019). However, cellulose has a disadvantage of being insoluble in the most organic solvent and aqueous media due to the strong hydrogen bonding, thus difficult to process and limits its applications. To overcome this limitation, cellulose was modified chemically by substituting the hydroxyl groups to disrupt hydrogen bonding, hence turns cellulose into a water-soluble polymer (Iglesias et al., 2019).

There are two crucial groups of cellulose; cellulose esters (insoluble in water) and cellulose ethers (soluble in water). Cellulose was modified into numerous types of water-soluble derivatives such as methylcellulose, carboxymethyl cellulose,

hydroxyethyl cellulose, and hydroxypropyl cellulose (Barik et al., 2010; Glass, 2000; Iglesias et al., 2019; Kadajji & Betageri, 2011). These water-soluble polymers residing in many hydroxyl groups which are hydrophilic side groups in the chemical structure. The hydroxyl groups contain a lone pair of electrons to form hydrogen bonding in the aqueous medium (Glass, 2000).

The cellulose ethers possess many advantages such as biocompatible, biodegradability, and nontoxicity (Abd Manan et al., 2016; Barik et al., 2010; Iglesias et al., 2019; Kadajji & Betageri, 2011). Therefore, they have been used in variety of industrial applications such as cosmetics, foods, pharmaceuticals, coating agents, thickening agents, stabilizers, binders, gels, and adhesives (Iglesias et al., 2019; Kadajji & Betageri, 2011).

In recent years, cellulose has gained the attention of researchers to apply in biosensing application such as phenol sensor (Abd Manan et al., 2016), cholesterol sensor (Barik et al., 2010), uric acid sensor (Sohouli et al., 2020), and humidity sensor (Li et al., 2019; Shukla, 2012). Cellulose has been used as a part of sensor material in order to improve the physical properties such as electrical conductivity and biocompatibility of sensing materials (Abd Manan et al., 2016; Barik et al., 2010).

In year 2016, nanocrystalline cellulose (NCC)/chitosan composite film sensor was successfully fabricated by Abd Manan and co-workers in phenol detection. The composite film was prepared through a drop-casting technique on a screen-printed carbon electrode (SPCE). Enzyme tyrosinase was used as a catalyst in the oxidation of phenol group to o-quinone. The redox reaction was measured electrochemically at low potential. Due to the abundance of hydroxyl groups, the nanostructure of NCC not only

provides high surface area but also enhances the transfer of an electron between the enzyme active sites and electrode. The sensor performance was evaluated by the chronoamperometric method. In the linear range of phenol concentration from 0.39 μM to 7.74 μM, the high sensitivity of 28.316 and the LOD of 0.38 μM were achieved. The nanocomposite showed a notable enhancement in the enzyme-biosensor performance and has good potential in the determination of phenolic compounds in industrial applications (Abd Manan et al., 2016).

In the fabrication of a high-performance electrochemical uric acid analysis system, methylcellulose/graphene oxide/iron oxide nanocomposite (MC-GO-Fe3O4) was prepared and coated onto a modified glassy carbon electrode (GCE). MC was used to immobilize active molecules (Fe_3O_4) for better adsorption, meanwhile, graphene acted as a catalyst to improve electrocatalytic activity and to advance the electron transfer between the uric acid analyte and GCE during the reaction. The electrooxidation of uric acid was evaluated by differential pulse voltammetry (DPV) and cyclic voltammetry (CV) methods at a scan rate of 50 mV s^{-1}. During the oxidation of uric acid, a significant decrease in potential and increase in current (0.24 V) were observed. In a linear concentration range of uric acid from 0.5 μM to 140 μM, the LOD of 0.17 μM with good sensitivity of 0.9093 was achieved. indicating that the modified GCE has good potential as a biosensor to detect uric acid and could be applied in the clinical analysis (Sohouli et al., 2019).

Besides nanocrystalline and MC, HPMC also has been used as a sensing material in the humidity sensor. An optical fiber Fabry-Perot interferometer (FPI) relative humidity (RH) sensor was invented using hollow-core fiber (HCF) and hydroxypropyl methylcellulose (HPMC) hydrogel film. The HPMC hydrogel was formed due to the

swelling property and its ability to absorb water. Besides swelling, good hygroscopicity, good adhesion, and biocompatibility are the few factors that made HPMC a suitable candidate as humidity-sensitive material. In the range of 40 – 99 % RH at constant temperature (29 °C) and humidity, HPMC hydrogel exhibited a fast response time of 2.25 s and a good recovery time of 3.15. Principally, when the RH decreased, the water content of HPMC and the thickness of the hydrogel film reduced, hence causes the shifting of resonance wavelength to the short-wave direction. As the RH increased, the reflection spectrum of the sensor shifted to the long-wave direction. The proposed sensor successfully developed with fast response time and recovery time (Li et al., 2019).

Table 2.4: A list of cellulose-based sensors

Cellulose sensor	Technique	Analyte	LOD	References
Nanocrystalline cellulose/chitosan composite film	Chronoamperometric	Phenol	0.38 µM	Abd Manan et al., 2016
Methylcellulose/graphene oxide/iron oxide nanocomposite	Cyclic voltammetry	Uric acid	0.17 µM	Sohouli et al., 2019
Hollow-core fiber and hydroxypropyl methylcellulose hydrogel film	Optical fiber demodulator	Humidity	-	Li et al., 2019

2.6 Development of Sensor for Hydrazine Detection

In the industrial fields, hydrazine has been used extensively in various productions such as in the manufacture of azo compounds, pesticides, rocket fuel propellants, oxygen scavenger, car airbags, and pharmaceutical drugs (Arulraj et al., 2015; Schirmann & Bourdauducq, 2012; Sinha et al., 2015; Tsubakizaki et al., 2009). The exposure to the high concentration of hydrazine may cause health damage to central nervous systems, respiratory systems, and reproductive systems to humans and animals (Sambasevam et al., 2015). According to the National Institute for Occupational Safety and Health (NIOSH), the recommended exposure limit (REL) is 0.03 ppm, NIOSH Immediately Dangerous to Life or Health Concentration (IDLH) is 50 ppm, and the Occupational Safety and Health Administration (OSHA) standard is 1 ppm. Therefore, it is crucial to develop a reliable and highly sensitive sensor to trace the hydrazine level in the environment.

Many methods had been proposed for the determination of hydrazine based on its basic character or reducing property using various analytical techniques such as conductometric (Lange & Mirsky, 2011), colorimetric (Zargar & Hatamie, 2013), electrochemical (Madhu et al., 2014), fluorescence spectroscopy (Sinha et al., 2015), resistivity measurement (Virji et al., 2005; Weiller et al., 2005), and spectrophotometry (Arulraj et al., 2015; George et al., 2008; Sambasevam et al., 2015).

Ulrich Lange and co-worker reported that LOD of 0.5 μM was achieved using nanocomposite of PdNP with PEDOT-PSS as a hydrazine sensor accompanied by a decrease in the conductance. However, this conductometric approach is not suitable for continuous monitoring of analyte concentration because it requires resetting the sensor to its initial potential before determining each concentration (Lange & Mirsky, 2011).

According to Zargar and partner, the colorimetric method also exhibited a good response in the recognition of hydrazine. The colour change was observable with the naked eyes and could be monitored spectrophotometrically. In the presence of hydrazine, gold ions were reduced to gold nanoparticles (AuNPs) as a sensor. This work achieved a good LOD of 1.1×10^{-6} M (Zargar & Hatamie, 2013).

Meanwhile, Rajesh Madhu et al. proposed a simple electrochemical approach to detect hydrazine using a glassy carbon electrode with gold nanoparticles (Au) decorated activated carbon (AC). The LOD of 6.3 nM attained (Madhu et al., 2014). Besides, the fluorescence spectroscopy technique has gained attention in the detection hydrazine. Sougata Sinha et al. suggested that the application of diester derivative based on 1,4-dihydroxyanthraquinone as a probe to trace hydrazine in mushroom cells resulted in a good LOD of 0.06 ppm (Sinha et al., 2015).

Virji and co-workers produced PAni thin films using hexafluoroisopropanol (HFIP) as an additive. The incorporation of the additive into the PAni may enhance the sensitivity during the exposure of hydrazine followed by the changes in resistance. Principally, most of the PAni sensor will produce PAni in the insulating state during hydrazine detection. Oppositely, PAni/HFIP films tend to become more conducting upon exposure to hydrazine because the reaction between PAni/HFIP films and hydrazine produces strong acid as a side-product. The LOD of 3 ppm hydrazine was gained (Virji et al., 2005).

During the detection of hydrazine, PAni will be converted from conducting emeraldine state (ES) to insulating leucoemeraldine state (LE) of PAni associated with the change in conductivity values as shown in **Figure 2.2.**

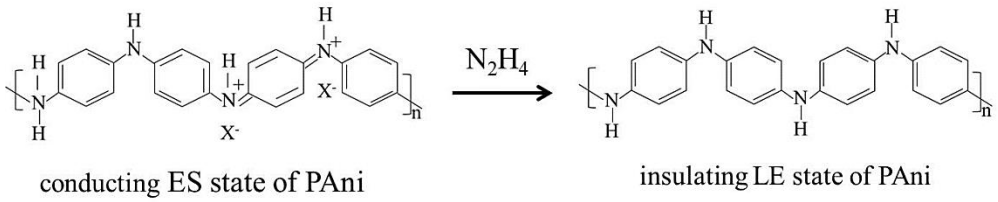

Figure 2.2: Conversion of emeraldine PAni to leucoemeraldine PAni with hydrazine (Virji et al., 2005).

The improvement of PAni in nanofiber size for hydrazine detection has been studied by Weiller and partners. The PAni nanofiber was fabricated through the chemical oxidation method in an immiscible organic/aqueous two phases system and was purified by the dialysis process. The organic solvents hexafluoroisopropanol (HFIP) and N-methylpyrrolidinone (NMP) were used. The smaller diameter of PAni nanofiber (30 – 50 nm) provides higher surface area and higher porosity that may result in a shorter time within ~2 s for the hydrazine to diffuse in the PAni sensor, eventually increases the sensor performance (Weiller et al., 2005).

Among the analytical techniques, spectrophotometry has received considerable attention because of its excellent sensitivity and relatively inexpensive instrumentation, rapid response time, easy operation, and can detect at low concentration levels of hydrazine (Arulraj et al., 2015; George et al., 2008). Based on reducing property of hydrazine, electrochemical techniques have been more popular than spectroscopic analyses but there are some drawbacks exhibited such as large over-potentials, lack of long-term stability, low sensitivity, expensive and complicated instruments (Arulraj et al., 2015).

Mary George and co-workers had developed a highly sensitive sensor for hydrazine detection. 2,4-dinitrochlorobenzene was used to react with hydrazine in the presence of sodium acetate under the boiling condition to form 2,4-dinitrophenylhydrazine. The LOD of 0.21 μg was obtained (George et al., 2008). The same analytical technique has been used by Arulraj et.al. in fabricating a very simple and rapid sensor for the determination of the pico-molar level of hydrazine using Alizarin red through spectrophotometry method. The LOD of 0.66 pM was achieved (Arulraj et al., 2015).

Besides, Sambasevam et.al has proposed a very simple and cost-effective PAni thin film doped with a dioctyl sodium sulfosuccinate (AOT) sensor for hydrazine detection. The sensor response was also evaluated by spectrophotometry. This material showed good sensitivity and a good LOD of 0.49 ppm (Sambasevam et al., 2015).

Table 2.4 showed a summary of previous works in hydrazine detection for the past few years. Among all the techniques, the resistivity method was used in this study. Although it is a conventional technique, it possesses some advantages such as analyte detectable at low concentration, facile method, and economical instrument (Bott & Jones, 1984).

Table 2.4: A summary of previous works in hydrazine detection.

Technique	Material	LOD	References
Conductometric	Palladium nanoparticles and PEDOT-PSS	0.5 μM	Lange & Mirsky, 2011
Colorimetric	Gold nanoparticles (AuNPs)	1.1×10^{-6} M	Zargar & Hatamie, 2013
Electrochemical	Gold nanospheres/activated carbon nanocomposite	6.3 nM	Madhu et al., 2014
Fluorescence	Diester derivative based on 1,4-dihydroxyanthraquinone as probe	0.06 ppm	Sinha et al., 2015
Resistivity	PAni thin films processed from HFIP	3 ppm	Virji et al., 2005
Resistivity	PAni nanofiber	3 ppm	Weiller et al., 2005
Spectrophotometry	2,4dinitrochlorobenzene in the presence of sodium acetate	0.21 μg	George et al., 2008
Spectrophotometry	Alizarin red S	0.66 pM	Arulraj et al., 2015
Spectrophotometry	PAni thin film with AOT dopant	0.49 ppm	Sambasevam et al., 2015.

CHAPTER 3: METHODOLOGY

3.1 Chemicals and Materials

Aniline (Ani, 99.5 %), ammonium persulfate (APS, 98 %), methylcellulose (MC), hydroxypropyl cellulose (HPC), and hydroxypropyl methylcellulose (HPMC) were purchased from Sigma-Aldrich, USA. Hydrochloric acid (HCl, 37 %) was supplied by RCI Labscan Sdn. Bhd, Thailand. Hydrazine hydrate (80 % in water) was attained from MERCK, Germany. For the interference study, 2-propanol (99.7 %), formic acid (FA, 98 %), sodium hydroxide (NaOH, 99 %), and ammonia (25 %) were purchased from Merck. All chemicals were used as received without further purification. Dialysis tubing with 14kDa molecular weight cut-off (MWCO) and an average flat width of 25 mm was purchased from Sigma-Aldrich, USA. Distilled water used was obtained from the water distillation set in the laboratory.

3.2 Apparatus

The apparatus such as beaker, measuring cylinder, magnetic stirrer, hot plate, thermometer, spatula, weighing paper, dropper, icebox, retort stand, dropping funnel, dialysis tube, thread, petri dish, and UV cuvette cells were used throughout this research study for polymer synthesis. Another set of apparatus such as volumetric flasks, measuring cylinders, pipettes, sample vials, syringes, and syringe filters (with a diameter of 25.00 mm and pore size of 0.22 μm) were used for hydrazine sensor application.

3.3 Synthesis of Water-soluble PAni

As shown in **Figure 3.1**, water-soluble PAni was synthesized by the chemical oxidation method using Ani as a monomer, MC as a steric stabilizer, HCl as a dopant, and APS as an initiator. In this study, water-soluble PAni was synthesized using different synthesis parameters with three different types of cellulose derivatives (**Figure 3.2**), and different monomer ratios.

The main criteria in the selection of cellulose derivatives (MC, HPC, and HPMC) is their properties as water-soluble polymer residing hydrophilic side groups (hydroxyl group) in the chemical structure. The hydroxyl groups of cellulose derivatives provide a lone pair of electrons to form hydrogen bonding with water molecules (Glass, 2000). Besides, they can improve the properties of PAni in terms of electrical conductivity, chemical stability, and biodegradability of PAni (Abd Manan et al., 2016; Barik et al., 2010; Casado et al., 2012).

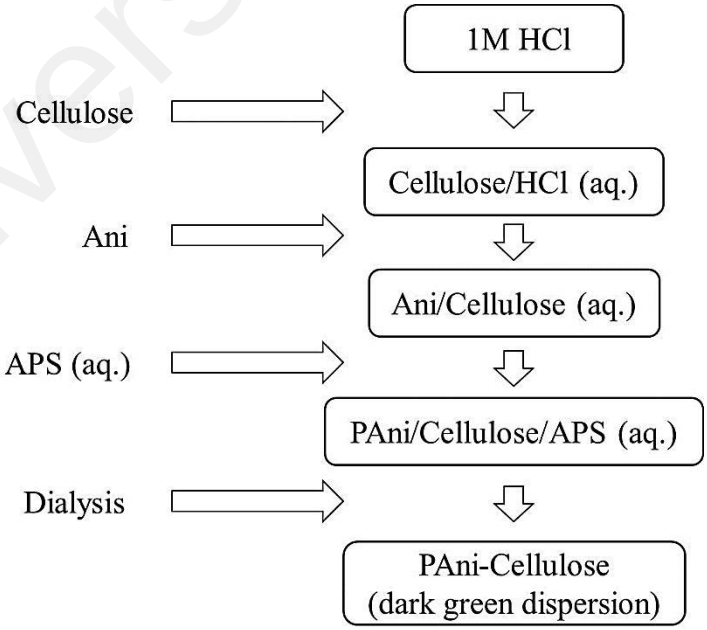

Figure 3.1: Preparation of water-soluble PAni via chemical oxidation method.

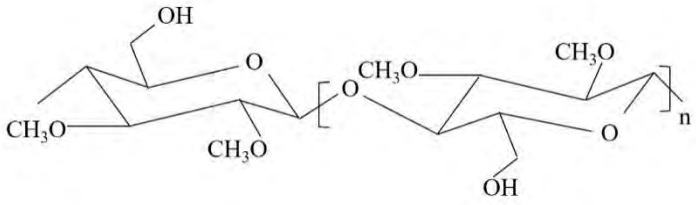

(a) MC

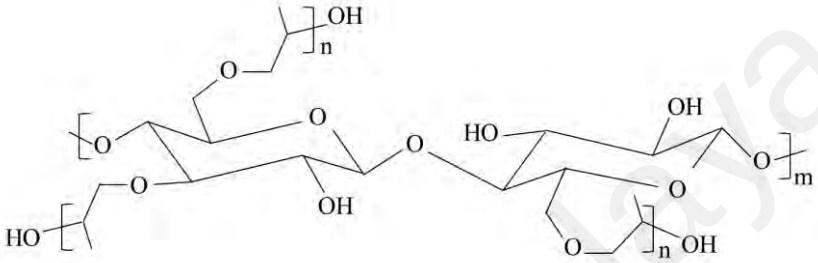

(b) HPC

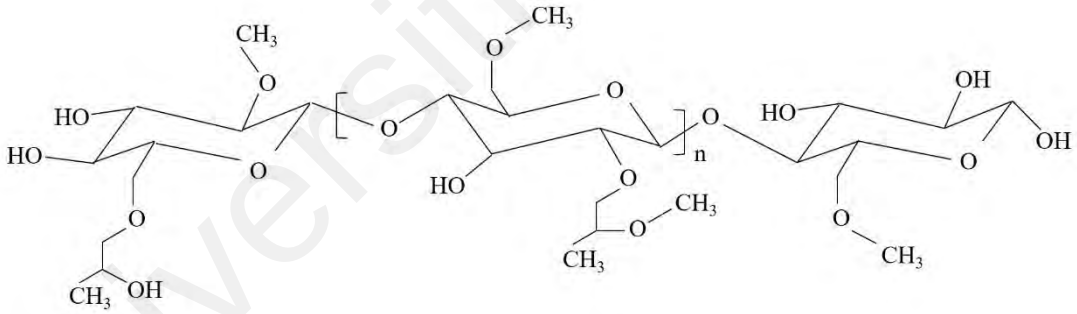

(c) HPMC

Figure 3.2: Chemical structure for different types of cellulose derivatives; (a) MC, (b) HPC, and (c) HPMC.

Initially, 1 M of HCl heated to 80 ˚C and MC (0.500 g) was added and stirred until getting a homogeneous solution of MC/HCl. The MC/HCl solution was cooled in an ice bath at 0 ˚C, then Ani (0.101 g) was dropped wisely under continuous stirring for 3 hours. Then, APS (0.210 g) aqueous solution was added slowly into the Ani/MC/HCl

solution to initiate polymerization. The polymerization was carried out at a specified temperature (0 °C) for 24 hours. The molar ratio of Ani: APS was kept to 1:1 as well as the mass ratio of MC: Ani was maintained at 1:0.2. After that, PAni was purified through a dialysis method using 1 M of HCl as dialysate. The purification process was carried out for 6 hours to remove the unreacted monomer, cellulose, APS, HCl, and oligomers. Finally, the dark green water-soluble PAni-MC dispersion was collected. The concentration of water-soluble PAni was calculated based on mass percentage (w/w %) using **Equation 3.1**.

$$\%\frac{w}{w} = \left(\frac{(Z-X)}{(Y-X)}\right) \text{ X } 100\ \% \qquad \textbf{(Equation 3.1)}$$

where;

X = mass of an empty petri dish

Y = mass of wet PAni and petri dish

Z = mass of dry PAni and petri dish

The same procedure was repeated to synthesize water-soluble PAni with different types of cellulose derivatives; HPC and HPMC (**Table 3.1**) by using the similar molar ratio of Ani: APS (1:1) and the mass ratio of cellulose: Ani (1:0.2).

Table 3.1: Different types of cellulose derivatives used to synthesize water-soluble PAni.

Samples	Cellulose Derivatives (g)	Ani (g)	APS (g)
PAni-MC	0.500	0.101	0.210
PAni-HPC	0.500	0.101	0.210
PAni-HPMC	0.500	0.101	0.210

The research work was continued for the variation of PAni-MC ratio based on the best performance towards hydrazine detection. PAni-MC with the different mass ratios of Ani: MC was synthesized following a similar procedure as shown in **Figure 3.1**. Besides, the amount of APS was adjusted to maintain the molar ratio of Ani: APS at 1:1. The different mass ratios of Ani: MC: APS was tabulated in **Table 3.2.**

Table 3.2: Different mass ratio of Ani: MC: APS used to synthesize water-soluble PAni.

Mass ratio Ani: MC	Ani (g)	MC (g)	APS (g)
0.1 : 1	0.050	0.500	0.105
0.2 : 1	0.101	0.500	0.210
0.5 : 1	0.251	0.500	0.525
1 : 1	0.500	0.500	1.047

3.4 Characterization of Water-soluble PAni

Water-soluble PAni that was synthesized with different types of cellulose derivatives were characterized using FTIR-ATR spectrometer, UV-Vis spectrophotometer, and conductivity meter.

3.4.1 Fourier-Transform Infrared (FTIR) Spectrometer

Infrared (IR) spectrometry is one of the crucial analytical techniques to investigate the absorption spectrum, functional groups, and the chemical structure of a molecule. Almost the molecules that consist of covalent bonds absorb different frequencies of electromagnetic radiation in the IR region. Each type of bond can be characterized

based on the absorption region. There are two types of IR spectrometers; dispersive and Fourier transform (FT) instruments. Both types provided absorption at wavenumber range of 4000 to 400 cm^{-1}. However, FT exhibits more advantages over dispersive such as high sensitivity, fast, and better signal-to-noise ratio of the spectrum (Pavia et al., 2009).

Attenuated Total Reflectance (ATR) is an IR sampling technique that performs by measuring the changes that happen in an internal reflected IR radiation when radiation in contact with the sample. ATR method gives great quality and the finest possible reproducibility of the data with faster sampling. ATR can analyze both solid and liquid sample including highly absorbing samples, surfaces, and thin-film (Grdadolnik, 2002; Perkin Elmer, 2005). A solid or liquid sample must be conducted near the optical element to ensure the IR beam is internally reflected and the sample contacts with the evanescent wave (Grdadolnik, 2002).

In this study, the chemical structures of water-soluble PAni were investigated using FTIR-ATR spectrometer (Perkin Elmer RX 1 model) in the wavenumber range of 400 to 4000 cm^{-1} at room temperature. PAni was dried in the oven at 80 °C for 24 hours. The dried PAni was placed on the surface of the ATR crystal. The holder was clamped with a strong force to have good optical contact between PAni and ATR crystal, thus producing an excellent spectrum. **Figure 3.3** displays the internal reflection of the ATR system during FTIR analysis for PAni. At a certain angle, an IR beam is reflected onto the ATR crystal and creates an evanescent wave that penetrates PAni. The evanescent wave will be attenuated when the PAni absorbs energy from the IR beam. Later, the attenuated wave will be directed to the IR detector and produces an IR spectrum (Perkin Elmer, 2005).

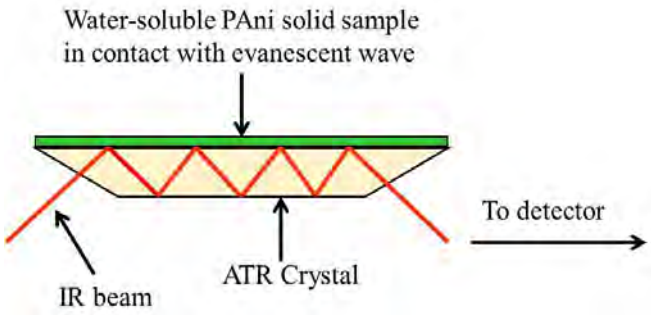

Figure 3.3: The internal reflection of the ATR system during FTIR analysis for PAni (Perkin Elmer, 2005).

3.4.2 Ultraviolet-Visible (UV-Vis) Spectrophotometer

Ultraviolet-visible (UV-Vis) spectrophotometer is the oldest analytical instrument that commonly used to analyze chemical behaviour and functional groups using visible light. Besides, UV-Vis also can be used in the determination of unknown concentration, identification of unknown compounds, detection of purity of substances, investigation of reaction kinetics, both quantitatively and qualitatively (RSC, 2009). The wavelength range from 190 nm to 800 nm of UV-Vis light has a particular energy to excite an electron (e^-). When the sample absorbs energy, the e^- will be excited from the highest occupied molecular orbital (HOMO) to the lowest unoccupied molecular orbital (LUMO), resulting in absorption of the spectrum. This electronic transition is depended on the types of orbital; sigma (σ) orbital, pi (π) orbital, nonbonding (n) orbital, and antibonding orbitals (π^* and σ^*) (Pavia et al., 2009; RSC, 2009).

In this research, the electrical conducting behaviours of water-soluble PAni-cellulose derivatives were identified using a UV-Vis spectrophotometer (Shimadzu UV-1650 PC model) in the wavelength range of 300 nm to 900 nm at room temperature. The sample

was prepared by diluting the water-soluble PAni with certain dilution factor (DF) in HCl solution to get a transparent solution and to reduce the noise during measurement. The DF was calculated using **Equation 3.2**. 1 M of HCl was used as a blank and the results were recorded as absorbance against wavelength.

$$\textbf{Dilution factor (DF)} = \frac{C_1}{C_2} = \frac{V_1}{V_2} \qquad \textbf{(Equation 3.2)}$$

where;

C_1 = initial concentration

C_2 = final concentration

V_1 = initial volume

V_2 = final volume

3.4.3 Electrical Conductivity Measurement

Electrical conductivity (EC) measurement is a measure of the capability of an aqueous solution, a metal, or a gas to conduct electrical current using conductivity meter. It is a quick, reliable, high sensitivity, and relatively low-cost measurement. Therefore, it has been used widely to determine the level of water impurities especially for domestic utilization and industrial need. For example, in the water treatment, clean in place (CIP), desalination, and quality control purposes (Eutech Instruments, 2014; Radiometer Analytical SAS, 2004; Rosemount Analytical Inc., 2010).

According to Ohm's law in **Equation 3.3**, conductance (G) can be defined as the inverse of resistance (R) as the alternating current (I) over the voltage (E) is applied to the electrodes that immersed in the solution. The R is determined from the voltage and

current values. The unit for conductance is the Siemens ($S = \Omega^{-1}$) or formally mho unit (Eutech Instruments, 2014; Radiometer Analytical SAS, 2004; RSAS, 2000).

$$G = \frac{1}{R} = \frac{I \text{ (amperes, A)}}{E \text{ (volts, V)}} \qquad \textbf{(Equation 3.3)}$$

In this study, the electrical conductivity of water-soluble PAni-cellulose derivatives was measured using conductivity meter (Eutech Instruments pc-510) at room temperature by immersing the conductivity probe in water-soluble PAni (**Figure 3.4**). A similar PAni from UV-Vis preparation was used in this analysis. The unit for all measurements is Siemens per centimeter (S/cm).

3.5 Application of Water-soluble PAni for Hydrazine Detection

In this study, the responses of hydrazine in water-soluble PAni-cellulose derivatives were monitored through electrical conductivity measurement. Before hydrazine detection, the conductivity probe was immersed into water-soluble PAni dispersion and the reading was recorded as initial conductivity (σ_i) as shown in **Figure 3.4 (a).** The same procedure was repeated for the combination of water-soluble PAni with various concentrations of hydrazine to get the readings after adding hydrazine as shown in **Figure 3.4 (b).** The readings were recorded as final conductivity (σ_f). The normalized conductivity of this sensor was calculated using **Equation 3.4.**

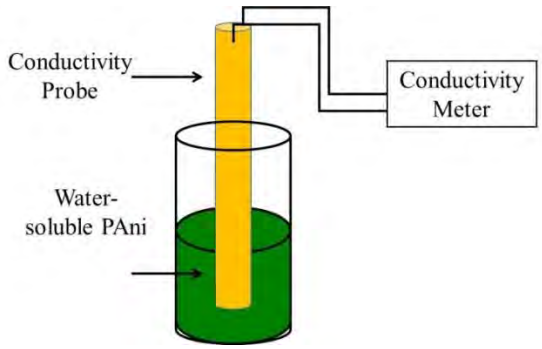

(a) Before hydrazine detection (σ_i)

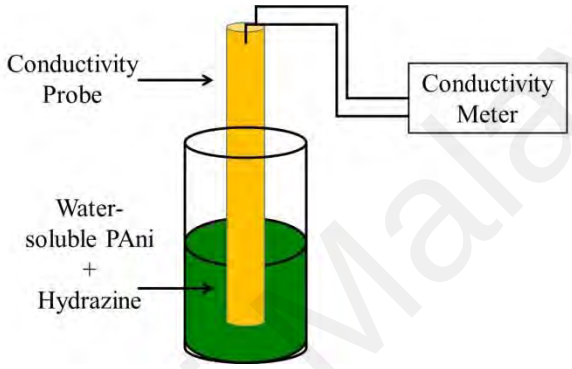

(b) After hydrazine detection (σ_f)

Figure 3.4: Conductivity measurement for water-soluble PAni (a) before (σ_i) and (b) after (σ_f) hydrazine detection.

$$\text{Normalized conductivity} = \frac{\sigma_f}{\sigma_i} \qquad \textbf{(Equation 3.4)}$$

Initially, the application of water-soluble PAni as a sensor was focused on hydrazine detection in the concentration range of 10 ppm to 100 ppm. The sensitivity and correlation determination (R^2) was manipulated using different parameters such as different volume ratio of water-soluble PAni-MC to hydrazine used; 1:5, 2:5, 5:5, 10:5, and 15:5 (**Table 3.3**), different types of cellulose derivatives; MC, HPC, and HPMC (**Table 3.1**), different mass ratio of Ani to MC; 0.1:1, 0.2:1, 0.5:1, and 1:1 (**Table 3.2**),

and different concentration range of hydrazine (1 ppm to 10 ppm). Throughout this study, the volume of hydrazine used was fixed in 5 mL.

Table 3.3: Different volume ratio of PAni-MC: hydrazine used to find the optimum volume of water-soluble PAni that can potentially react with hydrazine.

Volume ratio PAni-MC: Hydrazine	Volume of PAni-MC (mL)	Volume of hydrazine (mL)
1 : 5	1	5
2 : 5	2	5
5 : 5	5	5
10 : 5	10	5
15 : 5	15	5

The sensor performances of water-soluble PAni as hydrazine sensor were evaluated in terms of sensitivity, accuracy, the limit of detection (LOD), the limit of quantitation (LOQ), R^2, interference study, and real sample analysis. The LOD, LOQ, and standard deviation (SD) were calculated using **Equation 3.5**, **Equation 3.6,** and **Equation 3.7** respectively. For real sample analysis study, three different matrices were used; tap water from Polymer Research Laboratory (Chemistry Department, University of Malaya), drain water from Pengkalan Chepa Industrial Area (Kelantan), and mineral drinking water (brand: Spritzer). The known concentration of hydrazine was spiked into the real water samples for further investigations. The recovery and relative standard deviation (RSD) values of water-soluble PAni were analyzed at the end of this study.

The chemical interaction between water-soluble PAni and hydrazine during hydrazine detection was investigated using FTIR and UV-Vis analysis as the supporting data. Based on our knowledge, none of the research investigated the detailed proposed

mechanism between the analyte and water-soluble PAni as a sensor during chemical detection and firstly reported in this study. The summary of this research study was displayed in **Figure 3.5.**

$$\mathbf{LOD = 3\ x\ \left(\frac{SD}{k}\right)} \qquad \textbf{(Equation 3.5)}$$

$$\mathbf{LOQ = 10\ x\ \left(\frac{SD}{k}\right)} \qquad \textbf{(Equation 3.6)}$$

$$\mathbf{Standard\ Deviation\ (SD) = \sqrt{\frac{\Sigma\ (X\text{-}X'')^2}{N}}} \qquad \textbf{(Equation 3.7)}$$

where;

SD = standard deviation of the calibration curve

k = slope of the calibration curve (sensitivity)

Σ = the sum of squared deviations

X = each value in the data set

X" = mean of all values in the data set

N = number of values in the data set

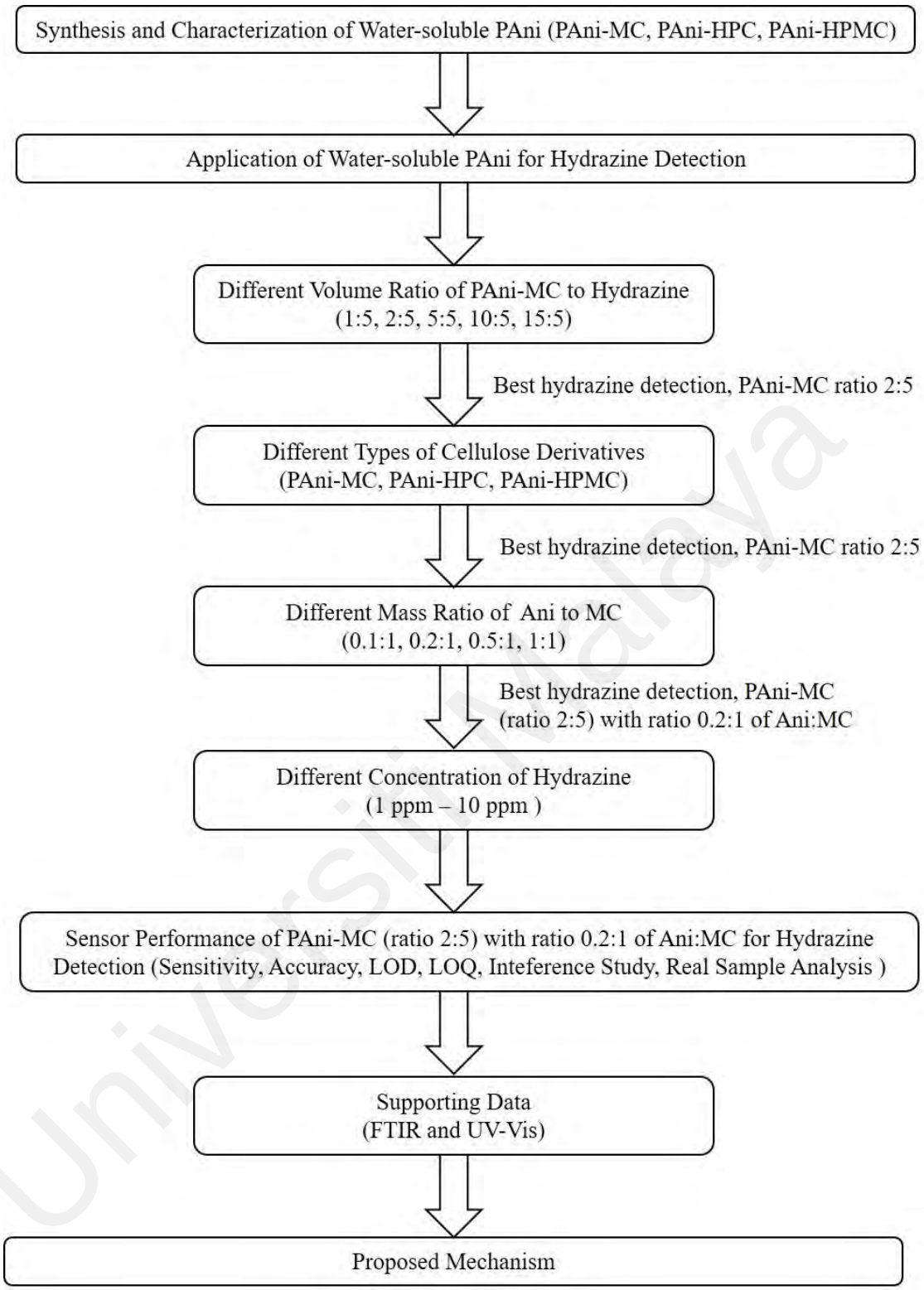

Figure 3.5: The summary of this research study.

CHAPTER 4: RESULTS AND DISCUSSION

4.1 Water-soluble PAni-cellulose Derivatives

4.1.1 FTIR Analysis

Figure 4.1, **Figure 4.2,** and **Figure 4.3** show the FTIR spectra for pristine PAni, cellulose derivatives (MC, HPC, and HPMC), PAni-MC, PAni-HPC, and PAni-HPMC. The discrete peaks of each functional group for all PAni were tabulated in **Table 4.1**. Pristine PAni was used as a control to observe the changes in the PAni structure after the incorporation of different types of cellulose derivatives. It can be seen that the three PAni-cellulose derivatives (PAni-MC, PAni-HPC, and PAni-HPMC) possessed the same FTIR pattern due to the similarity in the PAni backbone structures (Rahy et al., 2011).

For all cellulose derivatives, the broad band peaks in the range of 3400 – 3425 cm^{-1} was attributed to the O-H group of cellulose. It can be noticed that HPC and HPMC exhibit strong, broad band peaks (-OH groups) compared to MC because the HPC and HPMC consist of more OH groups than MC (**Figure 3.2**). Besides, the peaks at 2850 – 2920 cm^{-1} were ascribed to the C-H stretching vibration modes of MC, HPC, and HPMC (Barik et al., 2010; Chattopadhyay & Mandal, 1996; Jia et al., 2007). Moreover, the peaks in the range of 1047 - 1060 cm^{-1} were assigned to the C-O stretching vibration modes. All the characteristic peaks of cellulose as discussed above were present in the FTIR spectra of PAni-MC, PAni-HPC, and PAni-HPMC.

Referred to **Figure 4.1 - 4.3**, pristine PAni exhibited the essential characteristic peaks in the FTIR spectrum. The bands at ~3240 cm^{-1} identified as N-H stretching modes. Meanwhile, the bands in the range of 1450 - 1455 cm^{-1} and 1560 – 1585 cm^{-1} were

correlated to the C=C stretching modes of the benzenoid and quinoid ring, respectively. The bands in the range of 1290 – 1310 cm^{-1} were associated with the C-N stretching of PAni (aromatic amine nitrogen) (Barik et al., 2010; Jia et al., 2007). All these peaks were present in the PAni-MC, PAni-HPC, and PAni-HPMC.

For all PAni-cellulose derivatives, there was a significant shift of O-H bands from ~3407 cm^{-1} - 3430 cm^{-1} (cellulose derivatives) to ~3383 cm^{-1} – 3400 cm^{-1} (PAni MC, PAni-HPC, and PAni-HPMC) after the addition of cellulose derivatives into PAni. The intensity of N-H stretching bands for PAni-MC, PAni-HPC, and PAni-HPMC has also become lower than pristine PAni. This happened presumably because the environment at the molecular level has changed due to the formation of intermolecular hydrogen bonding between the N-H groups of PAni and the O-H groups of cellulose derivatives (Bin et al., 2013; Jia et al., 2007; Luong et al., 2013; Yue et al., 2016).

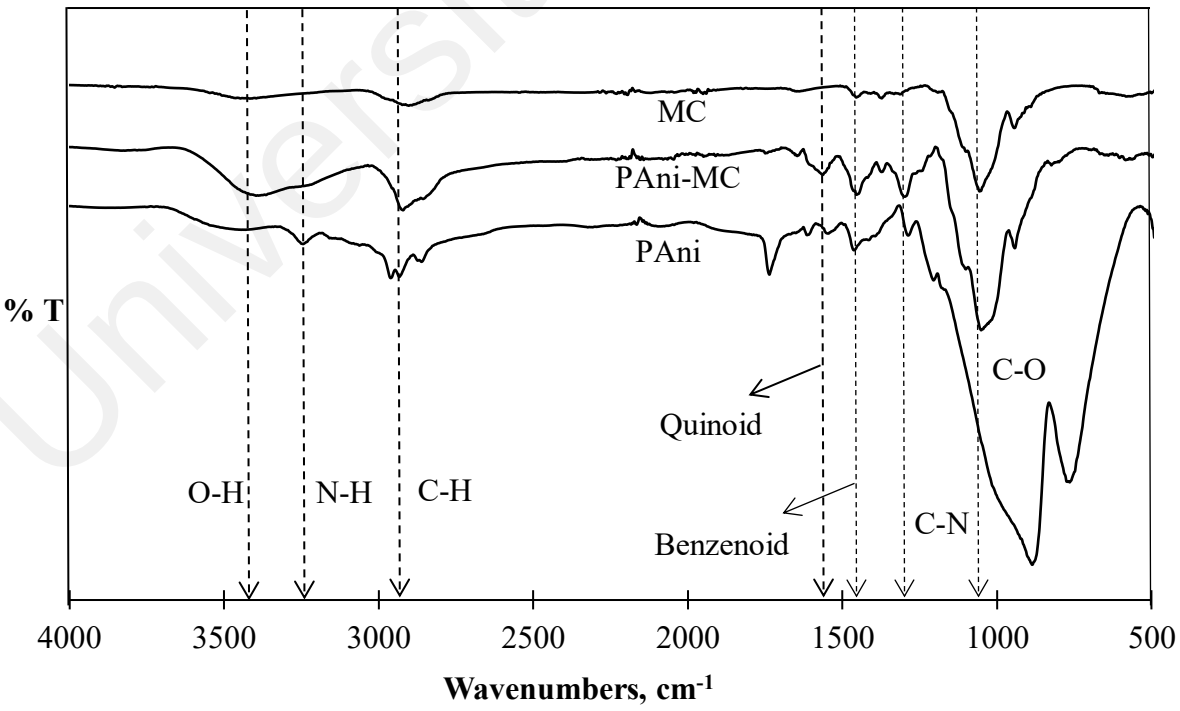

Figure 4.1: FTIR spectra of MC, PAni-MC, and pristine PAni.

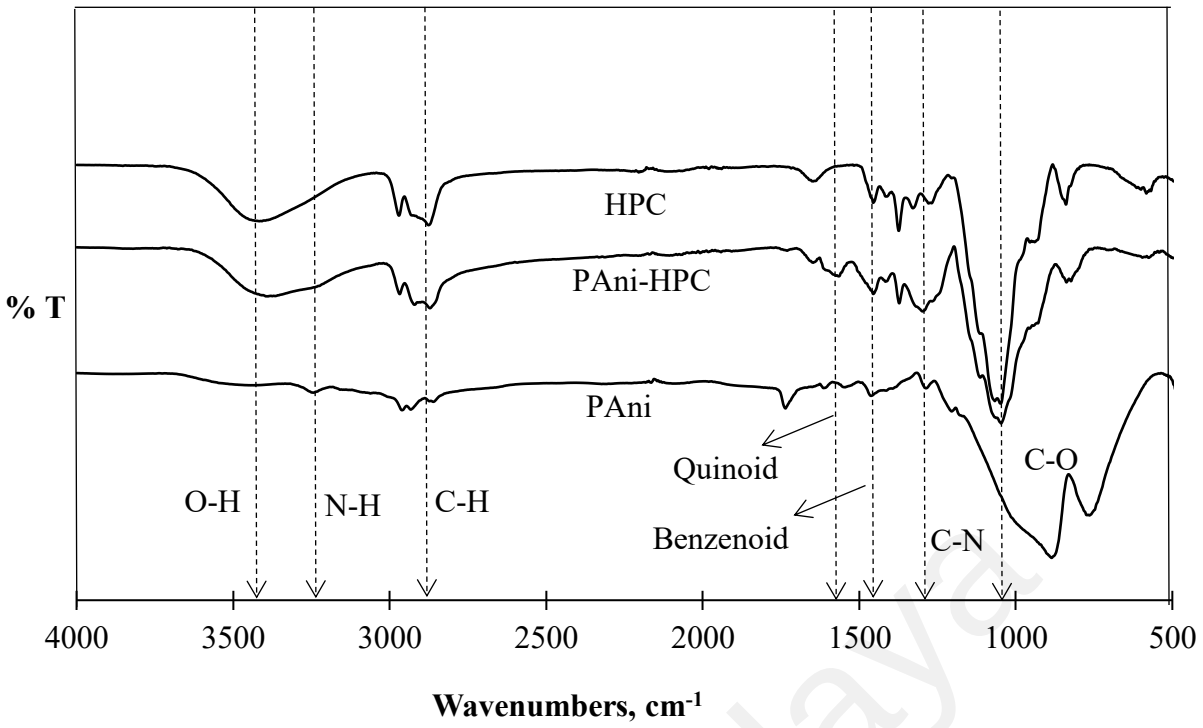

Figure 4.2: FTIR spectra of HPC, PAni-HPC, and pristine PAni.

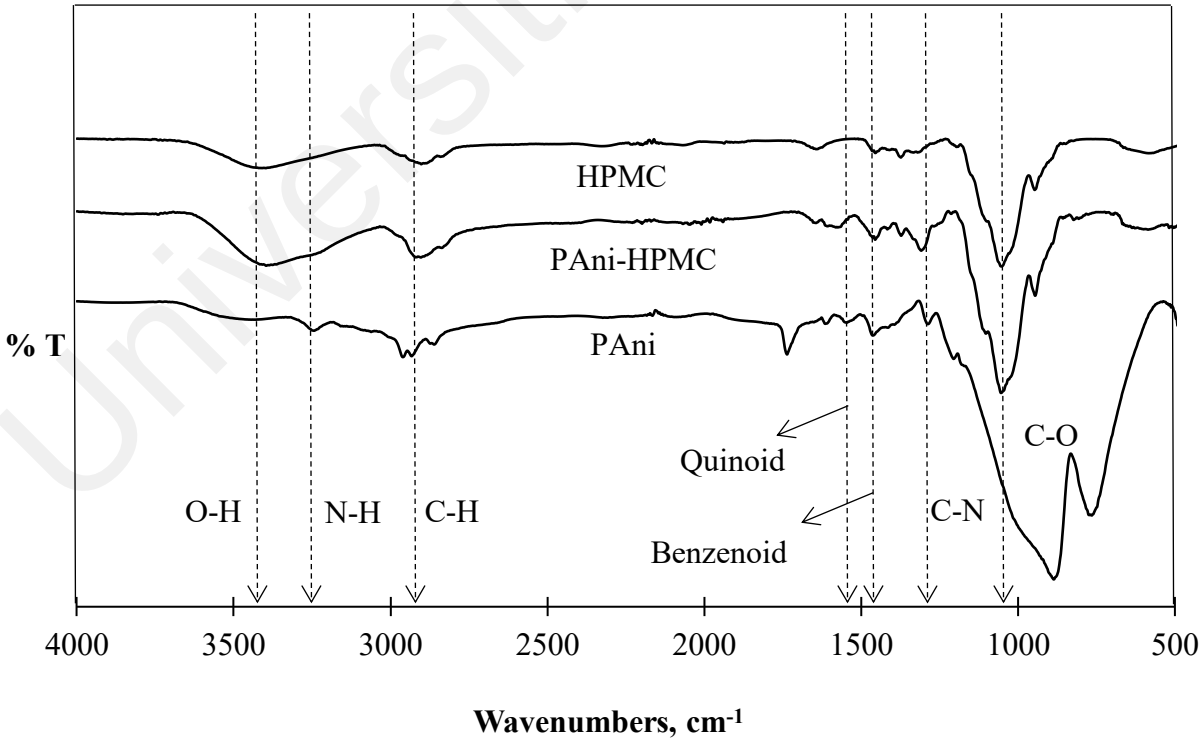

Figure 4.3: FTIR spectra of HPMC, PAni-HPMC, and pristine PAni.

Table 4.1: The characteristic peaks of FTIR spectra for pristine PAni, PAni-MC, PAni-HPC, and PAni-HPMC.

Characteristic peaks	Functional groups	Wavenumbers (cm^{-1})		
		PAni-MC	PAni-HPC	PAni-HPMC
Cellulose	O-H broad band	3400	3385	3383
	C-H stretching	2897	2874	2903
	C-O stretching	1049	1047	1058
PAni	N-H stretching	3187	3189	3195
	C=C quinoid	1560	1563	1561
	C=C benzenoid	1451	1454	1452
	C-N stretching	1298	1297	1299

4.1.2 UV-Vis Analysis

Figure 4.4 displayed UV-Vis spectra for water-soluble PAni-cellulose derivatives and pristine PAni. Principally, emeraldine salt of PAni may exhibit three essential absorption bands at ~350 nm, ~420 nm, and ~820 nm (free carrier tail) as shown by pristine PAni (Hino et al., 2006; Jia et al., 2007; Sambasevam et al., 2015; Shao et al., 2011; Yuan & Kuramoto, 2002). However, all PAni-cellulose derivatives produced two absorption bands only at ~430 nm and ~820 nm.

For all PAni-cellulose derivatives, the first absorption band at ~350 nm which attributed to π- π^* electron transition within the benzenoid ring almost disappeared owing to the interaction between PAni chains and cellulose derivatives (Jia et al., 2007). The disappearance of these peaks was caused by the formation of hydrogen bonding between hydroxyl groups in the steric stabilizer of cellulose with imine or amine groups

of PAni, hence leading to the formation of broad bands around 430 nm (Osorio-Fuente et al., 2014).

The second absorption bands were appeared in the range of 434 – 436 nm which specified as polaron- π^* transition caused by the protonation of the PAni backbone. The third absorption broad bands with free carrier tail were present in the range of 826 – 856 nm, represented the π–polaron transition that belongs to the emeraldine salt (ES) state of PAni and also a feature of CP with metal-like behaviour.

As reported by Jadwiga Laska, ultraviolet-visible-near infrared (UV-Vis-NIR) spectroscopy is an easy and effective method to ascertain the effects of a dopant, a solvent, and a polymer matrix on the conformation of the polymer. From the graph below, the absorption bands around 800 nm show a free-carrier tail which may be extended to the NIR region. Cellulose and its derivatives are rigid and mostly become expanded chains. They own many hydroxyl groups and oxygen atoms so that can form hydrogen bonding with amine groups on the PAni chain thus forcing the PAni to straighten along.

Therefore, PAni-cellulose derivatives give the band extended toward the NIR region indicates an expanded conformation. This conformation makes the PAni-cellulose derivatives coplanar, thus the π-electrons delocalize easily and creates more polaron structures of PAni, finally leading to higher conductivity (Laska, 2004; Patil et al., 2002; Xia et al., 1995). Herein, we can conclude that water-soluble PAni-cellulose derivatives are in an extended conformation (free-carrier tail).

Both characterizations from FTIR and UV-Vis analysis essentially verified the chemical structures of the resulted PAni-cellulose derivatives.

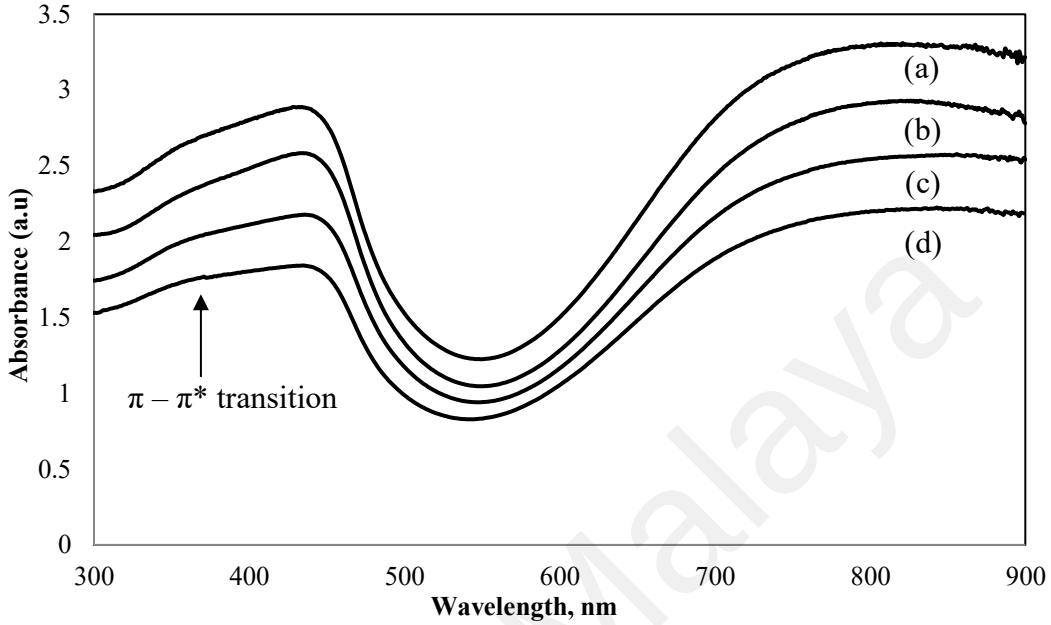

Figure 4.4: UV-Vis spectra for (a) PAni-HPC, (b) PAni-MC, (c) PAni-HPMC, and (d) pristine PAni.

4.1.3 Electrical Conductivity Study

All PAni-cellulose derivatives obtained in this study showed high water solubilities of 17.0 – 20.0 mg/mL (Bin et al., 2013). **Figure 4.5** showed the electrical conductivities of pristine PAni and water-soluble PAni-cellulose derivatives. After the inclusion of cellulose derivatives into PAni, the electrical conductivity increased from 0.068 S/cm for pristine PAni to 0.132 S/cm - 0.146 S/cm for all PAni-cellulose derivatives.

This phenomenon happened because the cellulose derivatives can form hydrogen bonding with PAni, hence contributing to higher delocalizations of charge carriers along the PAni backbone. Besides, these interactions also promoted PAni to disperse well in

the aqueous medium and prevent its aggregation in the reaction system. As a result, the electrical conductivity remarkably enhanced after the incorporation of cellulose derivatives into PAni (Casado et al., 2012; Laska, 2004; Shao et al., 2011).

Besides, many factors influence the conductivity behaviour such as dopant, a medium of preparation, amount of PAni content, and reaction temperature. In this work, 1 M of HCl which acts as a dopant and as a medium of preparation has been used to protonate PAni in the synthesis of water-soluble PAni-cellulose derivatives. This proved that the addition of HCl into PAni notably change PAni into ES state with high electrical conductivity of ~0.068 S/cm to ~0.132 – 0.146 S/cm (Bin et al., 2013; Chattopadhyay & Bain, 2008; Gosh et al., 1999; Shao et al., 2011). The electrical conductivities for all PAni-cellulose derivatives were almost similar, presuming that the types of cellulose do not give a significant effect on the electrical conductivity.

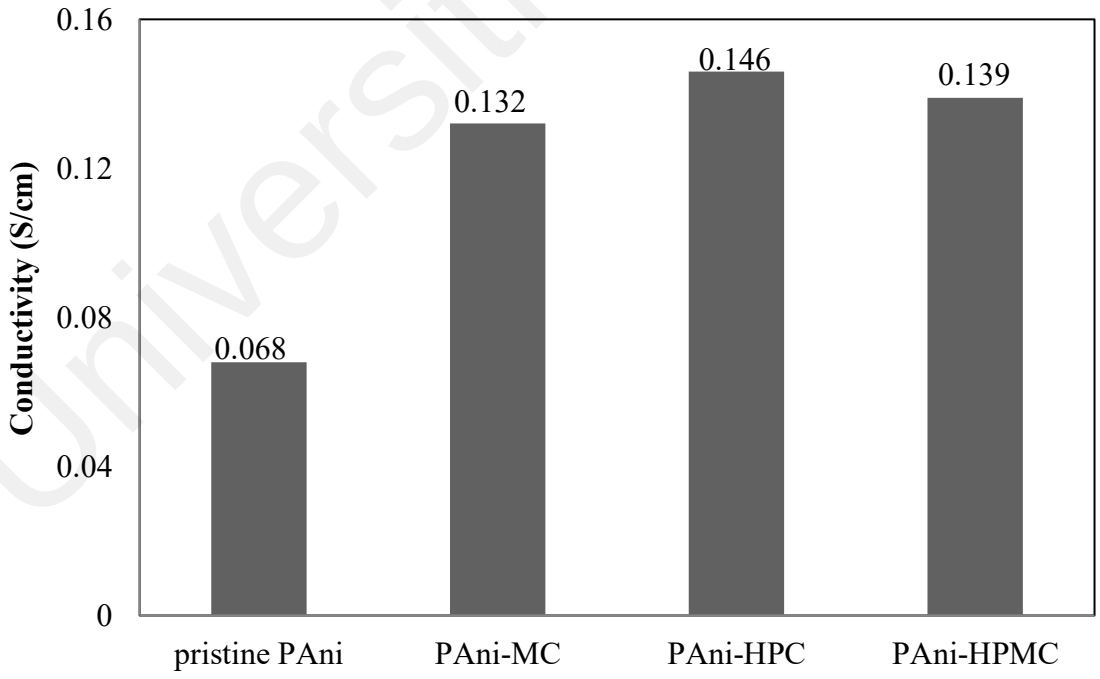

Figure 4.5: The electrical conductivities of pristine PAni, PAni-MC, PAni-HPC, and PAni-HPMC.

4.2 Application of Water-soluble PAni for Hydrazine Detection

4.2.1 Different Volume Ratio of PAni to Hydrazine

The sensor responses of water-soluble PAni in different concentration of hydrazine (10-100 ppm) were monitored through the changes in electrical conductivities as a principal study. **Figure 4.6** showed the normalized conductivities for the different volume ratios of PAni-MC to hydrazine (1:5, 2:5, 5:5, 10:5, and 15:5) against the various concentrations of hydrazine (10 ppm, 30 ppm, 50 ppm, 70 ppm, and 100 ppm). The normalized conductivity for each volume ratio was calculated using **Equation 3.4.** This part aimed to investigate the optimum volume ratio of PAni-MC (as sensing material) that could be possible to detect the hydrazine (as analyte) (Abd Manan et al., 2016).

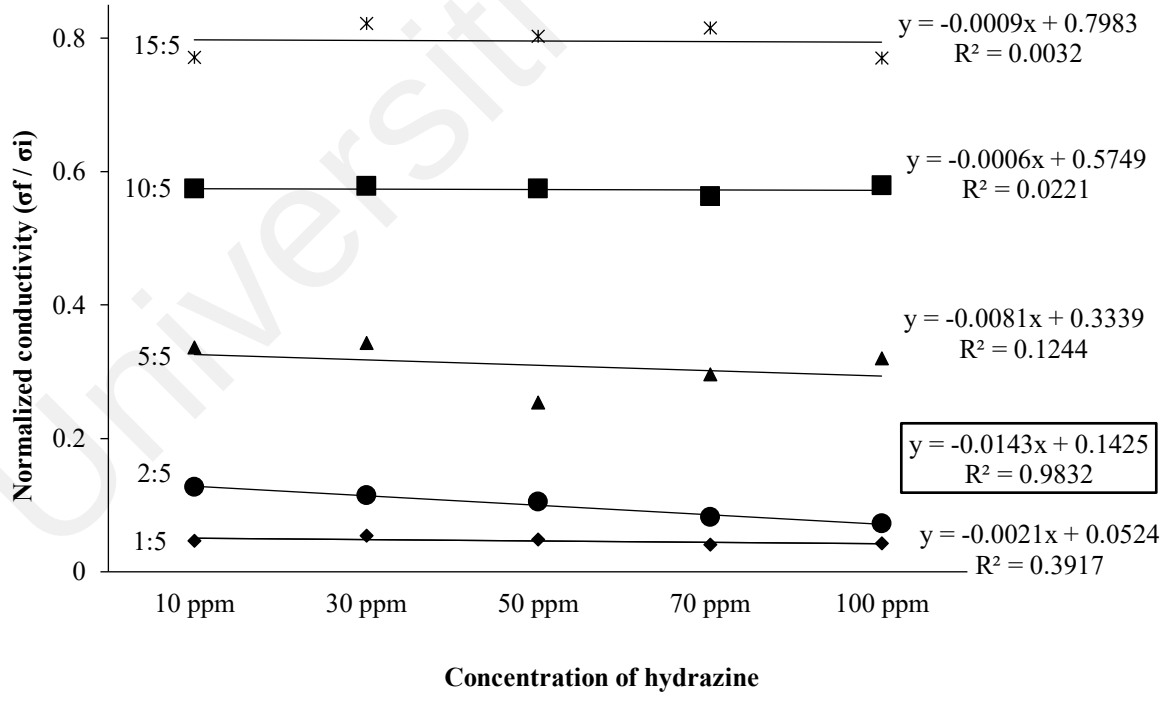

Figure 4.6: Normalized conductivities for the different volume ratios of PAni-MC to hydrazine against the various concentrations of hydrazine (10-100 ppm).

Generally, as depicted in **Figure 4.6**, all PAni-MC: hydrazine with the different volume ratios established a good linear relationship between the normalized conductivities and hydrazine concentrations. The sensitivity and coefficient of determination (R^2) values obtained were summarized in **Table 4.2**.

Table 4.2: The sensitivity and R^2 of PAni-MC: hydrazine with different volume ratios for hydrazine detection.

Volume Ratio (mL) PAni-MC: Hydrazine	Sensitivity (ppm^{-1})	R^2
1:5	0.0021	0.3917
2:5	0.0143	0.9832
5:5	0.0081	0.1244
10:5	0.0006	0.0221
15:5	0.0009	0.0032

As the hydrazine concentration increased from 10 ppm to 100 ppm, the normalized conductivities were reduced. The occurrences could be explained by the oxidation states of PAni. Hydrazine is known as a weak base and strong reducing agent which has an ability to reduce PAni state through the dedoping process. Before the addition of hydrazine, PAni resided in conducting ES state which occupied many free charge carriers. When hydrazine was added into PAni, the dedoping mechanism occurred by reducing the number of free charge carriers at PAni-ES backbone, thus cause the conducting of ES state converted into non-conducting of leucoemeraldine (LE) state (**Figure 4.7**).

As a result, the normalized conductivities were decreased. This condition could be seen apparently at a high concentration of hydrazine owing to the abundance of

hydrazinium ions that could make it to dedope a higher amount of conducting PAni-ES effectively. Therefore, the electrical conductivity becomes drop-off as the increment of hydrazine concentration (Phasuksom et al., 2018; Sambasevam et al., 2015; Stejskal et al., 2012; Virji et al., 2005; Wang et al., 2017).

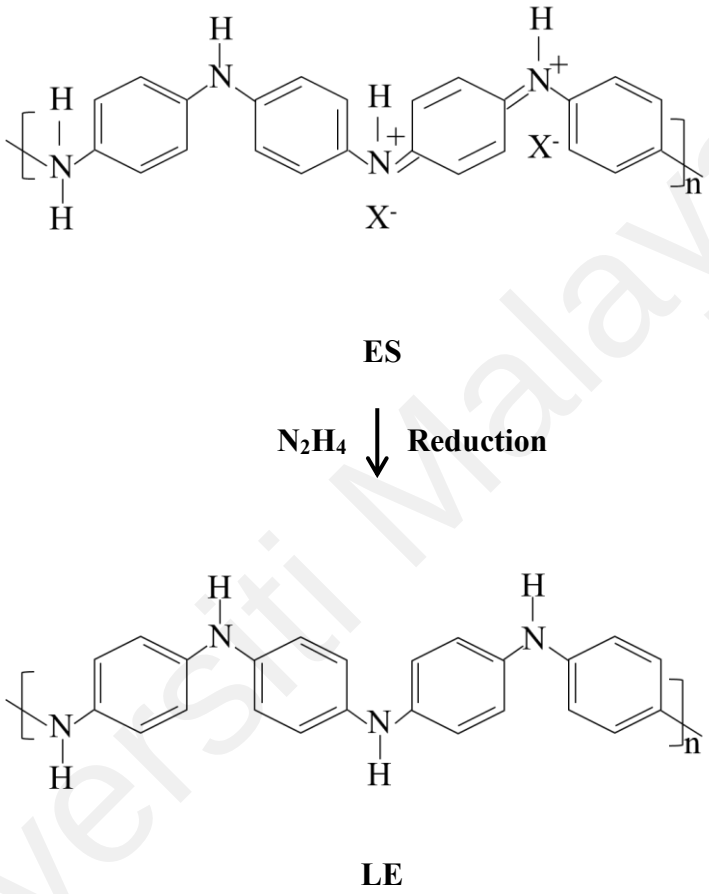

Figure 4.7: Conversion of ES state to LE state of PAni by hydrazine.

Among all the volume ratios used, the ratio 2:5 of PAni-MC: hydrazine possessed the highest sensitivity of 0.0143 ppm^{-1} with good R^2 of 0.9832. This happened because the PAni-MC with ratio 2:5 may provide a sufficient number of reactive sites of PAni (as sensing material), thus generate adequate chemical interaction between PAni and hydrazine. Consequently, the sensitivity of PAni-MC with ratio 2:5 towards hydrazine analyte detection was enhanced. On the other hand, the PAni-MC with ratio 1:5

exhibited a low sensitivity of 0.0021 ppm^{-1} with R^2 of 0.3917 due to the insufficient of reactive sites by PAni for the interaction with hydrazine. Besides, PAni at low concentration may provide more void and free volume of space in which hydrazine analyte moves randomly to access some of the binding sites in PAni's bulk. Finally, it significantly reduced the sensitivity of the sensor for PAni-MC with a ratio 1:5 (Li et al., 2004; Sambasevam et al., 2015).

Meanwhile, as the volume of PAni is 5 mL or more than 5 mL, the sensitivity and the value of R^2 eventually decreased to 0.0081 - 0.0006 ppm^{-1} and 0.1244 - 0.0221, respectively. As the volume of PAni increased, the concentration of PAni also significantly increased. At a higher concentration of PAni, the existence of a high amount of PAni in limited volume may cause the overlapping of the reactive sites. Consequently, it may induce stearic hindrance and block the interaction between PAni and hydrazine. Thus, the number of hydrazine analytes to interact with the binding sites of PAni became fewer, leading to a decrease in the sensitivity for hydrazine detection (Phasuksom et al., 2018).

Among all the volume ratio, the ratio 2: 5 of PAni-MC: hydrazine showed the optimum volume used to interact with hydrazine since it possessed the highest sensitivity of 0.0143 ppm^{-1} with R^2 of 0.9832. In conclusion, the volume ratio 2:5 of PAni: hydrazine will use for the next study of water-soluble PAni with different types of cellulose derivatives for hydrazine detection due to the sufficient number of reactive sites provided by PAni for adequate interaction with hydrazine.

4.2.2 Different Types of Cellulose Derivatives

As discussed in the previous part, the PAni-MC: hydrazine with a ratio of 2:5 produced the best sensitivity of 0.0143 ppm^{-1} and R^2 of 0.9832, hence was selected to study the effect of different types of cellulose derivatives (MC, HPC, and HPMC) used on the sensor performance during hydrazine detection. **Figure 4.8** displayed the normalized conductivities for different types of PAni-cellulose derivatives (PAni-MC, PAni-HPC, and PAni-HPMC) with the different concentrations of hydrazine in the range from 10 ppm to 100 ppm.

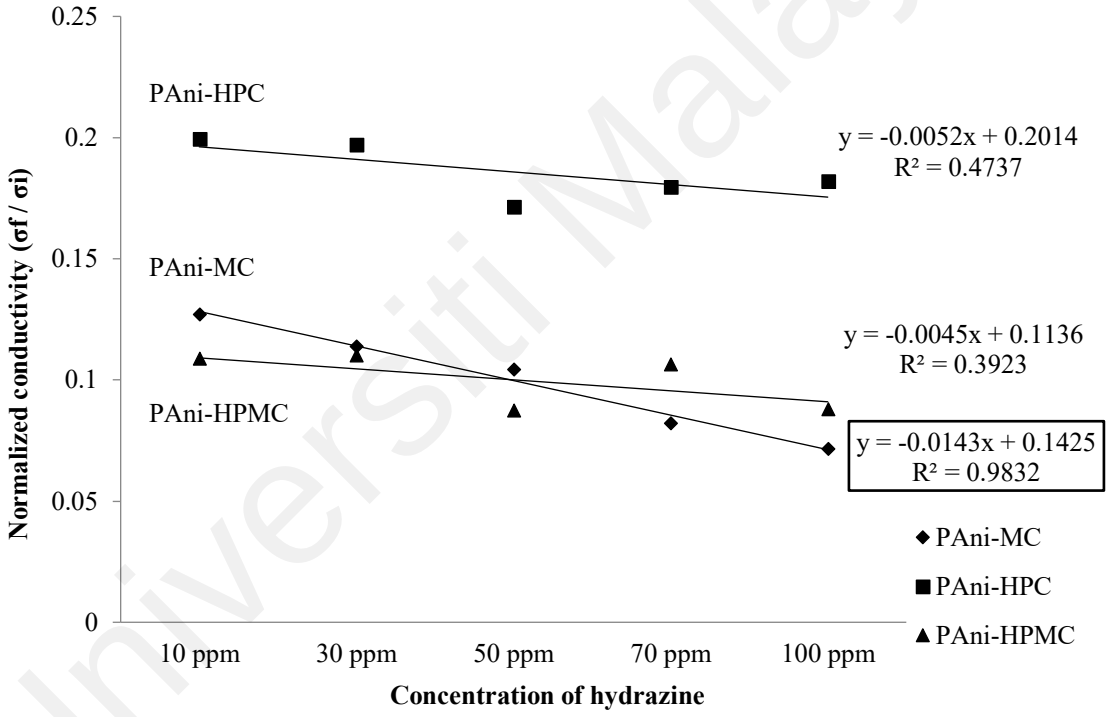

Figure 4.8: Normalized conductivities for PAni with the different types of cellulose derivatives against the various concentrations of hydrazine (10-100 ppm).

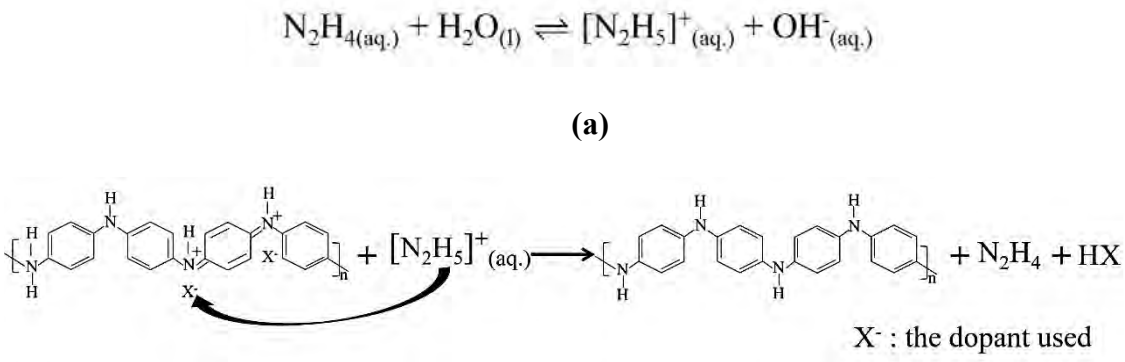

Figure 4.9: The protonation of hydrazine by water (a) and the general mechanism between PAni and hydrazine analyte (b) (Sambasevam et al., 2015; Virji et al., 2004).

All PAni-cellulose derivatives exhibited the decrement in normalized electrical conductivities as the increment of hydrazine concentration from 10 ppm to 100 ppm. This situation could be explained based on the general mechanism above. Before hydrazine detection, hydrazine (N_2H_4) firstly protonated by water to produce hydrazinium ion $[N_2H_5]^+$ as shown in **Figure 4.9 (a)**. During hydrazine detection, the $[N_2H_5]^+$ ion will attack the dopant anion (X^-) along the PAni-ES backbone (conducting state) to produce PAni-LE (non-conducting state), N_2H_4, and HX (**Figure 4.9 (b)**). The details of the proposed mechanism between PAni-cellulose derivatives and hydrazine for this research study will be discussed briefly in **Part 4.4** (Sambasevam et al., 2015; Virji et al, 2004; Wang et al., 2017).

The detection of $[N_2H_5]^+$ ion by PAni-cellulose derivatives will relatively change the conducting ES state of PAni into the non-conducting state of PAni in LE form. Therefore, the higher amount of hydrazine will significantly reduce the electrical conductivities of PAni-cellulose derivatives compare to those with fewer amount of

hydrazine. (Phasuksom et al., 2018; Sambasevam et al., 2015; Virji et al, 2005; Wang et al., 2017).

The sensitivity and R^2 values attained for PAni with different types of cellulose derivatives were tabulated in **Table 4.3**. Among all PAni-cellulose derivatives, the best sensitivity was achieved by PAni-MC (0.0143 ppm^{-1}), followed by PAni-HPC (0.0052 ppm^{-1}), and PAni-HPMC (0.0045 ppm^{-1}). These phenomena could be elucidated based on the interrelation between the PAni backbone with different types of cellulose derivatives that owned distinct molecular structures.

Table 4.3: The sensitivity and R^2 of PAni with the different types of cellulose derivatives for hydrazine detection.

PAni-cellulose derivatives	Sensitivity (ppm^{-1})	R^2
PAni-MC	0.0143	0.9832
PAni-HPC	0.0052	0.4737
PAni-HPMC	0.0045	0.3923

As shown in **Figure 4.10**, all cellulose derivatives connected each other via intramolecular hydrogen bonding and intermolecular hydrogen bonding through hydroxyl groups and aligned in parallel arrangements (Bochek, 2003; Luong et al., 2013; Tayeb et al., 2018). The plausible interactions between PAni and cellulose derivatives for PAni-MC, PAni-HPC, and PAni-HPMC were shown in **Figure 4.11, 4.12,** and **4.13,** respectively.

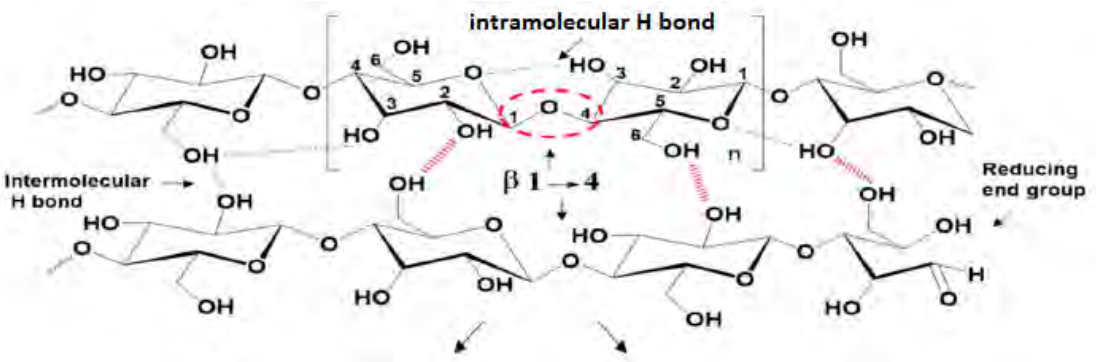

Figure 4.10: The intra- and intermolecular hydrogen bonding of cellulose (Tayeb et al., 2018).

Figure 4.11 showed the proposed interaction between PAni chains and MC. MC structure possessed methyl substituents (**I**) only and not bulky enough to hinder oxygen atom (**II**), thus permitting the formation of strong hydrogen bonding between hydroxyl groups of MC with amine groups of PAni. Besides, MC existed in fibrillar structure and oriented in parallel form, thus the reactive sites of MC were more opened in an extended form. As a result, PAni chains and MC were connected very well for intramolecular and intermolecular hydrogen bonding with opened and exposed binding sites, thus allowing hydrazine analytes to bind easily and effectively without affected by steric hindrance of methyl groups. Therefore, the responsiveness of PAni-MC as sensing material towards hydrazine analytes was enhanced and exhibited the best sensitivity than PAni-HPC and PAni-HPMC (Bochek, 2003; Bodvik et al., 2010; Li et al., 2007).

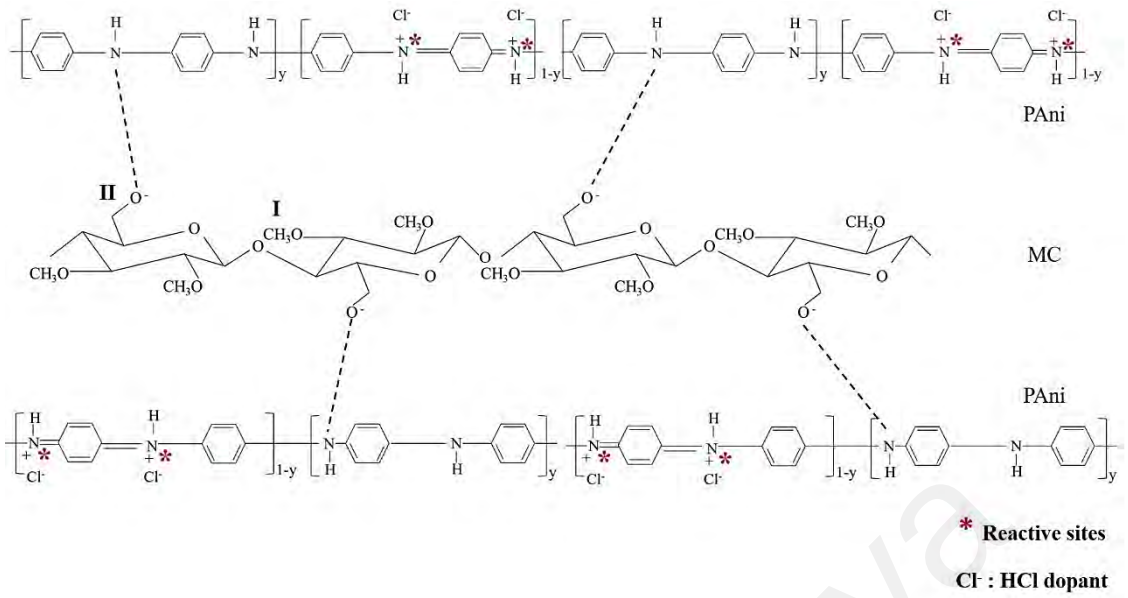

Figure 4.11: The proposed interaction between PAni and MC.

The vice versa situation happened for PAni-HPC and PAni-HPMC. PAni-HPC (**Figure 4.12**) exhibited hydroxypropyl substituents meanwhile PAni-HPMC (**Figure 4.13)** generated both methyl and hydroxypropyl substituents. The presence of hydroxypropyl and methyl substituents in the cellulose derivatives structures (HPC and HPMC) significantly affected the intermolecular hydrogen bonding between hydroxyl groups of cellulose and amine groups of PAni. The hydroxypropyl groups (**III**) in both HPC and HPMC exhibit hydrophobic character which are bulkier than the methyl groups (**I**), thus shielding the hydroxyl groups to form hydrogen bonds appropriately. Consequently, the fibril structure of HPC and HPMC with the steric hindrance group (**III**) significantly packed the PAni in the overlapping structures, finally block a big portion of the reactive sites. This is the main factor that reduced the sensitivity of both HPC and HPMC (Bodvik et al., 2010)

Besides, the bulkiness of steric hindrance by hydroxypropyl groups may induce aggregation. As a result, the reactive sites of PAni became shielded and hindered, makes

the attachment of hydrazine analytes to the PAni chain became more difficult for the reduction process. In addition, the steric hindrance of hydroxypropyl groups promoted the slow reaction of hydrazine with PAni-HPC and PAni-HPMC, leading to a little chance for adsorption of analyte on the PAni backbone (Bodvik et al., 2010; Phasuksom et al., 2018; Tayeb et al; 2018; Virji et al., 2005).

Therefore, the reactiveness of PAni-HPC and PAni-HPMC as sensing material towards hydrazine analytes was declined and exhibited a lower sensitivity than PAni-MC. It could be concluded that the excellent sensing performance may be attributed to the less hindrance of substituent groups to obtain great sensitivity (Li et al., 2007). Conclusively, PAni-MC with a ratio of 2:5 (PAni-MC: hydrazine) will be used for the next study of water-soluble PAni (as sensing material) with different ratios of aniline (Ani) to MC for hydrazine detection.

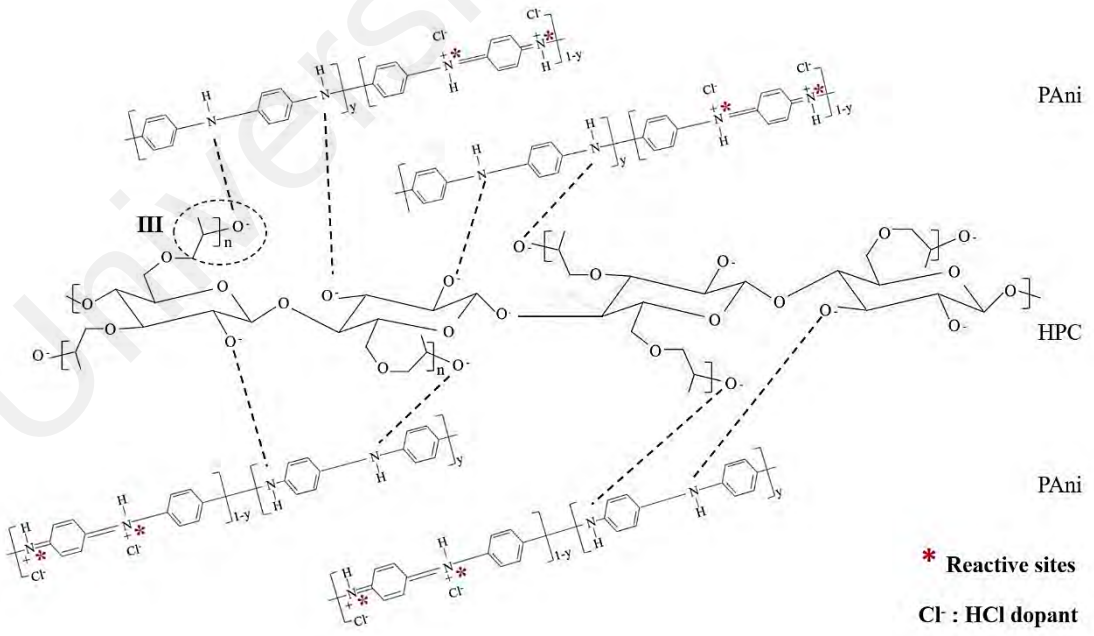

Figure 4.12: The proposed interaction between PAni and HPC.

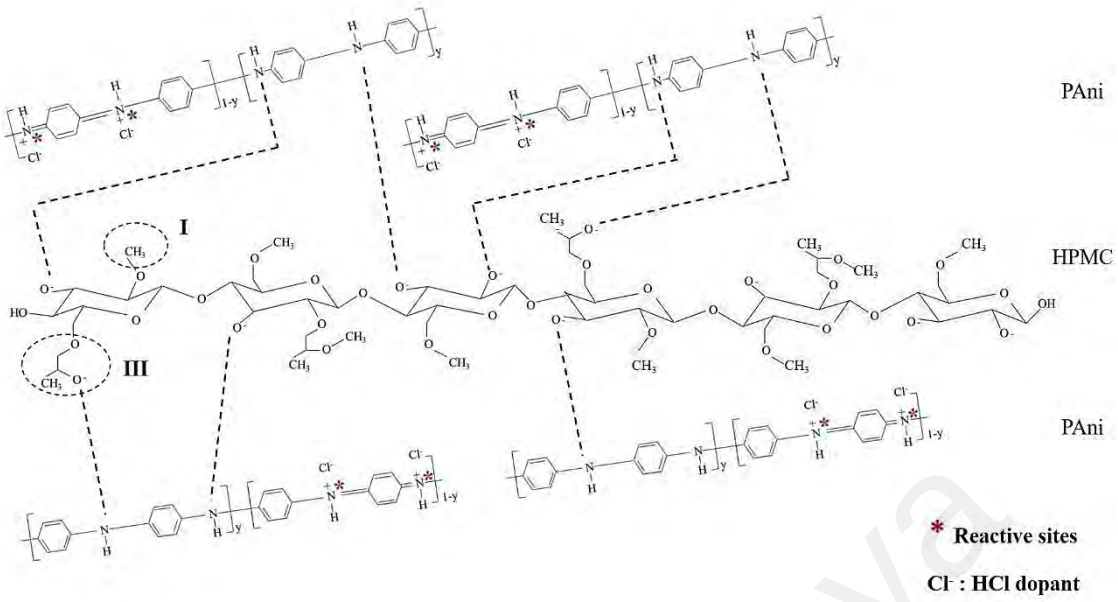

Figure 4.13: The proposed interaction between PAni and HPMC.

4.2.3 Different Mass Ratio of Aniline (Ani) to Methylcellulose (MC)

As reviewed earlier, the volume ratio 2:5 of PAni-MC: hydrazine exhibited the highest sensitivity of 0.0143 ppm^{-1} and R^2 of 0.9832, thus, it was selected to investigate the effect of the mass ratio of aniline (Ani) monomer to MC stabilizer used on the sensor performance for hydrazine detection. There were four different mass ratios of Ani to MC (0.1:1, 0.2:1, 0.5:1, and 1:1) were studied in order to examine the optimum monomer ratio of Ani to MC that could achieve the best sensor performance towards hydrazine (Chattopadhyay & Mandal, 1996; Luong et al., 2013; Shao et al., 2011). The normalized conductivities of PAni-MC (ratio 2:5) with the different mass ratios of Ani: MC against the concentration of hydrazine (10 ppm, 30 ppm, 50 ppm, 70 ppm, and 100 ppm) showed in **Figure 4.14**.

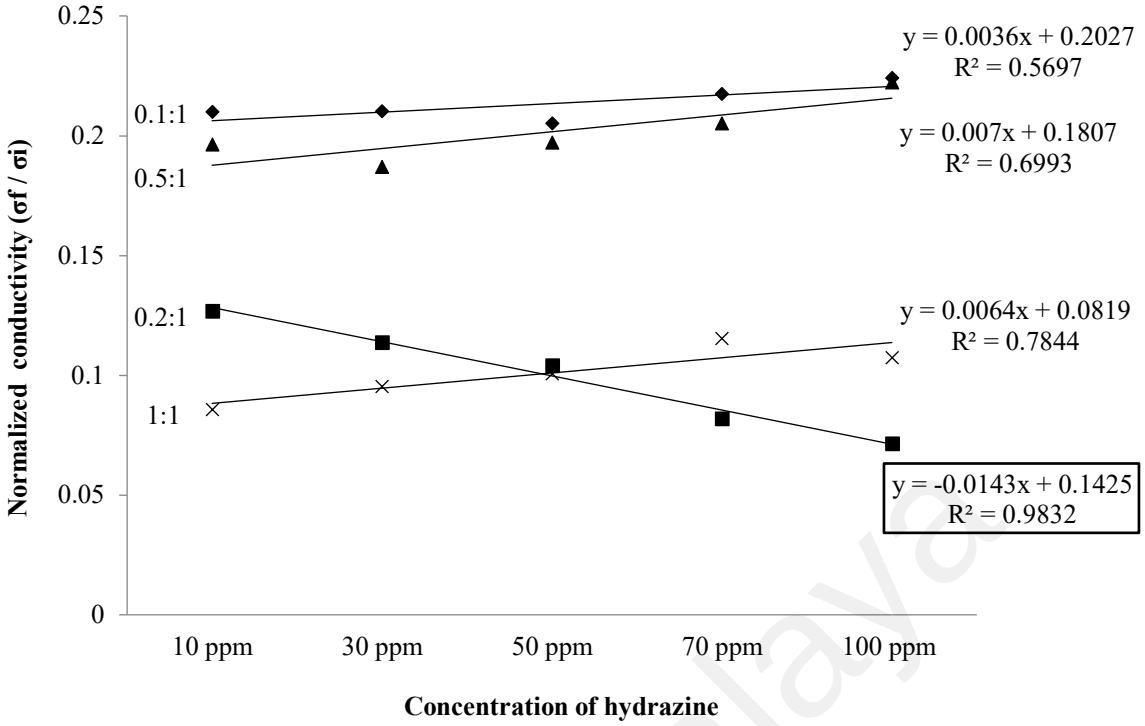

Figure 4.14: Normalized conductivities for the different mass ratios of Ani: MC against the various concentrations of hydrazine (10-100 ppm).

Generally, as represented in **Figure 4.14**, the ratio of 0.2:1 (Ani: MC) showed a notable decreased of normalized conductivities. Meanwhile, the mass ratio of 0.1:1, 0.5:1, and 1:1 increased linearly with hydrazine concentration for the normalized conductivities. The sensitivity and R^2 values obtained for PAni-MC (ratio 2:5) with the different mass ratios of Ani: MC summarized in **Table 4.4**.

Table 4.4: The sensitivity and R^2 of PAni-MC (ratio 2:5) with the different mass ratios of Ani: MC for hydrazine detection.

Mass ratio of Ani: MC (g)	Sensitivity (ppm^{-1})	R^2
0.1 : 1	0.0036	0.5697
0.2 : 1	0.0143	0.9832
0.5 : 1	0.0070	0.6993
1 : 1	0.0064	0.7844

Based on the general mechanism discussed earlier (**Figure 4.9)**, when PAni reacted with hydrazine, the quinoid ring converted to the benzenoid ring through the dedoping process by reducing the number of charge carriers along with PAni active sites. Thus, the normalized conductivities decreased significantly (negative gradient).

Among the mass ratios, the ratio of 0.2:1 (Ani: MC) showed the best sensitivity of 0.0143 ppm^{-1} with R^2 of 0.9832 with a negative gradient is in good agreement to the prior study. However, the ratio 0.1:1, 0.5:1, and 1:1 exhibited a positive gradient contrary to the mass ratio of 0.2:1. Notably, the counter ions that were supplied by the HCl dopant associate with the imine sites of PAni-MC resulting in protonation of charge carriers and thus increased the conductivity of PAni-MC. In the sensing mechanism, the hydrazinium ions attacked PAni-MC by seizing the counter ions from the PAni-MC chains through chemical absorption to form hydrazine molecules, leading to a decrease in the electrical conductivity of PAni-MC (Casado et al., 2012; Yin et al., 2017).

This sensing mechanism happened to the ratio of 0.2:1 (Ani:MC) because the amount of Ani present in the mass ratio of 0.2:1, provided sufficient active sites to interact with

hydrazine analyte for the charge-transfer interaction. Therefore, it possessed a negative gradient with the highest sensitivity of 0.0143 ppm^{-1} compared to the other ratios. **Figure 4.15** displayed the proposed interaction between PAni-MC and hydrazine analyte with adequate reactive sites (Virji et al., 2005).

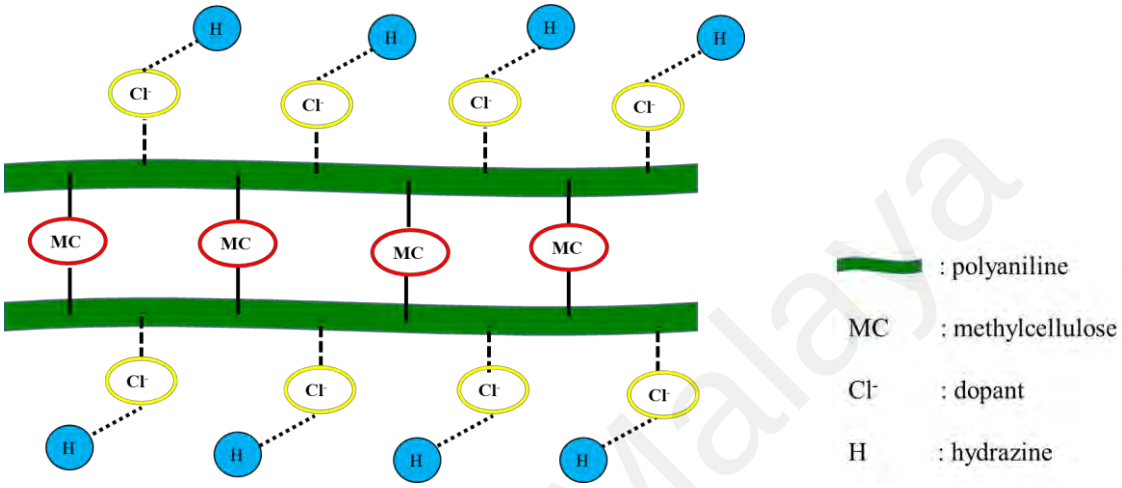

Figure 4.15: The proposed interactions of PAni-MC (ratio 2:5) with ratio 0.2:1 (Ani: MC) towards hydrazine analyte.

Meanwhile, the ratio of 0.1:1 for Ani: MC showed a slightly increment in normalized conductivities with the increase of hydrazine concentration (positive gradient) concomitant with the fluctuation values. When Ani is less than MC [Ani < MC], the MC is dominant along the PAni-MC chain. The formations of reactive sites along the PAni chain will be reduced, leading to the inadequate interactions between PAni-MC and hydrazine. Thus, the normalized conductivities exhibit slightly increase almost straight line was observed. Therefore, the ratio of 0.1:1 for Ani: MC possessed the lowest sensitivity of 0.0036 ppm^{-1} with the lowest R^2 of 0.5697 (Bhadra et al., 2017; Yin et al., 2017).

The opposite mechanisms had occurred for the ratio of 0.5:1 and 1:1 for Ani:MC [Ani > MC]. As the content of Ani is getting higher than MC in the PAni-MC chain, the aggregation of PAni may occur and disrupt the inter-chain and intra-chain interactions and leading to the blockage of the reactive sites (**Figure 4.16**). Due to the PAni aggregation, hydrazinium ions that attacked the PAni-ES will be recovered back by repossessing the hydrazine molecules. The reaction between PAni as sensing material and hydrazine analyte is reversible (**Figure 4.17**). So that, the conductivity of PAni will recover and the reduced PAni chain regain the ES state because the polaron was not taken away effectively by hydrazine in the excess of Ani contents. Therefore, the normalized conductivities for the ratios of 0:5:1 and 1:1 for Ani: MC were directly proportional to the hydrazine concentration and the responsiveness of both ratios as sensing material were less sensitive towards hydrazine (Moiz et al., 2012; Sambasevam et al., 2015; Tang et al., 2013; Yin et al., 2017; Yue et al., 2016).

(a) **(b)**

Figure 4.16: (a) The aggregation of PAni-cellulose, (b) The well-connected of PAni-cellulose (Shi et al., 2011).

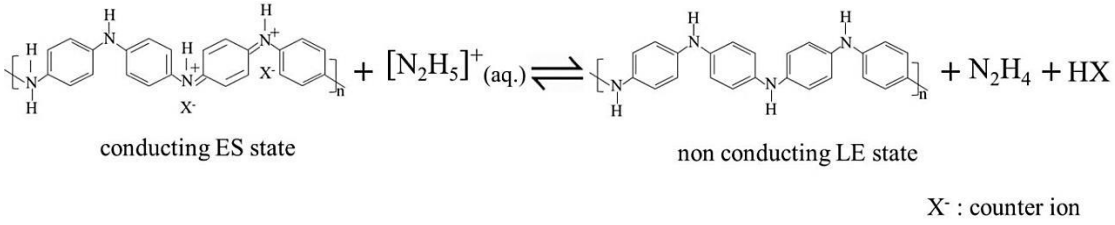

Figure 4.17: The reversible reaction between PAni and hydrazine in the excess of Ani contents.

Among all the ratios used, PAni-MC (ratio 2:5) with ratio 0.2:1 of Ani: MC exhibited the highest sensitivity of 0.0143 ppm^{-1} and best R^2 of 0.9832, hence it was used to study its effectiveness at different concentration of hydrazine (1 ppm-10 ppm).

4.2.4 Different Concentration of Hydrazine

Hydrazine is a well-known carcinogen and highly toxic chemical that may threaten human health and living organism for prolonging exposure. As stated by the NIOSH, the threshold limit value (TLV) permitted is 0.1 ppm, the odor threshold value is 3 ppm to 4 ppm, and the OSHA permissible exposure limit (PEL) is 1 ppm (NIOSH, 1988). Therefore, it is necessary to determine the ability of sensing material to detect hydrazine analyte at low concentration.

As evaluated from the prior study, the PAni-MC (ratio 2:5) with ratio 0.2:1 (Ani: MC) presented the finest sensitivity of 0.0143 ppm^{-1} and good R^2 of 0.9832, therefore it was preferred to examine the potentiality of PAni-MC as sensing material to trace hydrazine analyte at lower concentration varied from 10 ppm down to 1 ppm (Liu et al., 2019). The normalized conductivities of PAni-MC (ratio 2:5) with ratio 0.2:1 (Ani: MC) against the concentration of hydrazine (1 ppm, 2 ppm, 4 ppm, 6 ppm, 8 ppm, and 10 ppm) were presented in **Figure 4.18**.

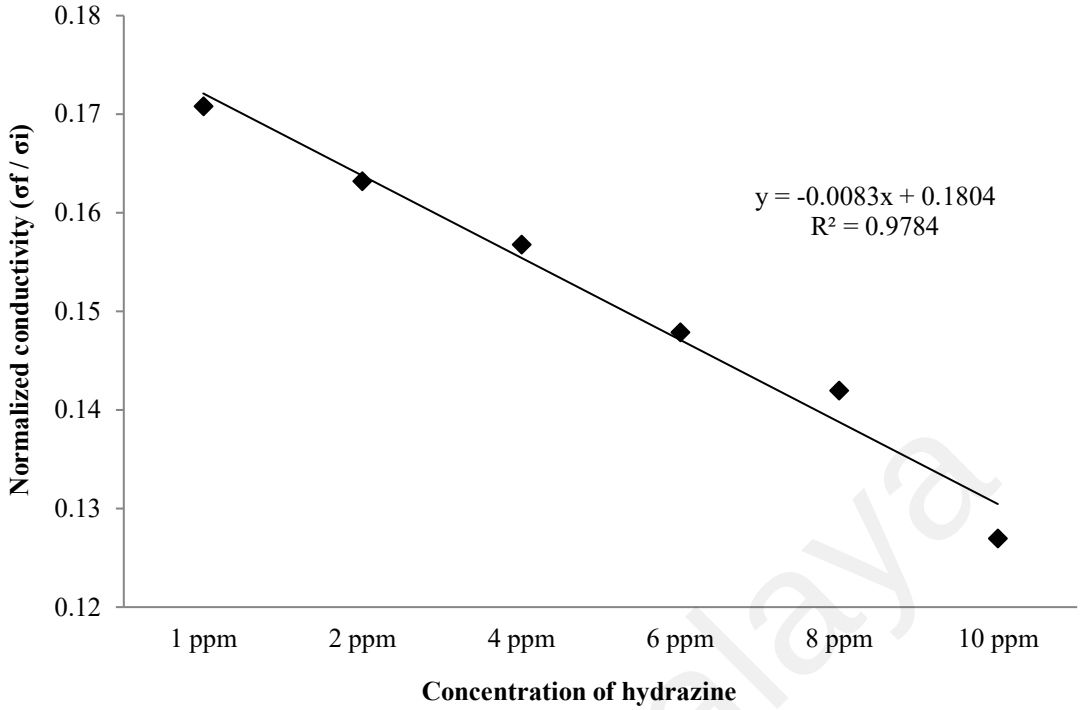

Figure 4.18: Normalized conductivities of PAni-MC (ratio 2:5) with ratio 0.2:1 of Ani: MC against the various concentrations of hydrazine (1-10 ppm).

Based on **Figure 4.18**, the good sensitivity of 0.0083 ppm^{-1} and valuable R^2 of 0.9784 was attained for PAni-MC (ratio 2:5) with a ratio of 0.2:1 (Ani: MC). The normalized conductivities decreased with the increasing of hydrazine concentration. This occurrence is in agreement with the expected theory as the higher concentration of hydrazine, more hydrazine may interact with reactive sites of PAni-MC, thus caused the significant decrease in the electrical conductivity by giving the lowest normalized conductivity as shown in **Figure 4.18**. The dedoping processes by hydrazine cause the changes of ES state to LE state and finally decrease the conductivity. Therefore, the normalized conductivities of PAni-MC decreased linearly (Wang et al., 2017). The data obtained showed a good linear relationship between the normalized conductivity and hydrazine concentrations from the low level of 1 ppm to a high level of 100 ppm was observed.

From all the parameters that have been investigated, it is worth noting that the PAni-MC (ratio 2:5) with ratio 0.2:1 (Ani: MC) was capable to trace hydrazine to as low as 1 ppm of concentration at room temperature. The sensor performance of PAni-MC as sensing material will be evaluated in the next study.

4.3 Sensor Performance of PAni-MC for Hydrazine Detection

In this study, different types of water-soluble PAni were synthesized using different parameters such as different volume ratios of PAni to hydrazine (**Part 4.2.1**), different types of cellulose derivatives (**Part 4.2.2**), and different monomer ratio of Ani to MC (**Part 4.2.3**). These entire water-soluble PAni were applied as a sensing material for hydrazine detection in the range of concentration from 1 ppm to 100 ppm.

Among all water-soluble PAni obtained (after optimization), PAni-MC (ratio 2:5) with a ratio of 0.2:1 (Ani: MC) possessed the best sensitivity of 0.0143 ppm^{-1} with R^2 of 0.9832 for the electrical conductivity responses as a principal study in hydrazine detection. Thus, the sensor performance of the optimized PAni-MC was investigated in depth as a potential sensor for hydrazine detection in terms of accuracy, linear range, sensitivity, R^2, the limit of detection (LOD), the limit of quantitation (LOQ), interference study, and real sample analysis.

The LOD is the lowest concentration of hydrazine that can be detected by sensor meanwhile the LOQ is the lowest concentration of hydrazine in a sample which can be determined with acceptable precision and accuracy. Both can be calculated from the calibration line at low concentrations using specified equations that had been stated earlier in **Part 3.5.** Besides, the LOD is an indicator to measure sensor sensitivity

towards hydrazine analyte (Ma et al., 2017; Phasuksom et al., 2018; Shivastava & Gupta, 2011).

4.3.1 Method of Validation

This part aims to determine the efficiency of water-soluble PAni-MC as a sensor. As mentioned earlier (**Part 4.2.4**), the LOD permitted by OSHA is 1.00 ppm and the TLV limit by NIOSH is 0.10 ppm. Therefore, the lower concentration range of hydrazine from 0.05 ppm to 5.00 ppm was selected to construct the calibration curve to find the LOD that could be achieved by the optimized PAni-MC as sensing material towards hydrazine analyte. This method is to justify the analytical procedure employed for a specific test or real sample analysis.

Figure 4.19 depicted the calibration curve of "-log normalized conductivity" against the different concentrations of hydrazine solution (0.05 ppm - 5.00 ppm) for the optimized PAni-MC as a sensor. The "-log normalized conductivity" was used to get a positive slope (Sambasevam et al., 2015). Based on the calibration curve attained, the "-log normalized conductivity" significantly increased with the increasing of hydrazine concentration. The sensitivity (slope) of 0.0132 ppm^{-1} with a good linearity of R^2 of 0.9953 was achieved. The accuracy of 97.0 ± 6.0 and the relative standard deviation (RSD) of 6.20 % were calculated using **Equation 4.1** and **Equation 4.2,** respectively. The percentage of RSD value is ≤ 10 % indicates the excellent precision data (Karnes 1993; Pellizzari & Clayton, 2006). Meanwhile, the LOD and LOQ were calculated using **Equation 3.5** and **Equation 3.6.**

Accuracy = mean ± SD **(Equation 4.1)**

$$\textbf{RSD} = \left(\frac{\textbf{SD}}{\textbf{means}}\right)\textbf{X 100\%} \qquad \textbf{(Equation 4.2)}$$

The optimized PAni-MC sensor exhibited the LOD of 0.55 ppm which is lower than the OSHA standard of 1.00 ppm with the LOQ of 1.82 ppm. Based on the overall results, the optimized PAni-MC possessed a good chemical sensor performance in hydrazine detection with a linear range from 0.05 ppm to 5.00 ppm of hydrazine.

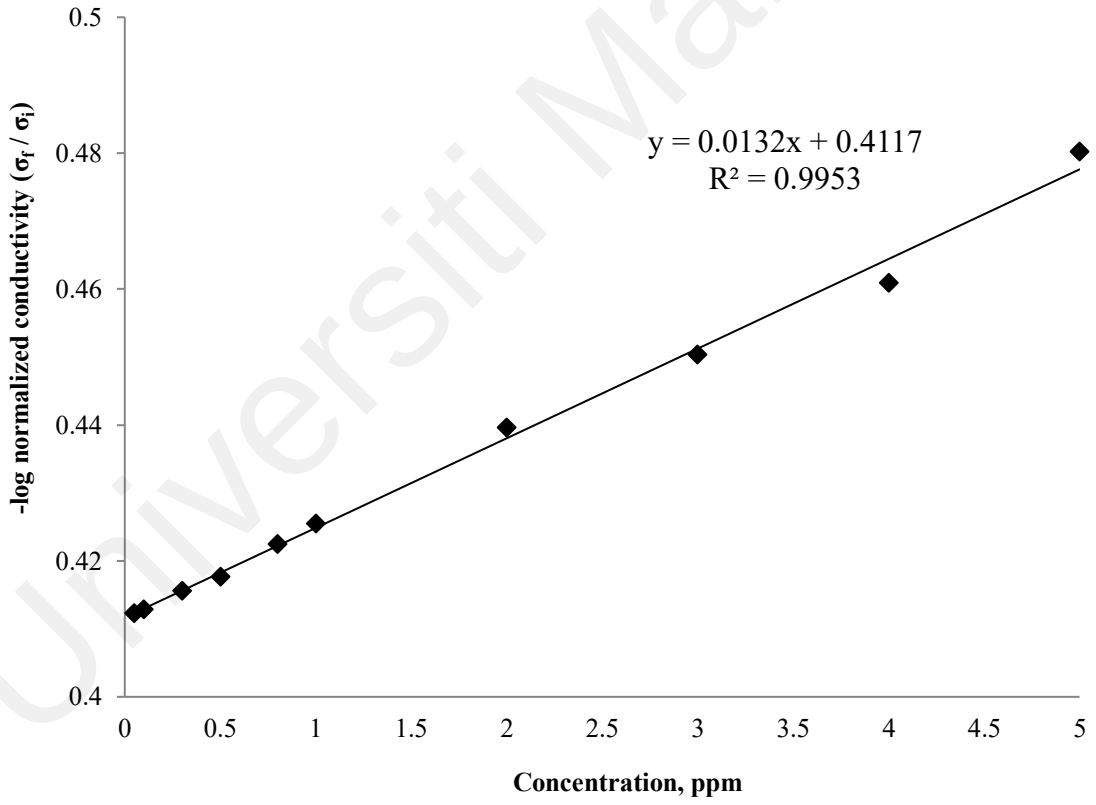

Figure 4.19: Calibration curve for the optimized PAni-MC as a sensor in the linear range of 0.05 ppm to 5.00 ppm.

The comparison of sensor performances between water-soluble PAni-MC sensor (present work) with organic PAni thin film (from the previous study) for hydrazine detection was tabulated in **Table 4.5** (Sambasevam et al., 2015).

Both of the sensing materials were performed well in the linear range from 0.05 ppm to 5.00 ppm. The sensitivity and R^2 of water-soluble PAni-MC sensor were higher than the organic PAni thin film. Meanwhile, the LOD and the LOQ of water-soluble PAni-MC sensor were slightly lower than the organic PAni thin film. However, the LOD obtained by water-soluble PAni-MC was successfully below the OSHA standard of 1.00 ppm.

It can be concluded that water-soluble PAni-MC has good potential as a chemical sensor. However, the water-soluble PAni-MC sensor exhibited the drawback of non-recyclability compared to the organic PAni thin-film sensor. Despite of this disadvantage, the water-soluble PAni-MC is more environmentally friendly because all the materials used were water-soluble materials compared to the organic PAni thin-film which used organic solvents that can cause toxicity to the environment.

Table 4.5: The sensor performance comparison between the present study with the previous study in hydrazine detection.

Sensor performance	Water-soluble PAni-MC	Organic PAni thin-film
Linear range	0.05 – 5.00 ppm	0.05 – 5.00 ppm
Sensitivity	0.0132 ppm^{-1}	0.0053 (L/mg)
R^2	0.9953	0.9900
LOD	0.55 ppm	0.49 ppm
LOQ	1.82 ppm	1.62 ppm

4.3.2 UV-Vis Analysis

In this study, the sensor performance for the optimized PAni-MC has been further researched in terms of UV-Vis and FTIR analysis to figure out the interactions existed between PAni-MC and hydrazine. **Figure 4.20** displayed the UV-Vis spectra for the optimized PAni-MC sensor before and after the addition of 1.00 ppm hydrazine solution. The UV-Vis response showed significant decreases in absorbance at the bipolaron band (~821 nm) from 3.27 to 0.63 and at the polaron band (~450 nm) from 2.89 to 0.55 upon the exposure to hydrazine. This happens due to the reduction of free charge carriers in the PAni-MC backbone through the dedoping process by hydrazine, thus producing PAni in LE form which is predominated in benzenoid units (Sambasevam et al., 2015; Tang et al., 2013).

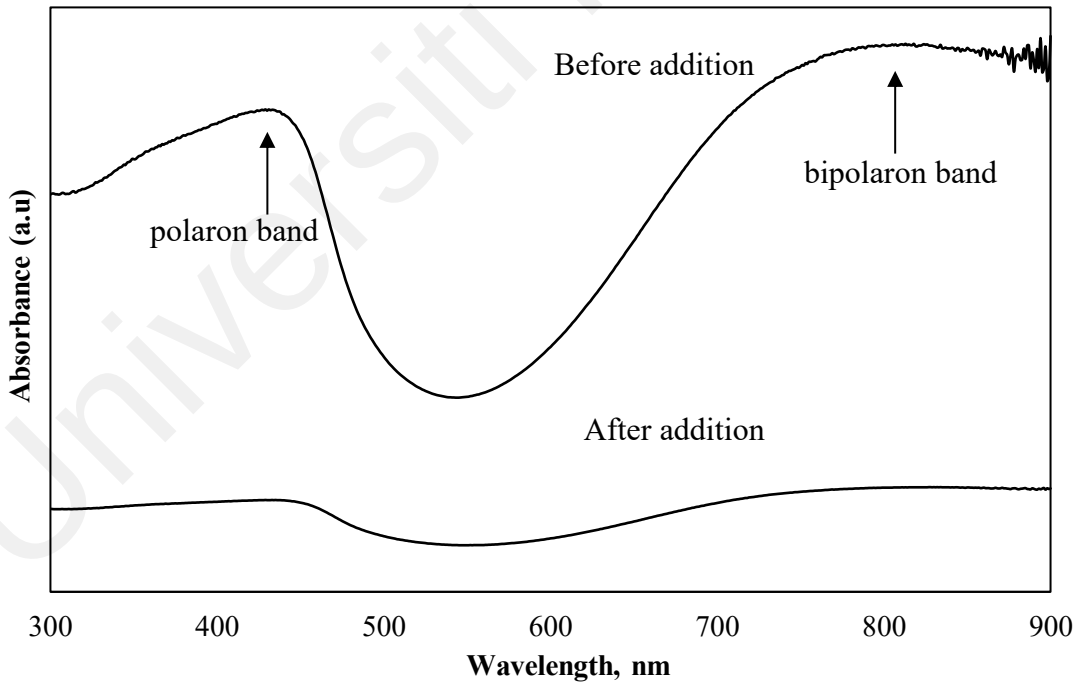

Figure 4.20: UV-Vis spectra of the optimized PAni-MC sensor before and after the addition of 1 ppm hydrazine.

4.3.3 FTIR Analysis

The FTIR analysis was evaluated to justify the structural changes occurred after the addition of hydrazine into the optimized PAni-MC. Initially, the ratio of the quinoid intensity to benzenoid intensity is equivalent in the PAni-ES state (I_Q/I_B = 1). When PAni-MC interacts with hydrazine, the hydrazine will remove the adsorbed counter-ions at the PAni causes the PAni to change from ES state into LE state. The quinoid structures along the PAni backbone will be converted into benzenoid structures. These changes can be observed by calculating the intensity ratios (I_Q/I_B) for both peaks. **Figure 4.21** showed the FTIR spectra of PAni-MC before and after the addition of 1.00 ppm hydrazine solution. The I_Q/I_B ratio has decreased from 1.03 to 0.97 after the addition of 1.00 ppm hydrazine. It has proven that the ES state of water-soluble PAni-MC has turned into LE state because LE state consists of the more benzenoid units compared to ES. This result is in agreement with the previous outcomes in this research study (Sambasevam et al., 2015; Tang et al., 2013; Virji et al., 2005).

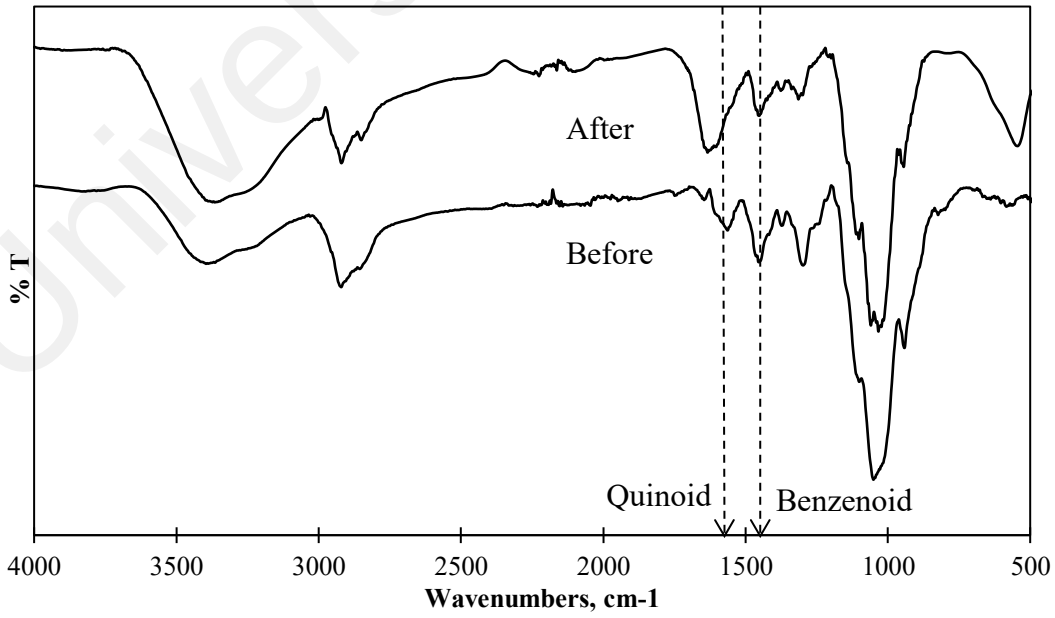

Figure 4.21: FTIR spectra of PAni-MC before and after adding 1 ppm hydrazine.

4.3.4 Interference Study

In this section, the interference study for the optimized PAni-MC as a sensor in hydrazine detection (target analyte) was monitored through the changes in the electrical conductivity measurement of PAni-MC before and after the addition of analytes. The interference or selectivity study is the ability of the optimized PAni-MC sensor to respond to a target hydrazine analyte in the presence of other analytes. It is one of the crucial factors needed in chemical sensor applications (Navale et al., 2014; Phasuksom et al., 2018).

The selection of the interfering analytes is based on the chemical properties of hydrazine which is a strong reducing agent and a weak base. Thus, these properties have been used as a guideline to choose the interfering analytes in this study. The interfering species that have been chosen are 2-propanol (reducing agent), formic acid (reducing agent), ammonia (base), and sodium hydroxide (base) (Sambasevam et al., 2015).

Figure 4.22 displayed the normalized electrical conductivities of the optimized PAni-MC before and after the addition of hydrazine, 2-propanol, formic acid, ammonia, and sodium hydroxide. All the concentration of analytes used was 1.00 ppm. Principally, the optimized PAni-MC resided in conducting ES state with a high electrical conductivity of 0.132 S/cm.

Upon the addition of the base and reducing agent such as hydrazine, the normalized conductivity of PAni-MC showed a significant decrease of 0.375. This happened due to the reduction from the ES state to the LE state of PAni-MC. As a comparison, the reducing agents such as 2-propanol and formic acid also exhibited a decrement in the normalized conductivity descending to 0.314 and 0.234, respectively. Besides, for the

base such as ammonia and sodium hydroxide, a declination of normalized conductivity to 0.237 and 0.304, were observed respectively. As a conclusion, hydrazine achieved the highest normalized conductivity among all the other interfering analytes.

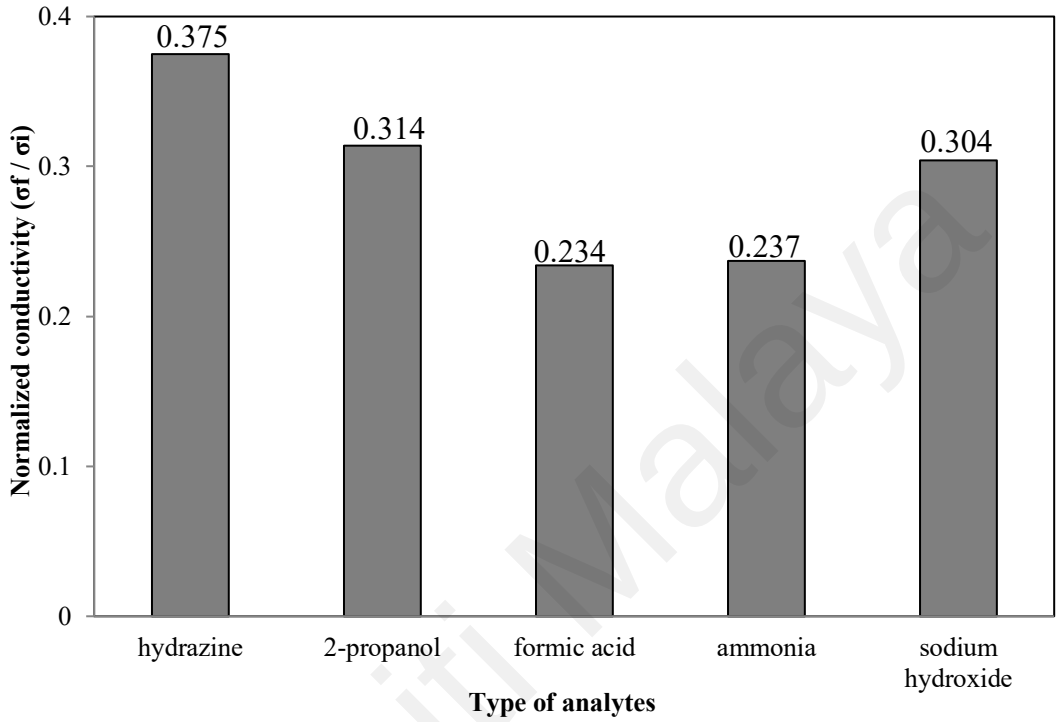

Figure 4.22: The normalized conductivities of the optimized PAni-MC after the addition of hydrazine and other interfering species.

The interference or selectivity study was evaluated using the selectivity coefficient (Q) and calculated using **Equation 4.3**. The Q is defined as the ratio of normalized conductivity of the target analyte (hydrazine) to the normalized conductivity of other interfering analytes (Gadzekpo & Christian, 1984; Navale et al., 2014). The Q values of the optimized PAni-MC sensor towards various interfering analytes were tabulated in **Table 4.6.** It can be seen that the Q values are 1.20 (2-propanol), 1.24 (sodium hydroxide), 1.58 (ammonia), and 1.61 (formic acid). The larger the Q value of the interfering species (formic acid: 1.61) towards hydrazine (target analyte), signify that the PAni-MC sensor has a better selectivity to hydrazine compared to the other

interfering analytes. It can be concluded that the optimized PAni-MC sensor has a good selective towards hydrazine compare to 2-propanol, sodium hydroxide, ammonia, and formic acid by giving significant and higher Q values of 1.20 – 1.61.

$$\textbf{Selectivity coefficient (Q)} = \frac{S_a}{S_b} \qquad \textbf{(Equation 4.3)}$$

where;

S_a: normalized conductivity towards hydrazine

S_b: normalized conductivity towards interfering analytes

Table 4.6: The Q values of the hydrazine sensor based on the optimized PAni-MC toward various interfering analytes.

Types of analytes	Q
Hydrazine	1
2-propanol	1.20
Formic acid	1.61
Ammonia	1.58
Sodium hydroxide	1.24

4.3.5 Real Sample Analysis

In this research, the real application of the optimized PAni-MC has been tested upon three matrix samples and monitored by the changes in electrical conductivity. The first matrix sample is tap water (**Sample 1**) which was collected from Polymer Research Laboratory (M014-M017) at the Department of Chemistry, University of Malaya. The second matrix sample is drain water (**Sample 2**) which was collected from an industrial

area near Pengkalan Chepa (Kota Bharu, Kelantan). The area is surrounded with a glove factory, food supplier factory, and tile contractor **(Figure 4.23)**. The third matrix sample is mineral drinking water (**Sample 3**) (brand: Spritzer). All the matrix samples were filtered using a nylon syringe filter with a pore size of 0.22 µm and a diameter of 25.00 mm to discard solid impurities in matrix samples (Isa et al., 2016; Sambasevam et al., 2015).

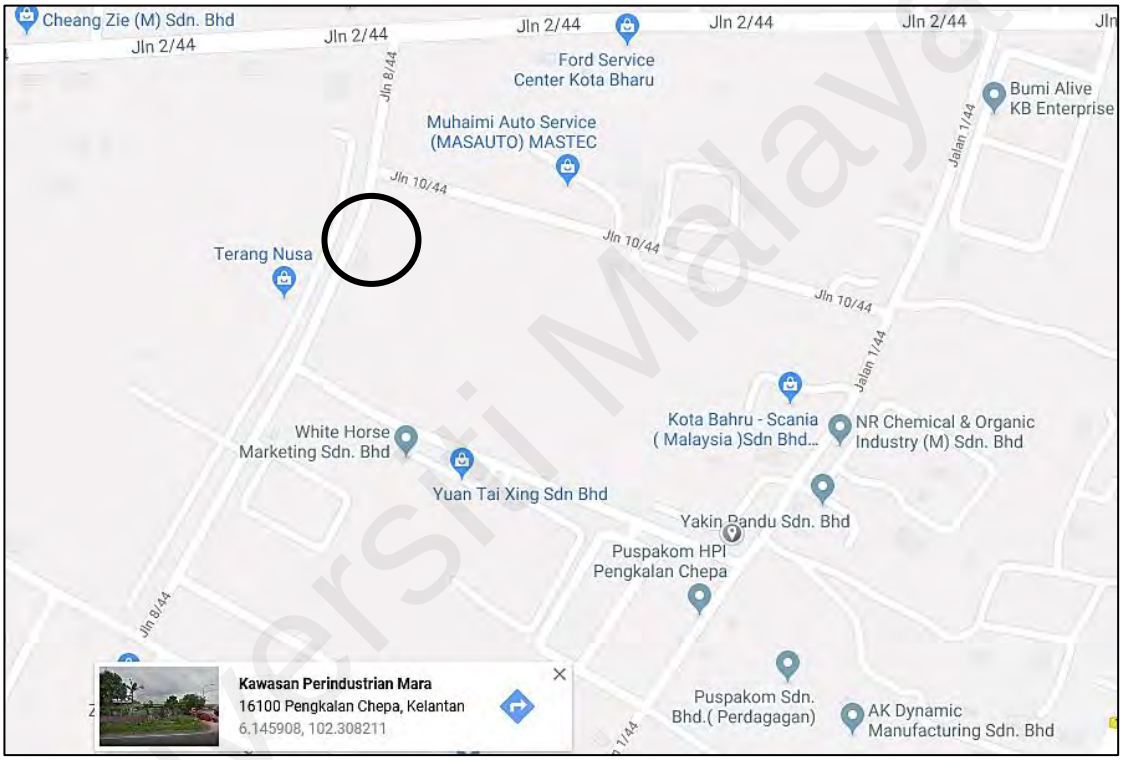

Figure 4.23: The industrial area that the matrix of Sample 2 was collected.

The optimized PAni-MC was analyzed by the electrical conductivity meter for the determination of the known concentration of spiked hydrazine in the matrix samples. The electrical conductivity response for each matrix sample was repeated three times (T1 – T3) in the different concentrations of hydrazine (1.00 ppm and 4.00 ppm). The found concentrations of hydrazine (T1 – T3) in all matrix samples were obtained by substituting in the linear equation of the calibration curve (y = 0.0132x + 0.4117). The

percentage of RSD and the recovery value of the optimized PAni-MC for all matrix samples were calculated using **Equation 4.2** and **Equation 4.4**, respectively and were tabulated in **Table 4.7**.

$$\textbf{Recovery} = \frac{\textbf{Amount of hydrazine determined}}{\textbf{Amount of hydrazine spiked}} \textbf{ X 100\%} \qquad \textbf{(Equation 4.4)}$$

The recovery was calculated to evaluate how well the instrumental analysis system performed on the check standards. According to Pellizzari and partner, the range from 100 % to 105 % is an excellent recovery and the range from 97 % to 122 % is very good to excellent recovery. Besides, the range from 66 % to 141 % is an acceptable recovery (Pellizzari & Clayton, 2006). Meanwhile, for the RSD percentage, the value less than 10 % is an excellent precision, less than 20 % is a very good precision, and less than 30 % is an acceptable precision (Karnes et al., 1993; Pellizzari & Clayton, 2006).

In this study, the optimized PAni-MC sensor possessed a very good to excellent recovery range of 96 - 113 % towards **Sample 1 – Sample 3**. However, PAni-MC exhibited an acceptable recovery of 136 % towards **Sample 2** in the concentration of 1.00 ppm. Besides, PAni-MC showed an excellent RSD range of 2.69 – 5.84 % in the matrix sample analyses. Generally, the results obtained were satisfactory based on the previous literature study.

Table 4.7: The spiked, found, mean, recovery, and RSD values of the optimized PAni-MC sensor in matrix samples during hydrazine detection.

Sample	Spiked (ppm)	Found (ppm)			Mean	Recovery (%)	RSD (%)
		T1	T2	T3			
Sample 1	1.00	0.98	0.98	0.92	0.96	96.0	3.61
	4.00	4.05	4.13	3.90	4.03	100.7	2.90
Sample 2	1.00	1.39	1.42	1.27	1.36	136.0	5.84
	4.00	4.27	4.16	4.61	4.35	108.7	5.40
Sample 3	1.00	1.13	1.11	1.17	1.14	113.7	2.69
	4.00	4.08	4.16	3.80	4.01	100.3	4.70

4.4 Proposed Mechanism

Figure 4.24 displayed the proposed chemical structure for the interactions of water-soluble PAni-MC sensor and hydrazine. In the detection of hydrazine using a PAni-based sensor, the doping and dedoping process play an essential character. The highly conductive PAni was achieved by the doping process. In this study, PAni-MC was doped with HCl dopant and used in hydrazine detection. During the doping reaction, PAni-MC molecules gain the protons from the HCl dopant to form N^{+}- H chemical bonding along the PAni backbone, leading to an increased in the number of charge carriers. Thus, the electrical conductivity of PAni-MC increased. The doping process of PAni-MC is reversible, which can be reversed to the undoped state by the dedoping process.

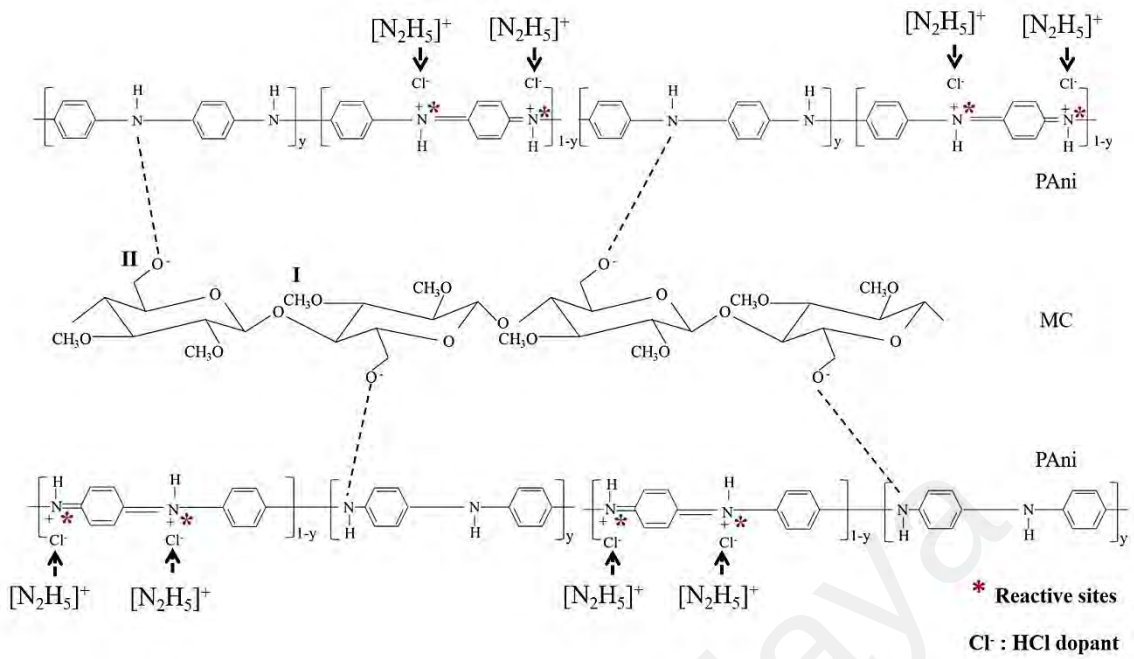

Figure 4.24: The proposed chemical structure for the chemical interactions of water-soluble PAni-MC sensor and hydrazine.

When hydrazine was introduced to the PAni-MC dispersion, the hydrazinium ions intercalated to the quinoid of PAni-MC and seize the protons, then wash away the counter ions at the PAni-MC backbone. As mentioned earlier, the chemical interaction between PAni-MC and hydrazine has changed the physical properties, thus alter the doping level of PAni-MC. As a result, the doping level and the number of charge carriers of PAni-MC significantly decreased eventually reduced the electrical conductivity of PAni-MC. The electron re-arrangement takes place and the quinoid units of PAni-MC have turned to the benzenoid units. Therefore, the PAni-MC in LE form was obtained and the hydrazinium ions forming back into neutral hydrazine molecules.

The proposed sensing mechanism of the water-soluble PAni-MC during hydrazine detection was shown in **Figure 4.25** (Lange et al., 2008; Sambasevam et al., 2015; Virji et al., 2004; Wang et al., 2017; Yoo et al., 2009). The proposed mechanism as discussed

above is strongly supported by the decreases in absorbance at the bipolaron band (~820 nm) and at the polaron band (~450 nm) in **Part 4.3.2**. Besides, and the intensity ratio of (I_Q/I_B) in FTIR decreased after the addition of hydrazine in **Part 4.3.3.**

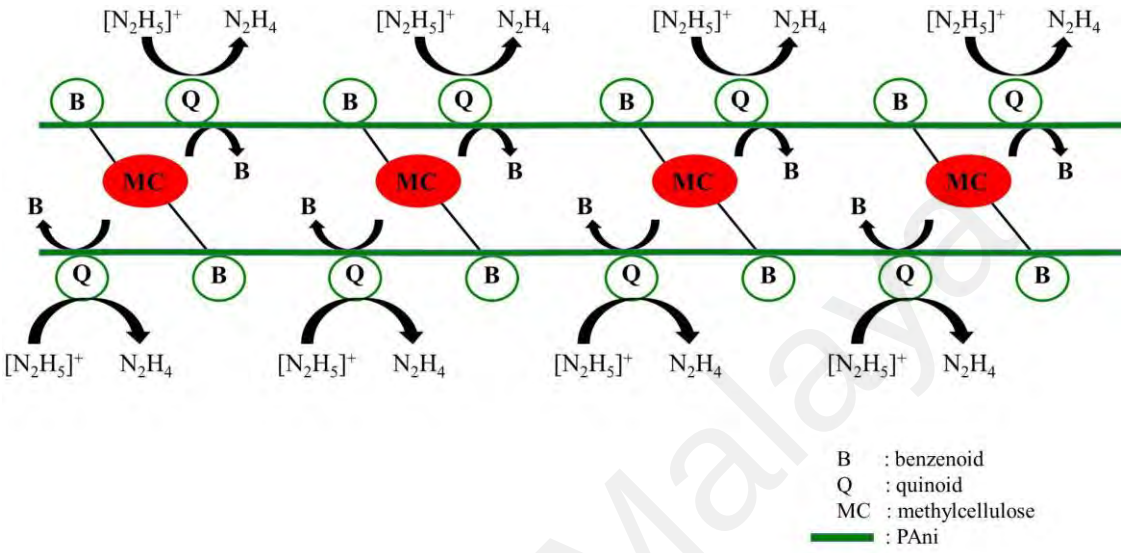

Figure 4.25: The proposed sensing mechanism of the water-soluble PAni-MC during hydrazine detection.

4.5 Summary of PAni-MC for Hydrazine Detection

At the beginning of this study (**Table 4.8**), the water-soluble PAni-MC was used to investigate the optimum volume ratio of PAni-MC as a potential chemical sensor for hydrazine detection. Among all the ratios used, the volume ratio of 2:5 (PAni-MC: hydrazine) possessed the highest sensitivity of 0.0143 ppm^{-1} with the most fitted R^2 of 0.9832 toward hydrazine detection due to the sufficient of reactive sites. Thus, the ratio of 2:5 (PAni-MC: hydrazine) was applied in further studies.

Table 4.8: A summary of PAni-MC (with different volume ratios) as a sensor for hydrazine detection.

PAni-MC: hydrazine	Sensitivity (ppm^{-1})	Sensor performance	Description
1:5	0.0021	Moderate	Moderate reactive sites
2:5	0.0143	Good	Sufficient reactive sites
5:5	0.0081	Moderate	Overlap reactive sites
10:5	0.0006	Poor	Overlap reactive sites
15:5	0.0009	Poor	Overlap reactive sites

The water-soluble PAni with different types of cellulose derivatives such as MC, HPC, and HPMC had been synthesized and applied as a hydrazine sensor. The effect of the substituent groups of cellulose derivatives on the sensor performance has been determined. **Table 4.9** displayed a summary of PAni with different types of cellulose derivatives as a hydrazine sensor. Among all the PAni-cellulose derivatives, PAni-MC exhibited the best sensitivity of 0.0143 ppm^{-1} due to the less steric hindrance effect by the methyl substituents in MC. It can be concluded that the sensitivity of the water-soluble PAni sensor is significantly affected by the substituent groups of cellulose.

Table 4.9: A summary of PAni with different types of cellulose derivatives as a hydrazine sensor.

PAni-cellulose derivatives	Sensitivity (ppm^{-1})	Sensor performance	Description
PAni-MC	0.0143	Good	Methyl substituents
PAni-HPC	0.0052	Moderate	Hydroxypropyl substituents
PAni-HPMC	0.0045	Poor	Methyl and hydroxypropyl substituents

Based on the previous results, the PAni-MC with ratio 2:5 has been selected for the next evaluation. The effect of the mass ratios of Ani to MC on the sensor performance of hydrazine detection has been investigated as shown in **Table 4.10**. Among all the ratios used, PAni-MC (ratio 2:5) with the ratio of 0.2:1 (Ani: MC) performed the highest sensitivity of 0.0143 ppm^{-1} due to the adequate of reactive sites for the interaction with hydrazine.

Table 4.10: A summary of PAni-MC (ratio 2:5) with the different mass ratios of Ani: MC for hydrazine detection.

Mass ratio of Ani: MC	Sensitivity (ppm^{-1})	Sensor performance	Description
0.1:1	0.0036	Poor	Inadequate reactive sites
0.2:1	0.0143	Good	Adequate reactive sites
0.5:1	0.0070	Moderate	Blockage of reactive sites
1:1	0.0064	Moderate	Blockage of reactive sites

After all the optimization of parameters, the PAni-MC (ratio 2:5) with the ratio of 0.2:1 (Ani: MC) has been examined its capability to trace hydrazine at a lower concentration from 10.00 ppm down to 1.00 ppm. This study is fundamental because of the PEL by the OSHA is 1.00 ppm. The good sensitiveness of 0.0083 ppm^{-1} with a good R^2 of 0.9784 was obtained and significantly proved that the optimized PAni-MC sensor has the potential to detect hydrazine until a low concentration of 1.00 ppm.

The efficiency of the optimized PAni-MC was validated through the calibration curve in the range of 0.05 – 5.00 ppm. This sensor possessed a sensitivity of 0.0132 ppm^{-1}, the LOQ of 1.82 ppm, and the LOD of 0.55 ppm which is lower than the OSHA standard of 1.00 ppm. For the interference study, this sensor significantly exhibited a

good selectivity toward hydrazine compared to the other interfering analytes. Besides, the optimized PAni-MC sensor eventually indicated a good recovery range of 96 – 136 % and a good RSD range of 2.69 – 5.84 % in the real sample analyses study.

CHAPTER 5: CONCLUSION AND SUGGESTION FOR FUTURE WORKS

5.1 Conclusion

In this research study, the water-soluble PAni-cellulose derivative has been applied as a chemical sensor in hydrazine detection. The water-soluble PAni was successfully synthesized using the different types of cellulose derivatives through the chemical oxidation method. The chemical structures of PAni-cellulose derivatives were confirmed through UV-Vis and FTIR spectra. Meanwhile, the electrical conductivities of the water-soluble PAni were in the ES state of 0.132 S/cm – 0.146 S/cm.

In the determination of hydrazine, the sensor responses were monitored using the electrical conductivity measurement. There were a few parameters that have been investigated for PAni-cellulose derivatives to find the optimized condition for hydrazine detection including the optimum volume of PAni: hydrazine, the effect of different types of cellulose derivatives, the effect of the mass ratio of Ani to MC, and the detection at a lower concentration of hydrazine (1 ppm to 10 ppm).

After the optimization, the PAni-MC (ratio 2:5) with the ratio of 0.2:1 (Ani: MC) sensor exhibited the best sensitivity of 0.0132 ppm^{-1} in hydrazine detection due to the sufficient of reactive sites provided by PAni-MC. Besides, the methyl substituents that were present in MC were not bulky enough to hinder the reactive sites, thus allowing hydrazine to bind effectively onto PAni-MC. The sensor performance of the optimized PAni-MC in hydrazine detection has been discussed in terms of the accuracy, LOD, LOQ, interference study, and real sample analysis.

In the linear range of 0.05 – 5.00 ppm, the optimized PAni-MC sensor showed good accuracy of 97.0 ± 6.0, an excellent LOD of 0.55 ppm, and a great LOQ of 1.82 ppm. Besides, this sensor also exhibited a good selectivity towards hydrazine as compared to the other interfering analytes such as ammonia, sodium hydroxide, 2-propanol, and formic acid. Moreover, in the real samples study, this sensor achieved a very good to excellent recovery range of 96 – 136 % and an excellent RSD range of 2.69 – 5.84 % for the tap water, drain water, and mineral drinking water.

As a conclusion, the water-soluble PAni-MC is highly proposed as a good chemical sensor due to the facile technique, economical set-up, and good sensor performance for hydrazine detection. Most importantly, this water-soluble PAni-MC is a more environmentally friendly material compared to organic PAni thin-film which can cause toxicity to the environment.

5.2 Suggestion for Future Works

As discussed in the previous chapter, the sensitivity of the water-soluble PAni-MC sensor was affected by several factors such as the volume used, the type of stabilizer, and the ratio of monomer. For future studies, the performance of the water-soluble PAni-MC sensor may be enhanced using secondary dopants, different concentrations of acid dopant, different types of dopants with different ratios level, different types of stabilizers, and different temperature during the polymerization.

Besides, the ability of the water-soluble PAni-MC as a sensor may be broadened by testing it in the high concentration range of hydrazine, for example, from 100 ppm to 10,000 ppm. Principally, hydrazine can reduce the ES state of PAni to LE state through

the dedoping process. When the high concentration of hydrazine used, the oxidation state conversion through the changing colour of PAni may be seen clearly by naked eyes due to the bountiful of hydrazinium ions to reduce PAni.

Therefore, the modification for the synthesis parameters and the detection at higher concentrations of hydrazine are highly recommended to enhance the sensitivity of the water-soluble PAni sensor as well as to broaden its application in the various fields.

REFERENCES

Abd Manan, F. A., Abdullah, J., Nazri, N. N., Abd Malik, I. N., Yusof, N. A., & Ahmad, I. (2016). Immobilization of tyrosinase in nanocrystalline cellulose/chitosan composite film for amperometric detection of phenol. *Malaysian Journal of Analytical Sciences, 20* (5), 978-985.

Aizawa, M., Karube, I., & Suzuki, S. (1974). A specific bio-electrochemical sensor for hydrogen peroxide. *Analytica Chimica Acta, 69*, 431-437.

Aizawa, M., Matsuzawa, M., & Shinohara, H. (1987). An optical chemical sensor using a fluorophor-embedded langmuir-blodgett film. *Elsevier Sequoia*, 477-481.

Arulraj, A. D., Vijayan, M., & Vasantha, V. S. (2015). Spectrophotometric determination of pico-molar level of hydrazine by using Alizarin red in water and urine samples. *Spectrochimica Acta Part A: Molecular and Biomolecular Spectroscopy, 148*, 355–361.

Barik, A., Solanki, P. R., Kaushik, A., Ali, A., Pandey, M. K., Kim, C. G., & Malhotra, B. D. (2010). Polyaniline-carboxymethyl cellulose nanocomposite for cholesterol detection. *Journal of Nanoscience and Nanotechnology, 10*, 1-10.

Bhadra, J., Al-Thani, N. J., Madi, N. K., & Al-Maadeed, M. A. (2017). Effects of aniline concentrations on the electrical and mechanical properties of polyaniline polyvinyl alcohol blends. *Arabian Journal of Chemistry, 10,* 664-672.

Bicak, N., Senkal, B. F., & Sezer, E. (2005). Preparation of organo-soluble polyanilines in ionic liquid. *Synthetic Metals, 155*, 105-109.

Bin, L., Konecke, S., Wegiel, L. A., Taylor, L. S., & Edgar, K. J. (2013). Both solubility and chemical stability of curcumin are enhanced by solid dispersion in cellulose derivatives matrices. *Carbohydrate Polymers, 98*, 1108-1116.

Bochek, A. M. (2003). Effect of hydrogen bonding on cellulose solubility in aqueous and nonaqueous solvents. *Russian Journal of Applied Chemistry, 76* (11), 1711-1719.

Bodvik, R., Dedinaite, A., Karlson, L., Bergstrom, M., Baverback, P., Pedersen, J. S., Edwards, K., Karlsson, G., Varga, I., & Claesson, P. M. (2010). Aggregation and network formation of aqueous methylcellulose and hydroxypropylmethylcellulose solutions. *Colloids and Surfaces A: Physicochem. Eng. Aspects, 354*, 162-171.

Bott, B. & Jones, T. A. (1984). A highly sensitive NO_2 sensor based on electrical conductivity changes in phthalocyanine films. *Sensors and Actuators, 5*, 43-53.

Casado, U. M., Quintanilla, R. M., Aranguren, M. I., & Marcovich, N. E. (2012). Composite films based on shape memory polyurethanes and nanostructured polyaniline or cellulose-polyaniline particles. *Synthetic Metals, 162*, 1654-1664.

Chattopadhyay, D. & Bain, M. K. (2008). Electrically conductive nanocomposites of polyaniline with poly(vinyl alcohol) and methylcellulose. *Journal of Applied Polymer Science, 110*, 2849-2853.

Chattopadhyay, D. & Mandal, B. M. (1996). Methyl cellulose stabilized polyaniline dispersions. *Langmuir, 12*, 1585-1588.

Ding, Y., Zhao, S., Wang, Q., Yu, X., & Zhang, W. (2018). Construction of a coumarin based fluorescent sensing platform for palladium and hydrazine detection. *Sensors and Actuators B, 256,* 1107-1113.

Eutuceh Instruments. (2014). *Eutech Instruments catalogue: Solutions for water analysis*. Ayer rajah Crescent, Singapore: Author.

Gadzekpo, V. P. Y. & Christian, G. D. (1984). Determination of selectivity coefficients of ion-selective electrodes by a matched-potential method. *Analytica Chimica Acta*, *164*, 279-282.

Gautama, V., Singh, K. P., & Yadava, V. L. (2018). Preparation and characterization of green-nano-composite material based on polyaniline, multiwalled carbon nano tubes and carboxymethyl cellulose: For electrochemical sensor applications. *Carbohydrate Polymers, 189*, 218–228.

George, M., Nagaraja, K. S., & Balasubramanian, N. (2008). Spectrophotometric determination of hydrazine. *Talanta, 75*, 27–31.

Glass, J. E. (2000). Water-soluble polymers. In *Kirk-othmer encyclopedia of chemical technology* (4th ed.).

Gosh, M., Barman, A., Meikap, A. K., De, S. K., & Chatterjee, S. (1999). Hopping transport in HCl doped conducting polyaniline. *Physics Letter A, 260,* 138-148.

Goswami, S., Das, S., Aich, K., Sarkar, D., & Mondal, T. K. (2014). A coumarin based chemodosimetric probe for ratiometric detection of hydrazine. *Tetrahedron Letters, 55,* 2695-2699.

Grdadolnik, J. (2002). ATR-FTIR spectroscopy: Its advantages and limitations. *Acta Chimica Slovenica, 49,* 631-642.

Hao, H. & Liu, R. (2014). Study on preparation and gas sensing property of water-soluble polyaniline/$SmBaCuMO_{5+\delta}$ (M=Fe, Co, Ni) for NH_3. *Journal of Rare Earths, 32* (1), 23-28.

Harun, M. H., Saion, E., Kassim, A., Yahya, N., & Mahmud, E. (2007). Conjugated conducting polymers: A brief overview. *Journal of the American Statistical Association, 2,* 63-68.

Hino, T., Namiki, T., & Kuramoto, N. (2006). Synthesis and characterization of novel conducting composites of polyaniline prepared in the presence of sodium dodecylsulfonate and several water soluble polymers. *Synthetic Metals, 156*, 1327-1332.

Hulanicki, A., Glab, S., & Ingman, F. (1991). Chemical sensors definitions and classification. *Pure & Applied Chemistry, 63* (9), 1247-1250.

Iglesias, M. R., Lizundia, E., & Mendez, S. L. (2019). Water-soluble cellulose derivatives as suitable matrices for multifunctional materials. *Biomacromolecules, 20*, 2786-2795.

Isa, I. M., Saruddin, S., Hashim, N., Ahmad, M., & Ab Ghani, S. (2016). Determination of hydrazine in various water samples by square wave voltammetry with zinc-layered hydroxide-3(4-methoxyphenyl) propionate nanocomposite modified glassy carbon electrode. *International Journal of Electrochemical Science, 11,* 4619-4631.

Jeon, S. S., An, H. H., Yoon, C. S., & Im, S. S. (2011). Synthesis of ultra-thin polypyrrole nanosheets for chemical sensor applications. *Polymer, 52*, 652-657.

Jia, B., Hino, T., & Kuramoto, N. (2007). Synthesis and chiroptical properties of water processable polyaniline using methylcellulose as a molecular template. *Reactive & Functional Polymers, 67*, 836-843.

Jones, T. P. & Porter, M. D. (1988). Optical pH sensor based on the chemical modification of a porous polymer film. *Analytical Chemistry, 60*, 404-406.

Jonsson, G. & Gorton, L. (1989). An electrochemical sensor for hydrogen peroxide based on peroxidase adsorbed on a spectrographic graphite electrode. *Electroanalysis, 1*, 465-468.

Kadajji, V. G. & Betageri, G. V. (2011). Water soluble polymers for pharmaceutical applications. *Polymers*, *3*, 1972-2009.

Karnes, H. T. & March, C. (1993). Precision, accuracy, and data acceptance criteria in biopharmaceutical analysis. *Pharmaceutical Research, 10* (10), 1420-1426.

Khan, M. D. A., Akhtar, A., & Nabi, S. A. (2015). Investigation of the electrical conductivity and optical property of polyaniline-based nanocomposite and its application as an ethanol vapor sensor. *New Journal of Chemistry, 39* (5), 3728-3735.

Kulys, J. & D'Costa, E. J. (1991). Printed electrochemical sensor for ascorbic acid determination. *Analytica Chimica Acta, 243*, 173-178.

Lange, U. & Mirsky. V. M. (2011). Chemosensitive nanocomposite for conductometric detection of hydrazine and NADH. *Electrochimica Acta, 56*, 3679-3684.

Lange, U., Roznyatovskaya, N. V., & Mirsky, V. M. (2008). Conducting polymers in chemical sensors and arrays. *Analytica Chimica Acta, 614*, 1-26.

Laska, J. (2004). Conformations of polyaniline in polymer blends. *Journal of Molecular Structure, 701,* 13-18.

Li, B., Santhanam, S., Schultz, L., Jeffries-EL, M., Iovu, M. C., Sauve, G., Cooper, J., Zhang, R., Revelli, J. C., Kusne, A. G., Snyder, J. L., Kowalewski, T., Weiss, L. E., McCullough, R. D., Fedder, G. K., & Lambeth, D. N. (2007). Inkjet printed chemical sensor array based on polythiophene conductive polymers. *Sensors and Actuators B, 123,* 651-660.

Li, G., Martinez, C., Janata, J., Smith, J. A., Josowicz, M., & Semancik, S. (2004). Effect of the morphology on the response of polyaniline-basedconductometric gas sensors: Nanofibers vs. thin films. *Electrochemical and Solid-State Letters, 7* (10), 44-47.

Li, J., Zhang, J., Sun, H., Hong, D., Li, L., Yang, Y., Yong, X., Zhang, C., & Cui, J. (2019). An optical fiber relative humidity sensor based on hollow-core fiber and hydroxypropyl methylcellulose hydrogel film. *Optik - International Journal for Light and Electron Optics, 195*, 1-7.

Li, X., Wang, Y., Yang, X., Chen, J., Fu, H., & Cheng, T. (2012). Conducting polymers in environmental analysis. *Trends in Analytical Chemistry, 39,* 163-179.

Li, Y., Ying, B., Hong, L., & Yang, M. (2010). Water-soluble polyaniline and its composite with poly(vinyl alcohol) for humidity sensing. *Synthetic Metals, 160,* 455-461.

Liu, H., Wang, H., Liu, G., Pu, S., & Zhang, H. (2019). Ultrasensitive sensing of hydrazine vapor at sub-ppm level with pyrimidine-substituted perylene diimide film device. *Tetrahedron, 75,* 1988-1996.

Luong, N. D., Korhonen, J. T., Soininen, A. J., Ruokolainen, J., Johansson, L. S., & Seppala, J. (2013). Processable polyaniline suspensions through in situ polymerization onto nanocellulose. *European Polymer Journal, 49*, 335-344.

Ma, X. S., Wang, D. H., Cui, Y. Z., Tao, F. R., Wang, Y. T., & Li, T. D. (2017). A novel hydrophilic conjugated polymer containing hydroxyl groups: Syntheses and sensing performance for NACs in aqueous solution. *Sensors and Actuators B, 251,* 851-857.

MacDiarmid, A. G. (2001). Synthetic metals: A novel role for organic polymers (nobel lecture). *Angewandte Chemie International Edition, 40,* 2581-2590.

Madhu, R., Veeramani, V., & Chen, S. M. (2014). Fabrication of a novel gold nanospheres/activated carbon nanocomposite for enhanced electrocatalytic activity toward the detection of toxic hydrazine in various water samples. *Sensors and Actuators B, 204,* 382–387.

Mo, Z., Zhao, Z., Chen, H., Niu, G., & Shi, H. (2009). Heterogeneous preparation of cellulose-polyaniline conductive composites with cellulose activated by acids and its electrical properties. *Carbohydrate Polymers, 75,* 660-664.

Moiz, S. A., Imran, S. M., Nahhas, A. M., Rehman, F., Ahmed, M. M., Kim, H. T., & Lee, J. H. (2012). Polaron hopping mechanism of conducting polymer. *2012 International Conference on Emerging Technologies.*

Nahar, R. K., Khanna, V. K., & Khokle, W. S. (1984). On the origin of the humidity-sensitive electrical properties of porous aluminium oxide. *Journal of Physics D: Applied Physics, 17,* 2087-2095.

Navale, S. T., Khuspe, G. D., Chougule, M. A., & Patil, V. B. (2014). Room temperature NO_2 gas sensor based on PPy/α-Fe_2O_3 hybrid nanocomposites. *Ceramics International, 40,* 8013-8020.

NIOSH. (1988). Occupational safety and health guidelines for hydrazine potential human carcinogen. Retrieved on 21 August 2019 from https://www.cdc.gov/niosh/docs/88-118/

Osorio-Fuente, J. E., Gomez-Yanez, C., Hernandez-Perez, M. D. L. A., & Perez-Moreno, F. (2014). camphor sulfonic acid-hydrochloric acid codoped polyaniline/polyvinyl alcohol composite: Synthesis and characterization. *Journal of the Mexican Chemical Society, 58* (1), 52-58.

Patil, R., Harima, Y., Yamashita, K., Komaguchi, K., Itagaki, Y., & Shiotani, M. (2002). Charge carriers in polyaniline film: A correlation between mobility and in-situ ESR measurements. *Journal of Electroanalytical Chemistry, 518,* 13-19.

Pavia, D. L., Lampman, G. M., Kriz, G. S., & Vyvyan, J. R. (2009). *Introduction to spectroscopy* (4th ed.). Bellingham, Washington: Brooks/Cole Cengage Learning.

Pellizzari, E. D. & Clayton, C. A. (2006). Assessing the measurement precision of various arsenic forms and arsenic exposure in the National Human Exposure Assessment Survey (NHEXAS). *Environmental Health Perspectives, 114,* 220-227.

Perkin Elmer. (2005). FT-IR spectroscopy: Attenuated total reflectance (ATR). Shelton, USA: Perkin Elmer.

Phasuksom. K., Prissanaroon-Ouajai. W., & Sirivat. A. (2018). Electrical conductivity response of methanol sensor based on conductive polyindole. *Sensors and Actuators B, 262*, 1013-1023.

Radiometer Analytical SAS. (2004). *Conductivity theory and practice*. Villeurbanne Cedex, France: Author.

Rahy, A., Rguig, T., Cho, S. J., Bunker, C. E., & Yang, D. J. (2011). Polar solvent soluble and hydrogen absorbing polyaniline nanofibers. *Synthetic Metals, 161*, 280-284.

Ramaprasad, A. T. & Rao, V. (2008). Electronic conduction mechanism in chitin-polyaniline blend. *Synthetic Metals, 158,* 1047-1053.

Rana, U., Paul, N. D., Mondal, S., Chakraborty, C., & Malik, S. (2014). Water soluble polyaniline coated electrode: A simple and nimble electrochemical approach for ascorbic acid detection. *Synthetic Metals, 192*, 43-49.

Rasmusssen, S. C. (2017). The early history of polyaniline: Discovery and origins. *Substantia, 1* (2), 99-109.

Rosemount Analytical Inc. (2010). *Theory and application of conductivity*. Irvine, CA: Emerson Process Management.

Royal Society of Chemistry. (2009). *Introduction to Ultraviolet - Visible Spectroscopy (UV).* Cambridge, UK: Royal Society of Chemistry.

Sambasevam, K. P., Mohamad, S., & Phang, S. W. (2015). Effect of dopant concentration on polyaniline for hydrazine detection. *Materials Science in Semiconductor Processing, 33*, 24-31.

Schirmann, J. P. & Bourdauducq, P. (2012). Hydrazine. In *Ullmann's Encyclopedia of Industrial Chemistry* (Vol. 18, pp. 79-96). Weinheim: Ullmann's Encyclopedia of Industrial Chemistry.

Seitz, W. R. (1984). Chemical sensors based on fiber optics. *Analytical Chemistry, 56* (1), 16-34.

Sen, T., Mishra, S., & Shimpi, N. G. (2017). A β-cyclodextrin based binary dopant for polyaniline: Structural, thermal, electrical, and sensing performance. *Materials Science and Engineering B, 220,* 13-21.

Shao, L., Qiu, J., Liu, M., Feng, H., Lei, L., Zhang, G., Zhao, Y., Gao, C., & Qin, L. (2011). Synthesis and characterization of water-soluble polyaniline films. S*ynthetic Metals, 161*, 806-811.

Shi, X., Zhang, L., Cai, J., Cheng, G., Zhang, H., Li, J., & Wang, X. (2011). A facile construction of supramolecular complex from polyaniline and cellulose in aqueous system. *Macromolecules, 44,* 4565-4568.

Shinohara, H., Chiba, T., & Aizawa, M. (1988). Enzyme microsensor for glucose with an electrochemically synthesized enzyme-polyaniline film. *Sensors and Actuators, 13,* 79-86.

Shirakawa, H., Louis, E. J., MacDiarmid, A. G., Chiang, C. K., & Heeger, A. J. (1977). Synthesis of electrically conducting organic polymers: Halogen derivatives of polyacetylene, $(CH)_x$. *Journal of the Chemical Society Chemical Communications*, 578-580.

Shivastava, A. & Gupta, V. B. (2011). Methods for the determination of limit of detection and limit of quantitation of the analytical methods. *Chronicles of Young Scientists, 2*, 21-25.

Shukla, S. K. (2012). Synthesis of polyaniline grafted cellulose suitable for humidity sensing. *Indian Journal of Engineering & Materials Sciences, 19,* 417-420.

Sinha, S., Gaur, P., Dev, S., Mukhopadhyay, S., Mukherjee, T., & Ghosh, S. (2015). Hydrazine responsive molecular material: Optical signaling and mushroom cell staining. *Sensors and Actuators B, 221*, 418–426.

Smith, J. A., Josowicz, M., & Janata, J. (2005). Gold-polyaniline composite. *Physical Chemistry Chemical Physics, 7*, 3614-3618.

Sohouli, E., Khosrowshahi, E. M., Radi, P., Naghian, E., Nasrabadi, M. R., & Ahmadi, F. (2020). Electrochemical sensor based on modified methylcellulose by graphene oxide and Fe_3O_4 nanoparticles: Application in the analysis of uric acid content in urine. *Journal of Electroanalytical Chemistry, 877*, 1-10.

Soni, A., Pandey, C. M., Solanki, S., & Sumana, G. (2019). Synthesis of 3D-coral like polyaniline nanostructures using reactive oxide templates and their high performance for ultrasensitive detection of blood cancer. *Sensors & Actuators: B. Chemical, 281,* 634-642.

Stejskal, J., Exnerova, M., Moravkova, Z., Trchova, M., Hromadkova, J., & Prokes, J. (2012). Oxidative stability of polyaniline. *Polymer Degradation and Stability, 97*, 10 26-1033.

Su, S., & Kuramoto, N. (2000). Synthesis of processable polyaniline complexed with anionic surfactant and its conducting blends in aqueous and organic system. *Synthetic Metals, 108*, 121-126.

Tang, S. J., Lin, K. Y., Zhu, Y. R., Huang, H. Y., Ji, W. F., Yang, C. C., Chao, Y. C., Yeh, J. M., & Chiu, K. C. (2013). Structural and electrical characterization of polyanilines synthesized from chemical oxidative polymerization via doping/de-doping/re-doping processes. *Journal of Physics D: Applied Physics, 46,* 1-8.

Tayeb, A. H., Amini, E., Ghasemi, S., & Tajvidi, M. (2018). Cellulose nanomaterials-binding properties and applications: A review. *Molecules, 23,* 1-24.

The Royal Swedish Academy of Sciences. (2000). *The Nobel Prize in Chemistry, 2000: Conductive polymers*. Stockholm, Sweden: The Royal Swedish Academy of Sciences.

Tsubakizaki, S., Gotou, H., Ishihara, N., Takada, M., Mawatari, K., & Kai, R. (2009). Alternatives to hydrazine in water treatment at thermal power plants. *Mitsubishi Heavy Industries Technical Review, 46*, 43-47.

United States Department of Labor. (2018). *Hydrazine*. Retrieved on 9 January 2019 from https://www.osha.gov/dts/chemicalsampling/data/CH_245900.html.

Urbano, E., Offenbacher, H., & Wolfbeis, O. S. (1984). Optical sensor for continuous determination of halides. *Analytical Chemistry, 56* (3), 427-429.

Virji, S., Huang, J., Kaner, R. B., & Weiller, B. H. (2004). Polyaniline nanofiber gas sensors: Examination of response mechanisms. *Nano Letters, 4* (3), 491-496.

Virji, S., Kaner, R. B., & Weiller, B. H. (2005). Hydrazine detection by polyaniline using fluorinated alcohol additives. *Chemistry of Materials, 17*, 1256-1260.

Wang, X., Meng, S., Tebyetekerwa, M., Weng, W., Pionteck, J., Sun, B., Qin, Z., & Zhu, M. (2017). Nanostructured polyaniline/poly(styrene-butadiene-styrene) composite fiber for use as highly sensitive and flexible ammonia sensor. *Synthetic Metals, 233*, 86-93.

Weiller. B. H., Virji. S., Baker. C., Huang. J., Li. D., & Kaner. R. B. (2005). Polyaniline nanofibers and composite materials for chemical detection. *NSTI-Nanotech, 2,* 1-4.

Wen, W. (2016). *Progresses in chemical sensor: What is chemical sensor?*. London, UK: IntechOpen.

Wolters, C. (2019). *Toxic waste, explained*. Retrieved on 14 October 2019 from https://www.nationalgeographic.com/environment/global-warming/toxic-waste/.

Xia, Y., Wiesinger, J. M., MacDiarmid, A. G., & Epstein, A. J. (1995). Camphorsulfonic acid fully doped polyaniline emeraldine salt: Conformations in different solvents studied by an ultraviolet/visible/near-infrared spectroscopic method. *Chemistry of Materials, 7,* 443-445.

Yadav, A., Kumar, J., Shahabuddin, Md., Agarwal, A., & Saini, P. (2019). Improved ammonia sensing by solution processed dodecyl benzene sulfonic acid doped polyaniline nanorod networks. *IEEE Access, 7*, 139571-139579.

Yin, W. & Ruckenstein, E. (2000). Soluble polyaniline co-doped with dodecyl benzene sulfonic acid and hydrochloric acid. *Synthetic Metals, 108*, 39-46.

Yin, C., Gao, L., Zhou, F., & Duan, G. (2017). Facile synthesis of polyaniline nanotubes using self-assembly method based on the hydrogen bonding: Mechanism and application in gas sensing. *Polymers, 9,* 1-14.

Yoo, K. P., Kwon, K. H., Min, N. K., Lee, M. J., & Lee, C. J. (2009). Effects of O_2 plasma treatment on NH_3 sensing characteristics of multiwall carbon nanotube/polyaniline composite films. *Sensors and Actuators B, 143,* 333-340.

Yuan, G. L. & Kuramoto, N. (2002). Water-processable chiral polyaniline derivatives doped and intertwined with dextran sulfate: synthesis and chiroptical properties. *Macromolecules, 35*, 9773-9779.

Yue, L., Zheng, Y., Xie, Y., Liu, S., Guo, S., Yang, B., & Tang, T. (2016). Preparation of a carboxymethylated bacterial cellulose/polyaniline composite gel membrane and its characterization. *RSC Advances, 6,* 68599-68605.

Zargar, B. & Hatamie, A. (2013). A simple and fast colorimetric method for detection of hydrazine in water samples based on formation of gold nanoparticles as a colorimetric probe. *Sensors and Actuators B, 182*, 706– 710.

Zhao, D., Li, L., Niu, W., & Chen, S. (2017). Highly conductive polythiophene films doped with chloroauric acid for dual-mode sensing of volatile organic amines and thiols. *Sensors and Actuators B, 243,* 380-387.

Zheng, Y., Lee, D., Koo, H. Y., & Maeng, S. (2015). Chemically modified graphene/PEDOT: PSS nanocomposite films for hydrogen gas sensing. *Carbon, 81,* 54-62.

Zuo, F., Jin, L., Fu, X., Zhang, H., Yuan, R., & Chen, S. (2017). An electrochemiluminescent sensor for dopamine detection based on a dual-molecule recognition strategy and polyaniline quenching. *Sensors and Actuators B, 244,* 282-289.

LIST OF PUBLICATIONS AND PAPERS PRESENTED

List of publications

1. **Hussin, H**., Gan, S. N., Mohamad, S., & Phang, S. W. (2017). Synthesis of water - soluble polyaniline by using different types of cellulose derivatives. *Polymer & Polymer Composites, 25*(7), 515-520.

Presentation

1. Synthesis of Water-soluble Polyaniline by Using Different Types of Cellulose Derivatives. 10th International Materials Technology Conference & Exhibition, International Symposium on Coatings and Corrosion (ISCC 2016): 16-19th May 2016, Putra World Trade Centre, Kuala Lumpur, Malaysia.